GEOLOGICA ULTRAIECTINA

Mededelingen van het
Instituut voor Aardwetenschappen der
Rijksuniversiteit te Utrecht

No. 27

HYDROTHERMAL PROCESSES IN MYLONITIC ROCKS AT THE NW EDGE OF THE GRONG CULMINATION, CENTRAL NORWAY

HARRY STEL

GEOLOGICA ULTRAIECTINA

Mededelingen van het
Instituut voor Aardwetenschappen der
Rijksuniversiteit te Utrecht

No. 27

HYDROTHERMAL PROCESSES IN MYLONITIC ROCKS AT THE NW EDGE OF THE GRONG CULMINATION, CENTRAL NORWAY

HYDROTHERMAL PROCESSES IN MYLONITIC ROCKS AT THE NW EDGE OF THE GRONG CULMINATION, CENTRAL NORWAY

HYDROTHERMALE PROCESSEN IN MYLONIETISCHE GESTEENTEN AAN DE NOORD-WESTELIJKE RAND VAN DE GRONG CULMINATIE, CENTRAAL NOORWEGEN. (MET EEN SAMENVATTING IN HET NEDERLANDS)

PROEFSCHRIFT

TER VERKRIJGING VAN DE GRAAD VAN DOCTOR IN DE WISKUNDE EN NATUURWETENSCHAPPEN AAN DE RIJKSUNIVERSITEIT TE UTRECHT, OP GEZAG VAN DE RECTOR MAGNIFICUS PROF. DR. O.J. DE JONG, VOLGENS BESLUIT VAN HET COLLEGE VAN DEKANEN IN HET OPENBAAR TE VERDEDIGEN OP MAANDAG 10 DECEMBER 1984 DES NAMIDDAGS TE 2.30 UUR

DOOR

HARM STEL

GEBOREN OP 29 MAART 1954 TE ASSEN

PROMOTOR: PROF. DR. H.J. ZWART

REFERENT: DR. J. N. BOLAND

Aan de nagedachtenis
van mijn vader

VOORWOORD

Voor de hulp die ik gekregen heb bij het vervaardigen van dit proefschrift gaat mijn dank uit naar

Mijn promotor, Prof. Dr. H.J. Zwart voor de kritische begeleiding tijdens mijn onderzoek, zowel in het veld als op de afdeling;

Dr. J. N. Boland, die mij wegwijs heeft gemaakt op het gebied van de electronenmicroscopie;

Prof. Dr. P. Hartman, Dr. R.J. Lisle, Dr. G.S.Lister, Dr. A. Senior, Dr. I. v.d. Molen en Drs C. Woensdregt voor stimulerende discussies.

Aan F. Stanley (tekeningen), H. Schiet (fotografie), C. Laman, ing. J. Pieters, J. Janssen (TNO) en J. de Groot voor diverse werkzaamheden en suggesties.

Aan mijn studievrienden Herman van Roermund en Peter Verhoef.

Veel dank ben ik verschuldigd aan mijn ouders, die mij in staat hebben gesteld om te studeren.

Dit proefschrift kwam tot stand dank zij de financiele steun van de organisatie voor Zuiver Wetenschappelijk Onderzoek (ZWO), waarvoor ik speciale dank verschuldigd ben.

INDEX

ABSTRACT

The cataclasite and mylonites, and the brittle/ductile deformation processes that produced them, were studied in relation to the regional geology at exposures along the northern rim of the Grong culmination, a transverse basement antiform in the Scandinavian Caledonides.

Autochthonous basement in the centre of the Grong culmination consists of leucocratic gneisses and granites. In cataclasites in the basement rocks hydrothermal growth of silica minerals took place, crystallization products vary from chalcedony aggregates to euhedral quartz crystals in veins. By cathode-luminescence microscopy euhedral crysts show growth bandings parallel to crystallographic planes, fine grained quartz aggregates in the matrix of the cataclasites show an agate-type banding. By TEM, growth banding was identified as dislocation arrays associated with bubbles, these structures were found in euhedral crystals and in small matrix grains. It is interpreted that during cataclasis a silica-gel was formed in the rocks from which crystallization took place. Older quartz veins have been plastically deformed, while undergoing rotation towards parallellism. It is thought that a similar process caused a foliation defined by an alternation of quartz-rich and feldspar-rich bands in the basement gneisses.

The microstructure of cataclasites and basement gneisses appears to be the result of a repeated alternation of brittle deformation (associated with crystal growth) and plastic deformation of the crystallization products.

The Granite-mylonite nappe is a basement unit which was emplaced on the autochthon during the Caledonian orogeny. The unit is found at the limbs of the Grong antiform. The rocksuite comprises augengneisses and augen-bearing mylonites of granodioritic composition. In shear zones in relatively undeformed granodiorites the transformation of non-foliated rock to platy mylonites was studied. Plastic deformation of the rocks appears to be associated with retrograde metamorphism: the original mineral association plagioclase + brown biotite + hornblende is transformed to the paragenesis green biotite + white mica + albite + epidote.

Syntectonic K-feldspar/chlorite veins are found throughout the entire

rocksuite, deformed veins show boudinage, the boudins constitute new K-feldspar augen. The modification of the feldspars is maximum microcline. Some crystals are partly or completely cross-hatched twinned by albite and pericline twin lamellae. Twins are predominantly found in kink bands and at grainboundaries. By TEM it is demonstrated that albite and pericline twin lamellae occur in dislocation loops, suggesting that the twins are formed by plastic deformation, precluding an origin by a symmetry inversion of a high temperature modification. It is concluded that the K-feldspar crystals in the rocks have a low temperature, syntectonic origin, and the microstructure of the rocks is formed by alternation of brittle deformation (with the formation of veins) and subsequent plastic deformation (with the formation of the augen). Each deformation regime is associated with a specific metamorphism:
During brittle deformation K-feldspar/chlorite veins are formed, probably by incongruent pressure solution of micas. During plastic deformation of the rocks this mineral association is transformed to white mica and green biotite following the reaction:

$$5 \text{ biotite} + 3 \text{ white mica} + 9 \text{ quartz} + H_2O = 8 \text{ K-feldspar} + 9 \text{ chlorite}$$

During this reaction plagioclase is overgrown by mica and epidote and K-feldspar crystals are replaced by albite. Albitization of K-feldspars occurred in two manners: by an ion-exchange mechanism which leaves the Si-Al-O framework intact, or by the formation of small new albite grains, the latter process took place in dislocation-rich specimens.

An alternation of brittle and ductile deformation is also found on a regional scale: cataclasites and mylonites show transitional relations to each other. Two large cataclasite zones have been formed by vertical movement of the basement during a late stage of the formation of the Crong culmination. Of other zones no movement direction could be deduced.

Mylonites occurring at the northern edge of the Grong culmination are the centres of large dextral shear zones formed by nappe emplacement during the Caledonian orogeny. The pattern of the orientations of the foliation and the extension lineations indicates that the nappes moved around an existing basement culmination.

At the southern edge of the Grong culmination basement units and metamorphic nappes are concordantly folded in large scale structures. It is thought that the Grong culmination was synchronously formed with these folds. At the southern rim of the Grong culmination, apparently, nappe emplacement pre-dated the formation of the Grong culmination. It follows that the relative age of nappe emplacement north of the Grong culmination (in the central Scandinavian Caledonides) is different from that south of this structure (in the southern Caledonides). It is interpreted that this age difference is due to the fact that in the central Scandinavian Caledonides the nappes moved ca. 150 km further to SE. This interpretation is in accordance with differences in stratigraphy, structure and intrusion pattern between these two parts of the Caledonian orogeny.

SAMENVATTING

De hydrothermale processen die plaatsvinden tijdens brosse en plastische deformatie en de relatie van mylonieten en cataclasieten met de regionale geologie zijn bestudeerd aan gesteenten die voorkomen aan de noordrand van de Grong culminatie, een transversale antiform in het grondgebergte van de Scandinavische Caledoniden.

De kern van de Grong culminatie bestaat uit leucocrate granieten en gneizen van het autochthone grondgebergte, deze gesteenten worden doorsneden door cataclasietzones. In de cataclasieten heeft hydrothermale groei van silicaten plaats gevonden, de kristallisatieprodukten varieren van chalcedoon aggregaten tot idiomorfe kwartskristallen. Met cathode-luminiscentie werden groeibanden in kwartskristallen waargenomen; kwarts-rijke delen van de matrix van de cataclasieten vertonen een banding die lijkt op die in agaten. Met transmissie electronen microscopie (TEM) werd vastgesteld dat groeibanden in kwarts worden begrensd door dislokatie netwerken met vloeistof insluitsels, deze substruktuur werd ook waargenomen in fijnkorrelige kwarts in de matrix van de cataclasiet. De microstrukturen zijn geïnterpreteerd als het product van kristallisatie uit een silica-gel die tijdens cataclase werd gevormd. Oudere kwartsaders in de cataclsieten zijn plastisch vervormd, de korrels zijn unduleus uitdovend en er is rekristallisatie opgetreden. Het blijkt dat in de cataclasieten een afwisseling van brosse deformatie, gerelateerd met kristalgroei, en plastische deformatie heeft plaatsgevonden.

De foliatie in de gneizen van het grondgebergte wordt gevormd door een afwisseling van veldspaat- en kwarts-rijke banden. Deze microstruktuur wordt geinterpreteerd als te zijn veroorzaakt door afwisselend bros en plastisch gedrag van het gesteente, de kwarts-rijke banden zijnde gevormd door afplatting en rotatie van kwartsaders die tijdens een vroegere fase van brosse deformatie zijn gevormd.

Het Graniet-myloniet dekblad is een grondgebergte-eenheid die tijdens de Caledonische orogenese over het autochthoon is geschoven. Het gesteentepakket bestaat uit ogengneizen en mylonieten van granodiorietische samenstelling. In shearzones in relatief weinig gedeformeerde granodioriet werd

de transformatie van ongefolieerd gesteente naar myloniet bestudeerd. Het blijkt dat de plastische deformatie van het gesteente is geassocieerd met retrograde metamorfose: de granodiorietische mineraalassociatie plagioklaas + bruine biotiet + hoornblende wordt vervangen door groene biotiet + witte mica + albiet + epidoot, hetgeen erop wijst dat de deformatie plaatsvond onder groenschist facies condities.

In het gesteente komen syntektonische K-veldspaat aders voor, vaak in combinatie met chloriet. De modificatie van de K-veldspaat is maximum mikroklien. Gedeformeerde aders zijn geboudineerd, de boudins vormen K-veldspaat ogen in het gesteente. Sommige K-veldspaten vertonen een gehele of gedeeltelijke ontwikkeling van gekruiste albiet en periklien tweelingen. De tweelingslamellen komen voornamelijk voor op plaatsen waar het mineraal sterk plastisch is vervormd. Met TEM werd aangetoond dat er albiet en periklien mikro-tweelingslamellen voorkomen binnen dislokatielussen. Het blijkt dat de gekruiste tweelingen in de bestudeerde mikroklien-kristallen het produkt zijn van van plastische deformatie en niet ontstaan zijn door inversie van een hoge-temperatuur modificatie. Geconcludeerd is dat de meeste K-veldspaat in het gesteente een laaggradige oorsprong heeft.

De microstruktuur van de ogengneizen is gevormd door een afwisseling van brosse deformatie (met vorming van K-veldspaat aders) en plastische deformatie (tijdens welke door boudinage de K-veldspaat ogen ontstaan). De deformatie-regiems zijn elk geassocieerd met een bepaald type metamorfose: Tijdens brosse deformatie van het gesteente vindt K-veldspaat-chloriet groei in aders plaats. Bij plastische deformatie van het gesteente wordt deze mineraal associatie gedeeltelijk omgezet in witte mica en groene biotiet volgens de reactie:

$$\begin{matrix} 5\text{biotiet} + 3\text{witte mica} \\ +9\text{kwarts} + H_2O \end{matrix} = \begin{matrix} 8\text{K-veldspaat} \\ +9\text{chloriet} \end{matrix}$$

Deze reaktie is geassocieerd met de omzetting van plagioklaas naar mica en epidoot en vervanging van K-veldspaat door albiet. Albitisatie van K-veldspaat kan plaatsvinden door ionen-uitwisseling waarbij het Si-O-Al bouwwerk intact blijft, of door groei van nieuwe albietkorrels, het laatste proces vindt plaats als de K-veldspaat sterk gedeformeerd is en veel kristaldefecten bevat.

De afwisseling van brosse en plastische deformatie die op micro-en mesoscopische schaal in het gesteente werd waargenomen, heeft ook op macroscopische schaal plaatsgevonden: cataclasiet-zones zijn gemylonitiseerd en myloniet-zones zijn op veel plaatsen bros gedeformeerd.

Twee cataclasiet-zones zijn aantoonbaar gevormd door verticale beweging van het grondgebergte tijdens een late fase van de vorming van de Grong culminatie. Van de meeste cataclasieten kon geen bewegingsrichting worden vastgesteld.

Mylonieten die voorkomen op de noordelijke grens van het grondgebergte en de daarop liggende dekbladen zijn de centra van grootschalige dextrale shearzones die gevormd zijn tijdens de verplaatsing van de dekbladen. Het patroon van de orientatie van de foliatie en van de uitrekkingslineaties toont aan dat de dekbladen langs een al bestaande Grong culminatie 'gevloeid' zijn.

Aan de zuidrand van de Grong culminatie zijn eenheden van het grondgebergte en metamorfe dekbladen samen verplooid in grootschalige strukturen. De Grong culminatie is gelijktijdig met de vorming van deze plooien ontstaan. Dit wijst erop dat in het zuiden de beweging van de dekbladen vóór de vorming van de Grong culminatie plaatsvond. De relatieve ouderdom van de dekbladbeweging ten noorden en ten zuiden van de culminatie is dus verschillend. De interpretatie van dit fenomeen is dat ten noorden van de Grong culminatie (in de centrale Caledoniden) de dekbladen ca. 150 km verder zijn verplaatst dan ten zuiden van deze struktuur. Deze interpretatie wordt gesteund door het bestaan van grote verschillen in de stratigrafie, struktuur en metamorfose van de beide gedeelten van het Caledonische orogeen.

CHAPTER I INTRODUCTION.

1.1. Terminology.

The term mylonite was introduced by C.Lapworth (1885) to classify rocks which occur in movement zones in the Moine region (NW Scotland). Because Lapworth differentiated between mylonites and rocks which were deformed by plastic yielding, accompanied by recrystallization (augenschists) it is likely that the term initially covered rocks formed by crushing and grinding of the minerals.

In more modern literature it is demonstrated that in a number of planar movement zones the rocks deformed plastically, while undergoing dynamic recrystallization (Bell and Etheridge, 1973, White et al.,1980). The common occurrence of folds in these rocks is an evidence of ductility (cf. Carreras et al., 1977). It is now believed that most mylonites have been formed by such processes, however the term still causes confusion. Detailed classifications have been published which never gained general acceptance (Christie, 1960, Spry, 1969, Higgins, 1971, Sibson, 1977). Hence it is still necessary to begin this work with definitions of mylonites and cataclasites.

A mylonite is defined here as a finely foliated (laminated), well lineated tectonite which is found in narrow, usually planar zones of very strong deformation and in which during the deformation history coherency was retained. The grainsize of mylonites is usually small relative to that in the country rocks. This definition is in accordance with the modern usage of the term (Christie, 1960, 1963, White, 1977, 1979, Bell and Etheridge, 1973, 1976, Wilson, 1973, 1980, Mitra, 1978, 1979. Carreras et al., 1977, Lamouroux et al., 1980, Passchier, 1982, Behrmann and Platt, 1982).

A cataclasite is a tectonite in which during deformation coherency was lost, the rocks are predominantly built up by crush fragments.

1.2. Deformation history of mylonites.

Mylonites represent zones in which the strain is large relative to that in the country rocks. This implies that if coherency is retained throughout a rocksuite and if deformation occurs at constant volume the deformation history of mylonites must have a non-coaxial component. For instance, a narrow planar zone of intense flattening would cause extrusion, leading to space problems in most geological settings. Bell (1981) argues that mylonites may form by bulk flattening without causing space problems if there are zones of localized shear strain which anastomose, his argument is a question of scale.

From the literature it appears that mylonites have been related mostly to relative displacement of rock bodies. Mylonite zones are the most frequently cited associate of thrusts (Lapworth, 1885; Christie, 1960; Trouw, 1973; Zwart, 1974; Wakefield, 1977; Gee, 1980; Behrmann and Platt, 1982). Other occurrences are related to vertical or steeply dipping displacement zones which can be of strike slip nature (e.g. Yuen et al., 1978; Carreras et al., 1980; Sibson et al., 1981) or were formed by reverse faulting (Zwart, 1958; Passchier, 1982).

1.3. Mylonitization, some processes.

Mylonites are formed by strong ductile deformation. Because the microstructures of minerals in ductilely deformed rocks resemble those in plastically deformed metals (Ramberg, 1952; Voll, 1960) it is thought that the deformation of rocks and metals follow basically the same principles. Experimental rock deformation studies, combined with electron microscopy have confirmed this correlation. It was demonstrated that minerals such as calcite (Griggs, 1938; Griggs and Handin, 1960; Spiers, 1979), quartz (Carter et al, 1964; Tullis, 1970; Tullis et al., 1973), olivine (Kohlstedt and Goetze, 1974; Boland, 1974) and feldspars (Marshall et al., 1976; Willaime and Gandais, 1977; Willaime et al.,1979) deform plastically at appropriate physical conditions (high temperature, high confining pressure).

The detailed mechanisms of plastic deformation are different when the physical conditions change. The relations can be visualized by deformation

mechanism maps (Stocker and Ashby, 1973; Rutter, 1976). Figure 1.1. shows the relation of strain rate, differential stress and temperature and deformation mechanisms in calcite (from Rutter, 1976). The different deformation mechanisms will be briefly discussed below.

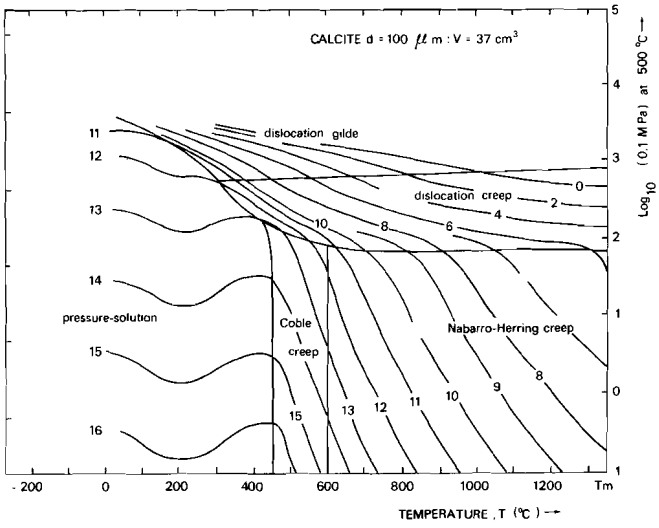

Figure 1.1. Deformation mechanism map of calcite. (from Rutter, 1976).

Dislocation glide. Polycrystalline material can be plastically strained by intracrystalline deformation of the constituent minerals. This deformation can be achieved by movement of dislocations along a slip plane, causing a relative displacement of parts of a crystal (Read, 1953; Friedel, 1964; Hull, 1975). Dislocations are present in each natural crystal, but they are also generated during deformation by high local stresses (Friedel, 1964), leading to a high dislocation density which causes hindrance to further slip, and eventually to brittle failure (Paterson, 1978; Atkinson, 1982). Processes which tend to minimalize the dislocation density in crystals (e.g. annihilation, network formation) involve diffusion (Friedel, 1964) and such processes are critical for crystals to undergo large plastic strain and hence for the formation of mylonites (cf. White, 1977).

Dislocation glide assisted by diffusional processes (notably climb) is called dislocation creep. As this mechanism is governed by diffusion, it is a high temperature deformation.

Higher temperatures ($>\frac{1}{2}T_{melt}$) will promote diffusion in crystals and processes such as Coble creep (involving grain boundary diffusion) and Nabarro-Herring creep (involving bulk diffusion) take place. By these processes plastic strain is achieved by diffusion of interstitial atoms and vacancies to sites of low and high stresses respectively (Nabarro, 1967). It is thought that Coble creep is an important deformation mechanism in high temperature mylonites, as it allows grain boundary sliding. Superplastic deformation (involving diffusion accomodated grain boundary sliding) is thought to be the dominant deformation mechanism in many fine grained mylonites (Boullier and Gueguen, 1974; Schmidt et al., 1977).

At lower temperatures grain boundary sliding may be accomodated by pressure solution (Rutter, 1976; Kerrich, 1977). Basically the process involves solution of material at sites of high stress and redeposition at low stress sites: i.e. Riecke's principle. Of course, for this mechanism to be operative a pore fluid has to be present in the rocks.

The application of deformation mechanism maps to unravel the tectono-metamorphic history of a rock is still rather limited. In particular mechanisms which are driven by a high grain boundary mobility are difficult to pin-point to a specific field on deformation-mechanism maps because

several factors (impurity content, composition of the pore fluid and the effect of ongoing metamorphic reactions) have not yet been quantified.

Cataclasites by definition have been formed by brittle deformation, i.e. processes which involve the loss of coherency on a (sub)microscopic scale (microcracking). Microcracks develop when locally tensile or shear stresses exceed the strength of the material, i.e. the stress required to overcome the interatomic forces.
Two independent factors control operation of microcracking: external factors which determine the differential stress and intrinsic factors controlling the stress distribution and strength of a crystal (cf. Paterson, 1978; Fyfe et al., 1978).
Impurities, crystal defects such as dislocation pile-ups, twin tips and pre-existing microcracks are sites of stress concentration in a crystal, the ratio of microstresses at these sites and the "bulk stress" may approach 1000:1 (Griffith, 1924). Growth of cracks will markedly be enhanced by hydrolysis of broken bonds in silicates (by lowering surface energy), and more generally by reactions at pre-existing microcracks (stress corrosion cracking), which tend to lower the strength of the material (cf. Kerrich et al., 1980).
Recently fracture mechanism maps, which are analogous of deformation mechanism maps were introduced (Atkinson, 1982). The author differentiates between four mechanisms of fracture: fracture controlled by pre-existing defects, by defects generated by microplasticity, by grainboundary sliding and by creep.
After formation of microcracks sliding along the fault surfaces can produce a permanent bulk strain of the faulted material (cataclastic flow). The rate of this process is controlled by the differential stress, the mineralogy of the faulted rocks (influencing the roughness of fault surfaces) and the formation of ground-wear or gouge (Byerlee, 1967; Dieterich, 1972; Scholz et al., 1972), and the pore pressure (Jaeger, 1943; Hoskins et al., 1968; Byerlee and Brace, 1972).
Large brittle faults are the loci of mineral growth, a process which is attributed to "tectonic pumping" (Sibson et al., 1975) causing fluids and dissolved material to migrate to faulted zones. Ramsay (1980) defined a deformation mechanism based on mineral growth in relation to cracking; namely the crack-seal process.

1.4. Geological setting of the studied mylonites.

The mylonite belt discussed in this thesis occurs at or near the basal thrust of the Scandinavian Caledonides. The zone outcrops at the edges of the Grong culmination, a N.W.-S.E. trending antiformal structure in which the Precambrian granitic basement transects the N.E.-S.W. trending Caledonian belt in central Norway and Sweden (Fig. 1.2). The basement rocks are mainly composed of leucocratic (alkali)granitic rocks (Foslie, 1958, 1959, 1960; Oftedahl, 1956; Aukes et al., 1979). Whole rock age determinations (Rb-Sr) yield values of 1700-1500 Ma (Reymer, 1979; Klingspor and Troëng, 1980). Locally the granites are crosscut by mafic dykes (cf. Johansson, 1980).
There is discussion in the literature whether the Grong and Olden granites (the Swedish extension of the Grong culmination) are autochthonous, parautochthonous or allochthonous (Asklund, 1938; 1955, Gee, 1975a, 1980; Stephansson, 1976). Recent aeromagnetic interpretation indicates that the Grong-Olden granites are continuous with the basement of the Baltic shield, suggesting an autochthonous nature (Dyrrelius, 1980).

In the studied area three "basement" units have been recognized (Fig. 6.2):

i) Autochthonous basement; this unit, which outcrops in the central part of the culmination consists largely of alkali-granites and gneisses with an alkali-granitic composition. There are parts in which the rocks have an undeformed appearance, but in most cases the rocks are foliated and at some places mylonites and cataclasites are found (Aukes et al., 1979).

ii) Parautochthonous: a unit consisting of strongly deformed marbles and phyllites, which is thought to represent the original, Cambro-Ordivician sedimentary cover of the autochthonous (Gee and Zachrisson, 1974; Aukes et al., 1979).

iii) Granite-mylonite or Offerdal nappe (Strömberg, 1961), this is interpreted as a basement slice, tectonized and thrust over the autochtonous during the Caledonian orogeny (Gee, 1975 a&b, 1980). Gee (1978) argues that the root zone of this nappe is located West of the present Norwegian coast. Johansson (1981) noted petrographic similarities between the granite-mylonites and the rocks of the Western gneiss region (West coast of Norway). The Granite-mylonite nappe comprises granodiorites, augengneisses

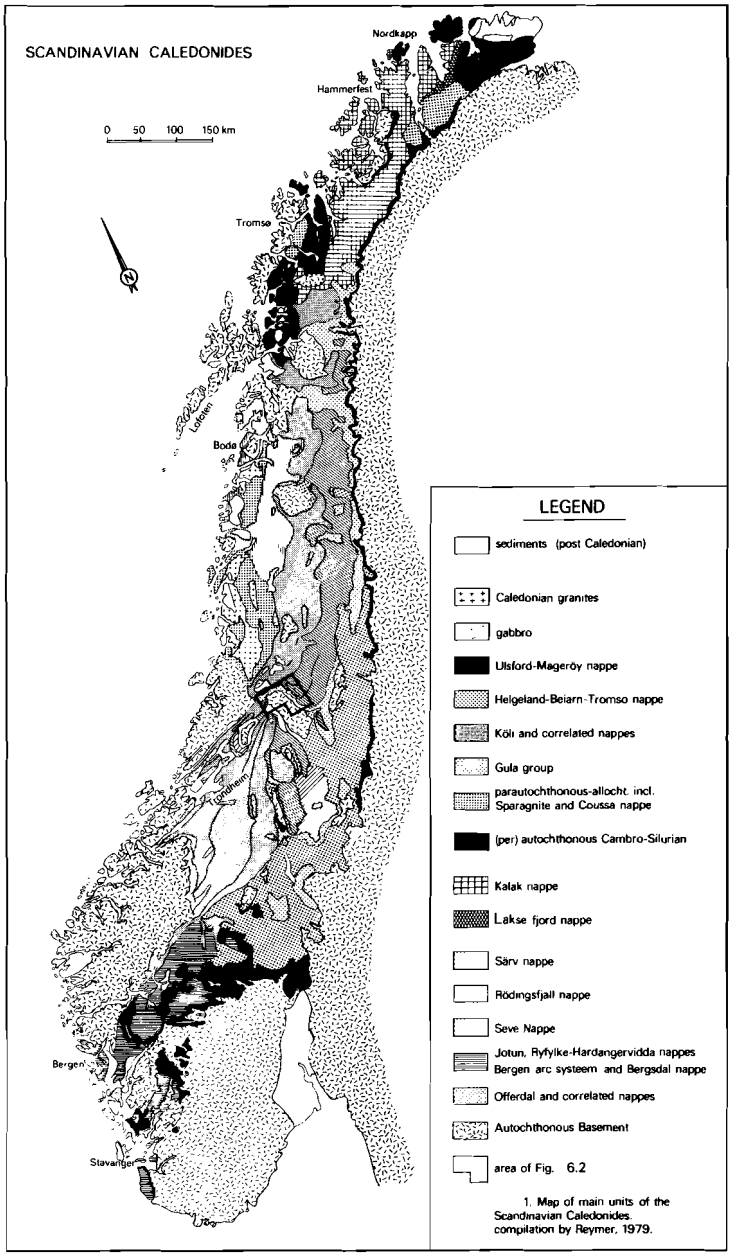

1. Map of main units of the Scandinavian Caledonides. compilation by Reymer, 1979.

Figure 1.2

and mylonites of comparable whole-rock chemical compositions. Mylonites are found throughout the whole rock suite, but they are predominantly found near the contact with the autochthonous. Whole rock age determinations (Rb-Sr) of weakly deformed augengneisses yield values of 1650 ± 50 Ma , whereas phengites from the mylonitic rocks have a Caledonian age: 431±13Ma (Reymer, 1979). Claesson (1980) dated rocks which belong to the Tännas augengneiss nappe, a rock unit which has been correlated with the Granite-mylonite nappe in the presently discussed area (Gee, 1975b; Röshoff, 1978). He arrived at similar results, with this respect that slightly higher ages for minerals in the mylonites are found (475±25 Ma). Both authors conclude that mylonite formation was an (early) Caledonian event. A Precambrian origin as suggested by Råheim et al. (1979) is therefore rejected.

The mylonites discussed in this work are all found in the autochthonous. basement and in the Granite-mylonite nappe. Distinction is made between three types of tectonized granitoids:

- -Banded gneiss: rocks of which the chemical composition is close to alkali-granite; the structure of the rock is a compositional banding of quartz and feldspar rich layers. This rock type is found solely in the autochthonous.
- -Augengneisses: foliated rocks of granodioritic composition, charactarized by megacrysts of K-feldspar in a fine grained mica-rich matrix.
- -Mylonites: well foliated, well lineated fine grained rocks with a chemical composition close to granodiorite.

Augengneisses and mylonites are found in the Granite-mylonite nappe.

The Granite-mylonite nappe is overlain by the Seve and Köli nappes, consisting of meta-sediments and metavolcanics, emplaced during the Caledonian orogeny (Gee, 1975b; Aukes et al., 1979; Kollung, 1979). The relation of internal structures of these nappes with the mylonites of the basement is discussed in this publication.

Cataclasites are found in zones near and at contacts of different rock units, or are cross-cutting these contacts and other (later) structures.

1.5. Tectonic significance of mylonites in the Scandinavian Caledonides.

Törnebohm (1889) presented a theory explaining the structure of the Scandinavian Caledonides as being due to large nappe movement. At present this theory is generally accepted by geologists, although there is still discussion about the extend of nappe structures and distance of transport (e.g. Gee, 1975a; Ramberg, 1977+reply of Gee). Many authors have stressed the relation of mylonites with the emplacement of the nappes (Asklund, 1955; Trouw, 1973; Zwart, 1974; Gee, 1975a; Ramberg, 1977; Point, 1975; Röshoff, 1978; Stephansson, 1977; Cooper, 1981).
In this section the possible formation of mylonites in the Scandinavian Caledonides is discussed in relation with two tectonic models of nappe emplacement.

(i) During their emplacement nappes are relatively rigid blocks or sheets.
(ii) Alternatively, relative displacement of rock units is achieved by internal ductile deformation e.g. by gravity spreading or laterally outflowing diapirs (Ramberg, 1967, 1981; Elliot, 1976), and closely related to this development of fold nappes (e.g. Williams and Zwart, 1977).

ad i) Figure 1.3. illustrates the rigid nappe emplacement model. Clearly such a nappe requires a basal zone of weakness on which transport takes place (Murrel, 1981). Such zones can be original weak materials such as saline or clay horizons (e.g. Behr, 1981), or can be weakened during deformation, notably by grain size reduction to produce mylonites (White, 1977). The tectonic significance of mylonites in this model is rather straightforward: they are zones in which strain took place to accomodate the displacement of relatively rigid blocks.
The deformation history of such mylonites is basically a progressive simple shear, and the sense of shear is consistent with the relative displacement of the blocks. A geologically feasible situation in which such a mechanism of nappe formation could take place is gravity sliding (like décollement thrusts in the pre-Alps, Graham, 1981). Gee (1975a) proposed a tectonic model for the central Scandinavian Caledonides which includes such a mechanism of nappe formation by subduction of the Baltoscandian margin under the Greenland block during continental collision, followed by a stage of décollement type nappe formation.

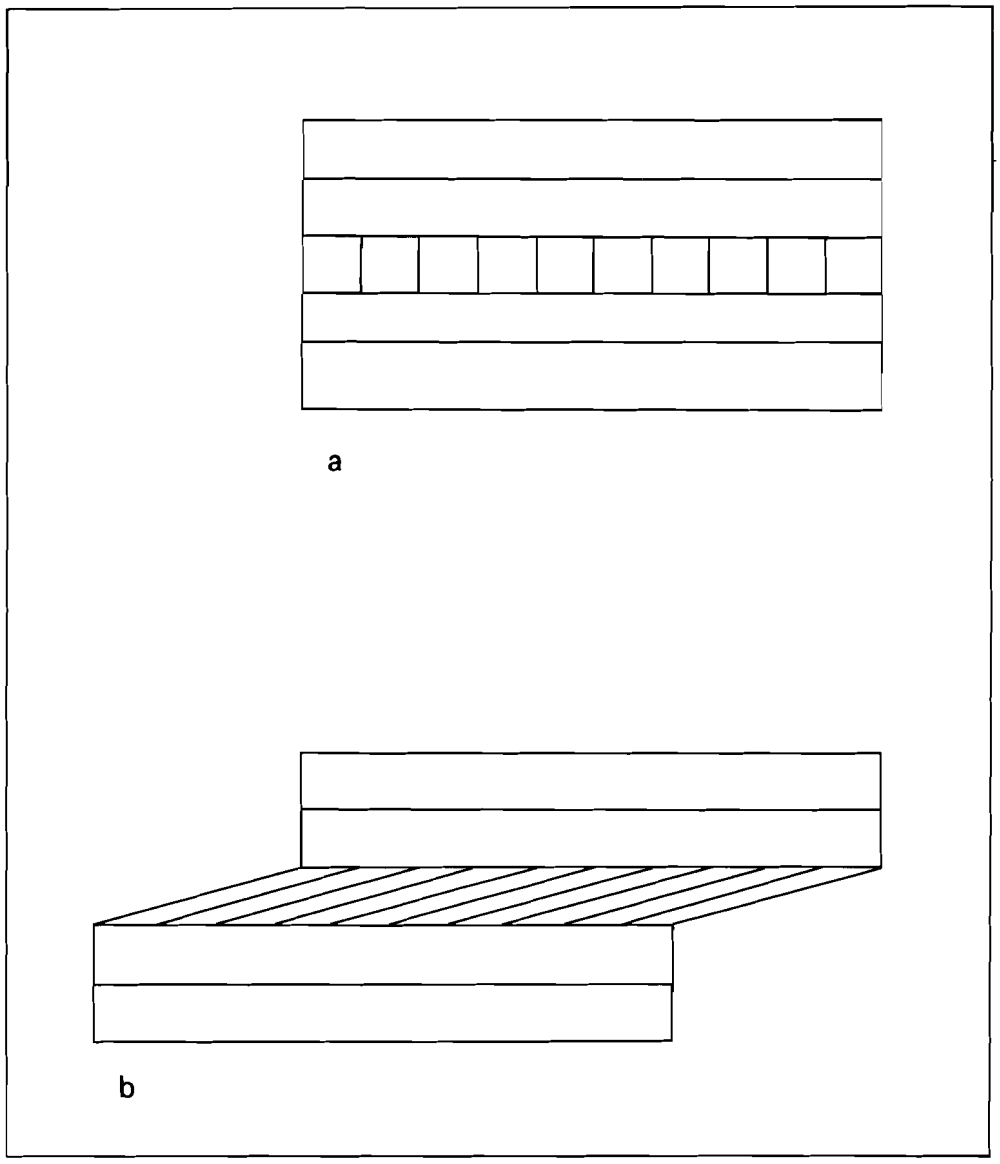

Figure 1.3. Illustration of nappe emplacement by movement of rigid sheets. Fig. 1.3a.: pre-thrusting; Fig. 1.3b.: after thrusting of the upper two layers with respect to the lower by simple shear in the central layer.

ad ii) Figure 1.4 illustrates the ductile nappe model. The relation between nappe emplacement and mylonites in this model is more complicated than in the "rigid block model".

On the basis of experimental data and theoretical studies Ramberg (1981) constructed a profile showing the deformation of an initially rectangular body (Fig. 1.4a) after a certain amount of gravity spreading while at the base coherency is retained (Fig. 1.4 b). Due to increasing load the rate of flow will gradually increase from the top layer to lower levels of the body, until at a certain level the line of maximum flow is reached. From this level downward the amount of flow decreases due to the influence of the basal friction. The differential flow is associated with a shear strain, the sense of shear above and below the level of maximum flow being opposite.
Whether or not mylonites will develop in a nappe which behaves accordingly depends on the position of the line of maximum flow. If this line is located relatively high in the profile there is no zone in which the strain reaches extremely high values relative to the bulk, hence no mylonites will be formed. If the level of maximum flow is relatively low the volumes of material between this and the base undergo a shear strain which exceeds strain values in the bulk and mylonites may develop. The strain history of this mylonites will be approximately a progressive simple shear, the sense of shear being consistent with the direction of relative movement of the spreading body, but opposite to the sense of shear in the bulk. Figure 1.4c illustrates a spreading body on a frictionless base. In this case within the entire body the material will undergo a shear strain of which the sense of shear is opposite to the direction of relative movement.

Ramberg (1967, 1977, 1981) argues that nappe formation in the Scandinavian Caledonides may have taken place by diapirism of granitic basement in the core of the orogen and subsequent outflow of the rocks by gravity spreading. Williams and Zwart (1977) and Gee (1978) presented tectonic models which include the late stage gravity spreading mechanism of nappes, but propose that the initial high is not caused by diapirism but by crustal thickening due to continental collision.
So the study of the involvement of the autochtonous basement in the orogeny and the relation of structures in the basement to those in the overlying

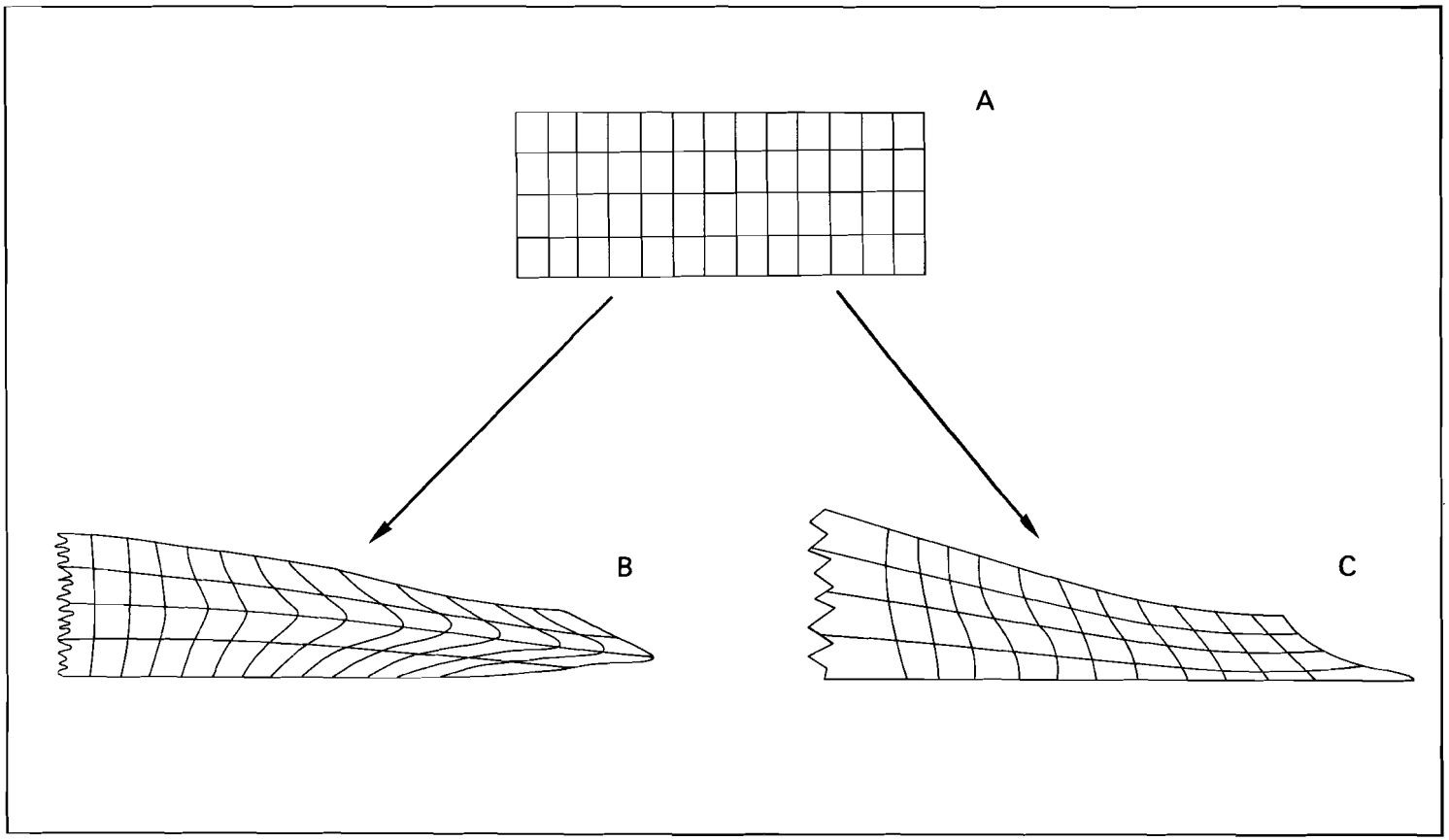

Figure 1.4. Illustration of nappe emplacement by gravity collapse of an initial rectangular body ("A"). "B": at the base of the collapsing body coherency is retained, "C": the base of the collapsing body is frictionless.

nappes is an important problem. Due to a deep erosion level basement-cover relations can be studied directly in a number of windows (Fig. 1.2). These windows are basement domes which are formed either by diapirism or by lateral compression in which case they would represent the cores of large antiforms.

Diapirism involves vertical movement of the basement with respect to the cover, which may provide an alternative cause for the formation of mylonites. Stephansson (1977) studied the structural relations of basement and cover at the eastern edge of the Olden dome in Sweden and concluded that both diapirism and thrusting caused formation of mylonites; he was however not able to distinguish between the contribution of either process in the deformation history of the rocks.

The present study also deals with this problem. Structural relations indicate that both vertical and horizontal movements took place. Micro- and mesostructures provide information on the relative contribution of either process. These matters are discussed in chapter 6.

CHAPTER II CRYSTAL GROWTH IN CATACLASTIC BASEMENT GRANITES, DIAGNOSTIC MICROSTRUCTURES AND STRUCTURAL IMPLICATIONS.

2.1. Introduction.

The autochthonous basement outcrops in the core of the Grong culmination. Typically the rocks are pink coloured, leucocratic, relatively coarse grained granitoids and gneisses (grain sizes 0.5-1cm). The mineralogical composition is rather uniform throughout the rocksuite: ca. 50 vol.% alkali feldspar and ca. 50 vol.% quartz, accessoria are chlorite, epidote, ore (predominantly haematite), rutile, sphene and calcite.
The whole-rock chemical composition of 12 samples is given on a Streckeisen diagram (Fig. 2.1); all samples fall within the fields of alkali-granite and syenite.

In chapter 1 the pre-Caledonian history of the rock unit is discussed. The present chapter deals with deformation-induced microstructures which are probably of Caledonian origin. The large scale tectonic history and setting of the unit are discussed in chapter 6.

Predominantly at the northern and eastern rim of the basement, near the contacts with higher units, relatively narrow planar zones (width varying from 10-100 m) are found in which extremely fine grained, predominantly red coloured (occasionally green coloured), not foliated rocks are found. The rocks are composed of a flint-like ground mass in which angular rock-fragments float (Fig. 2.2), the size of these fragments varies from 0.5-5cm. Feldspar fragments contain numerous microcracks which are stained by fluid inclusions, clay minerals and haematite particles. Haematite is also found in the flinty ground mass, it causes the red colouring of the rocks.
Throughout the zones there is ample evidence for hydrothermal activity. For instance there is extensive quartz-veining at some localities (Fig.2.3), and occasionally microstructures which indicate replacement of feldspar by epidote-group minerals (saussuritization) have been found.
The occurrence of numerous microcracks throughout the rocks, the angular shape of the rock fragments, the presence of veins and the absence of a

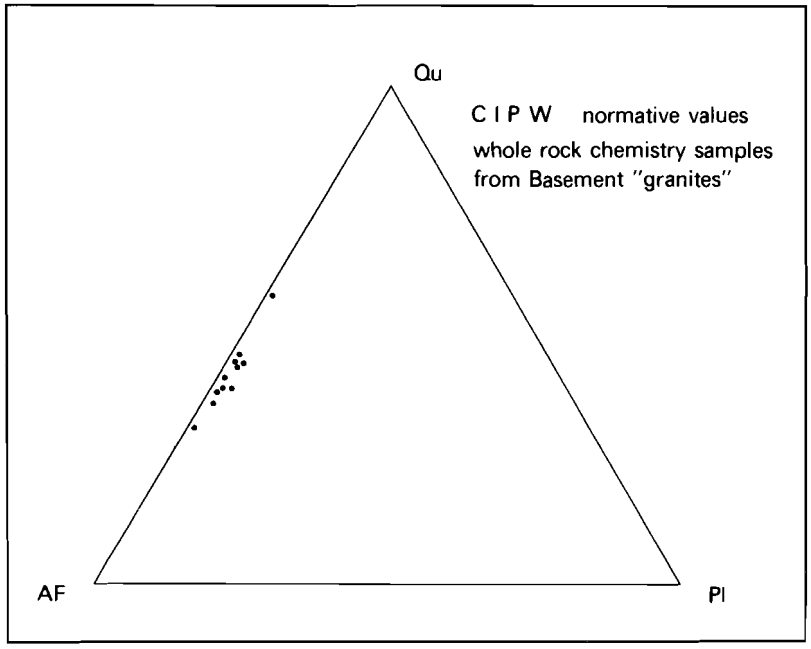

Figure 2.1. CIPW normative values of whole rock chemistry of 12 samples from the authochthonous. Qu= quartz; AF= alkali feldspar; Pl=plagioclase.

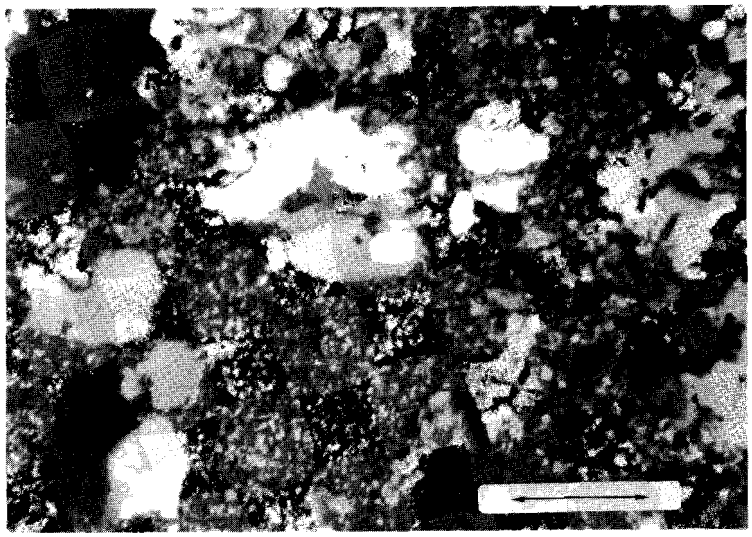

Figure 2.2. Micrograph of cataclasite showing relatively large crush-fragments in a fine grained matrix. Note absence of foliation. Crossed polarizers. Scale bar: 1mm.

Figure 2.3. Outcrop near Sandøla. Quartz veins in flinty cataclasite. Two directions of veining are indicated.

a foliation indicate that the rocks underwent predominantly brittle deformation. Figure 2.4 is an example of a microstructure formed by brittle deformation; a microfault with offset of a quartz vein.

Whole-rock chemistry of cataclasites devoid of veins is similar to that of the country rock. Heavily veined specimens show quartz-enrichment relative to the country rock (see appendix, table 1).

2.2. Cataclasites.

Recent work on faulting and the products of faulting has been carried out because of interest in modern and ancient seismic processes (Scholz et al., 1972; Friedman et al., 1974; Rutter and White, 1979). The presently discussed zones allow examination of brittle processes at shallow levels (upper crust).

The microstructure of the rocks suggests that there are several processes active in relation with the movement of the faults. Intensive cracking has taken place on mesoscopic and microscopic scales. Most cracks have been opened and may contain crushed feldspar and other rock fragments. The brittle processes have been accompanied by plastic deformation of some minerals, especially quartz, which in some cases shows undulose extinction, deformation bands, deformation lamellae and incipient grain boundary recrystallization.
In the cracks there is clear evidence that crystal growth has occurred, possibly in relation with partial solution of brittly deformed material. Figure 2.5 shows a TEM photograph of a corroded surface of a quartz grain covered with clay minerals which were possibly formed in situ. The microstructures indicate activity of a fluid phase during or after a cataclastic event. A fluid phase plays an important role in the behaviour of rocks undergoing brittle deformation, it facilitates the initiation of cracks by lowering the surface energy by hydrolysis of broken Si-O bonds and it allows diffusional processes which assist grain boundary sliding in the faulted material (Paterson, 1978; Fyfe et al., 1978; Rutter and White, 1979). Secondly, fluids play an important role in the healing of cracks, by allowing crystal growth. It is not difficult to imagine ongoing deformation in a rock in which interaction of brittle processes, crystal growth and eventually plastic deformation takes place. Dieterich (1978), Ramsay

Figure 2.4. Micro-cataclasite (black, running approximately N-S). Note offset of quartz vein. Crossed polarizers. Scale bar: 1mm.

Figure 2.5. TEM photograph showing corroded quartz grain (q) overlain by clay mineral. Scale bar: 0.2um.

(1980) and Augevine et al. (1982) have described such processes. It is of critical importance to evaluate the role of growth processes during the deformation of rocks. For this reason the microstructures in the cataclasites have been investigated by means of optical microscopy, cathode luminescence and transmission electron microscopy (TEM). It was attempted to find diagnostic microstructures which indicate crystal growth in free space, in order to separate these from those which are formed by solid state recrystallization.

2.3. Microstructures related to crystal growth.

a) Optical microscopy.

In most specimens there are domains in which the old granitic microstructure can still be recognized (see Fig. 2.6, near "A"). Microcline crystals show perthitic exsolution and cross-hatching twins (albite and pericline), microstructures which are typical for alkalifeldspars in granites (see Ch. 4). In these domains feldspar and quartz grains are fragmented by microcracks in which fine-grained aggregates of haematite, clay minerals, feldspar fragments and quartz crystallites are found. The width of the cracks is rather variable (0.1mm - 1cm). The microstructure of specimens which contain a dense network of relatively broad cracks filled with fine-grained material can be described best as "rock fragments floating in a flinty matrix". Transitional to the fine-grained polycrystalline domains are zones composed of quartz crystallites. Fine-grained quartz aggregates may be transitional to coarse-grained, strain-free quartz grains (Fig. 2.6, near "B"). In some cases, as is illustrated by figure 2.7, there is evidence that the larger grains have grown in free space, since they occur with euhedral terminations in vug-like structures. Large euhedral grains often have inclusion trails which are defined by haematite particles, tiny mica flakes and fluid inclusions parallel to crystallographic planes (Fig. 2.8). In some cases, as is shown on Fig. 2.7 and 2.8, euhedral crystals are associated with chalcedony aggregates.

b) Cathode luminescence.

Cathode luminescence microscopy has proved to be a useful technique in visualizing overgrowth structures in sedimentary rocks, volcanites and in granitoids (Zinkernagel, 1978). Four thin sections of the presently discussed cataclasites have been examined by using this method in order to

Figure 2.6. Microstructure of cataclasite. Near "A" a relatively coarse-grained relict of granite. Near "B" the fine grained quartz in the matrix is transitional to coarser grains in a vein-like structure. Crossed polarizers. Scale bar: 1mm.

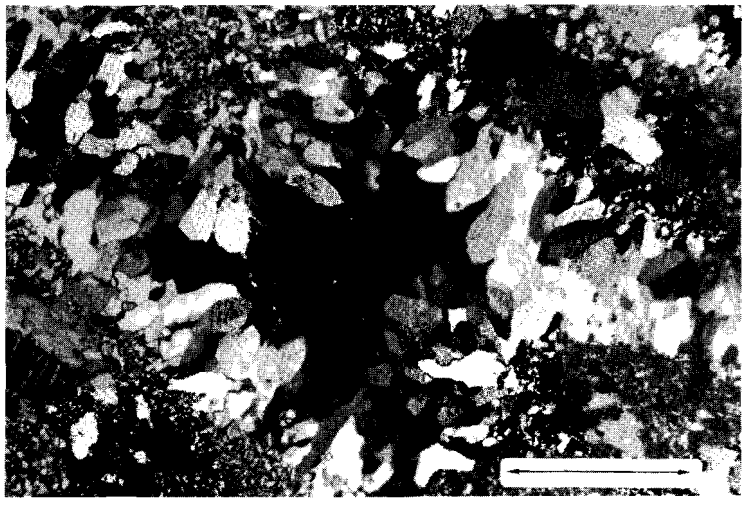

Figure 2.7. Coarse-grained euhedral terminated quartz crystals in vug-like structure which is filled with crypto-crystalline quartz. Crossed polarizers. Scale bar: 0.2mm.

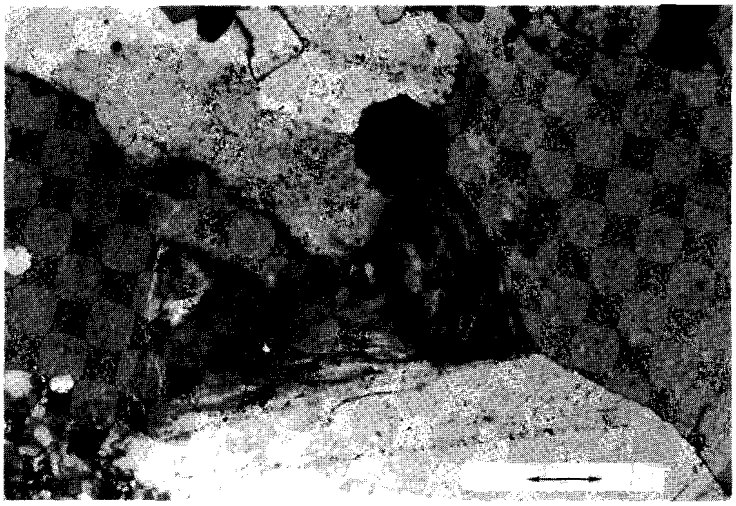

Figure 2.8. Inclusion trails parallel to crystallographic planes in euhedral terminated quartz crystals. Note fibrous chalcedony aggregate in "void". Crossed polarizers. Scale bar: 0.2 mm.

examine the growth induced microstructures. For the euhedral grains it was possible to correlate the luminescence characteristics directly with "normal" optical microscopy. As is shown on figure 2.9a bands which are characterized by different intensities of luminescence are found parallel to crystallographic planes of the crystal. This phenomenon is typical for all hydrothermally grown quartz (Zinkernagel, 1978). In optical microscopy the same crystal shows a similar type of banding which in this case is caused by small crystallographic misorientations (Fig. 2.9b).
Deformed quartz grains in flattened veins show no banding by cathode luminescence, instead they demonstrate a dull yellow colour, evenly distributed through the grains.
In optical microscopy also no banding was observed in these grains.

Zones rich in extremely fine grained quartz aggregates reveal in cathode-luninescence a surprising structure compared with optical microscopy (Fig. 2.10a and b). The individual grains were not resolved in cathode luminescence but a coarser structure encompassing many grains has been revealed. This structure is characterized by a concentric banding which is caused by differences in luminescence coulour. The interpretation of this structure is not straightforward. It resembles an agate-type banding which can be caused by a compositional layering produced by rhytmic precipitation from a silica gel (Webster, 1970).
Note also that small feldspar fragments (bright spots on Fig. 2.10b) are embedded in the fine crystalline quartz.

c) Transmission electron microscopy(TEM).
Ion-thinned specimens of euhedral grains and of fine grained material from the matrix of the cataclasites, as well as samples from deformed quartz grains were examined with a JEOL 200C transmission electron microscope operating at 200 kV.

A typical microstructure of the euhedral quartz crystals is a narrow banding (ca. 0.2 µm in width) which runs parallel to rhomb and prism planes (Fig. 2.11). The bands are characterized by small contrast differences. They are bounded by narrow zones along which electron beam damage occurs rapidly, giving rise to a cross hatching pattern (Fig. 2.12). Similar types of damage structures have been described by Rutter and White (1979) in overgrowth structures in experimentally produced fault gouges. In

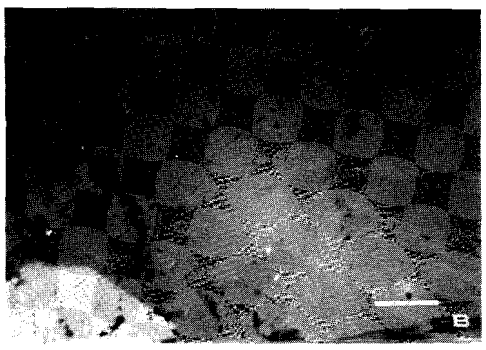

Figure 2.9a Cathode-luminescence micrograph of euhedral quartz grain, showing bands of intense luminescence parallel to crystallographic planes.

Figure 2.9b Same crystal , normal microscopy, showing similar outline of banding due to small crystallographic misorientation. Scale bar: o.4mm
Photographs by Dr. U. Zinkernagel

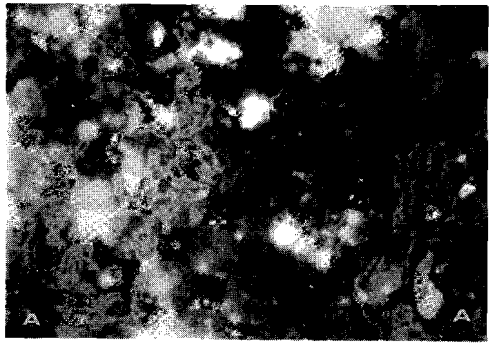

Figure 2.10a. Cathode-luminescence banding showing an agate-type bamding in fine grained quartz aggregate. Bands are defined by differences in luminescence colour.

Figure 2.10b Idem, optical microscopy.
Scale bar:0.4mm
Photographs by Dr. U. zinkernagel

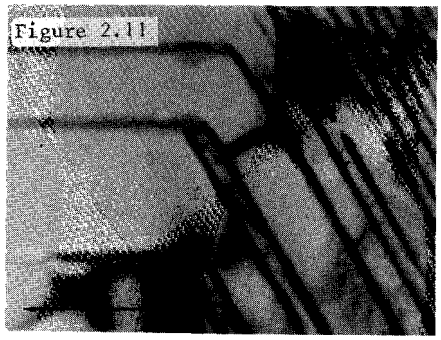

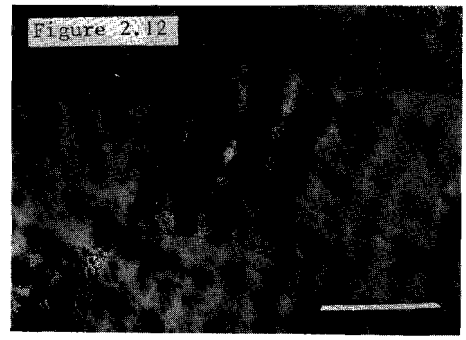

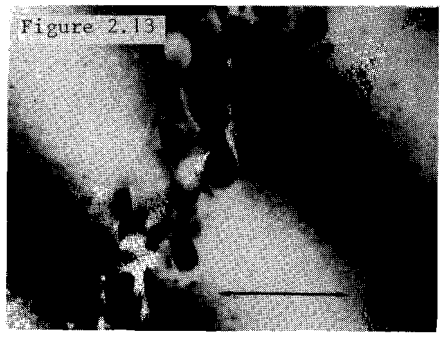

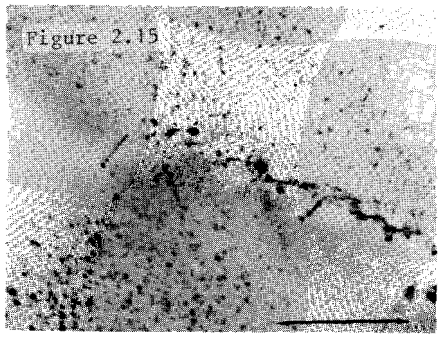

Figures 2.11-2.16 are TEM micrographs of quartz crystals from cataclasites.

Figure 2.11 Growth banding in euhedral quartz crystal, the bands are parallel to prism planes. Scale bar: 0.2 μm

Figure 2.12 Idem, banding parallel rhomb planes. Scale bar: 0.5 m

Figure 2.13 Growth band boundary showing the association of dislocations and bubbles. Scale bar: 0.2 μm

Figure 2.14 Closely spaced growth bands with bubble trails. Scale bar: 0.2 μm

Figure 2.15 Absence of growth structures in deformed quartz. Scale bar: 0.1 μm

Figure 2.16 Hexagonal growth-band pattern in quartz crystallite. Scale b.:0.2 μm

some cases, as is illustrated in figure 2.13 the growth band boundaries could be identified as dislocation arrays decorated with bubbles (see also Fig. 2.14).
Even in slightly deformed quartz grains such a type of banding is absent (Fig. 2.15), so it is thought to be a characteristic growth feature for undeformed crystals only.

The matrix of the cataclasite contains quartz crystallites. The microstructure of the crystallites is similar to that of the euhedral grains. There are bands parallel to crystallographic planes, due to the smaller grain-size many more orientations are present in a sample and complete hexagonal patterns could be visualized (Fig. 2.16). In these too there is a close association of growth band boundaries and bubble trails.

Discussion.

In optical microscopy the euhedral quartz crystals show banding which is defined by inclusion trails parallel to crystallographic planes. As the inclusions are partly solid (mica flakes, haematite particles) it is likely that they are primary and that the inclusion trails may delineate growth surfaces. Parallel to these bands there is a banding which is caused by small crystallographic misorientations (ca. 1° misfit). This banding can be directly correlated with bands visualized by cathode luminescence intensities. This feature has been reported only for hydrothermally grown quartz crystals (Zinkernagel, 1978). The origin of the luminescence banding lies in the distribution of impurities (Nickel, 1978) or lattice defects (Zinkernagel, 1978). As shown above, the luminescence bands can be correlated with dislocation arrays associated with bubbles, so there seems to be a correlation between lattice defects as well as impurity content with luminescence intensity.
In transmission electron microscopy similar types of banding have been observed. These bands show small image contrast differences due to orientation variation from one band to the other, and they are bounded by dislocation arrays in which bubbles are found. Both features can be correlated with microstructures found in optical microscopy. The growth structures reported by Nassau and Prescott (1978) and Yoshimura et al.(1979) in synthetical grown crystals and the striations parallel to growth surfaces

in quartz fibers (Frondel, 1978) might be compatible with the presently described substructure.
The origin of growth banding in quartz may be diverse. Yoshimura et al. (1979) reported growth sectors which are defined by small compositional changes, which induce lattice distortion; variations in the amount of structurally bound water have been demonstrated by Brunner et al. (1959) and Bambauer (1961). In chalcedony growth banding may be caused by twins (Miehe et al., 1984).
The present study shows that in the quartz crystals bubble trails occur in bands parallel to growth surfaces. This suggests that the observed banding could be due to periodic water concentration variations. Also the damage pattern induced by the electron beam in TEM indicates such a variation as this process appears to involve a reaction of impurities with structurally bound water (Stenina et al., 1984).
Because the microstructures are found solely in crystals grown in free space and are absent in plastically deformed and recrystallized quartz, it is concluded that they are diagnostic for growth. Because the microstructure of the quartz crystallites in microcracks and in the matrix of the cataclasites is identical to that of the euhedral grains, it is concluded that they also have grown from a fluid phase in free space. It appears that the crystallites have grown in a fluid-filled network of cavities, thus cementing the crushed fragments formed during cataclasisis. Given that the crystallites and large euhedral grains grew from a fluid, it follows that the observed transition from the former to the latter (Fig. 2.6) could represent a crystallization sequence. Such a sequence is reported from crystallization experiments of a silica gel (Oehler, 1976). The presence of colloidal fluids in the rocks is also suggested by the occurrence of fibrous chalcedony aggregates (Fig. 2.7) and by the agate-type growth band pattern viewed in the crystallite zone with cathode luminescence.
Crystallization of colloidal fluids in microcracks will lead to volume decreases in the faulted material because of the loss of water, and the resulting contraction will provide space for the growth of euhedral quartz in vein-like structures.

All the growth quartz described above is undeformed and thus could be interpreted as late stage structures. However, there are relatively old

veins the formation of which could be equivalent to those described above, but these have been progressively plastically deformed, as illustrated in figure 2.17. The grains become undulose and contain deformation bands and lamellae and incipient grain boundary recrystallization occurs as well. These features normally accompany plastic deformation (e.g. Hobbs et al., 1976; Nicolas and Poirier, 1976). As a result of this deformation the veins are flattened and rotated towards parallellism and produce a foliation. Flattened veins are transected again by cracks in which crystal growth has occurred to produce a new vein (Fig. 2.18).
Crystal growth processes apparently have operated during the early stages in the deformation history of the faults. The process of repetitive operation of brittle deformation, crystal growth, plastic deformation followed by brittle deformation, and so on, can be interpreted to indicate periodic stress release, a phenomenon which is prominent in modern seismic zones and which is attributed to a stick-slip behaviour (Scholz et al., 1972). The present study however shows that periodic stress release can be the result of a more complicated process, involving the restoration of fault surfaces by crystal growth (cf. Augevine et al., 1982).

2.4. Basement gneisses.

The interpretation of the microstructure of the cataclasites is used to explain the microstructure of the basement gneisses.
The foliation of the gneisses found in the basement is defined by an alternation of quartz-rich versus feldspar-rich bands, such as shown in figure 2.17. The quartz-rich bands show microstructures indicative of crystal-plastic deformation. Feldspar-rich bands are characterized by structures induced by brittle deformation, old perthitic alkali feldspars have been boudinaged, in the pressure shadows a new generation of alkali-feldspars has grown. These new phase differ from the older granitic alkali-feldspars because they are end-members in composition (pure $NaAlSi_3O_8$ and $KAlSi_3O_8$) and show no exsolution structures. It is interpreted that the growth of these phases took place at relatively low temperatures (greenschist facies conditions, see Ch. 4).
It is suggested that this type of compositional banding was formed by flattening and rotation of quartz veins during which process the feldspar crystals behaved brittly by undergoing boudinage.
It is thought that the quartz veins in the gneisses are analoguous to those

Figure 2.17. Progresively (from left to right on the picture) plastically deformed quartz vein. In the deformed part occurrence of deformation lamellae and incipient grain boundary recrystallization. Crossed polarizers. Scale bar:1mm.

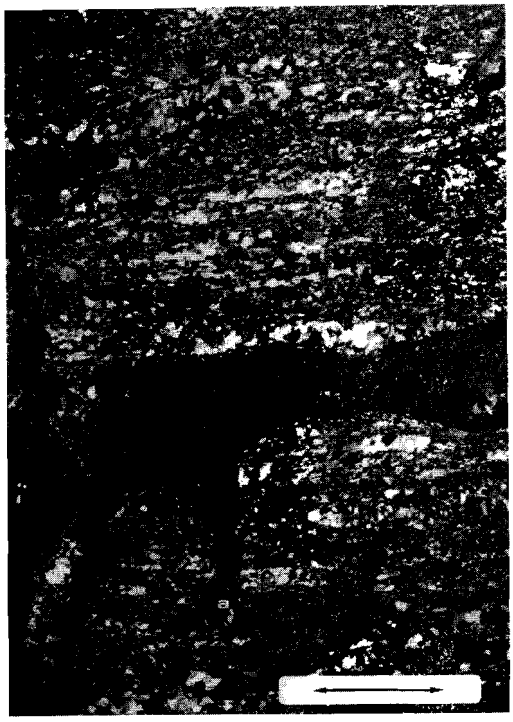

Figure 2.18. Micrograph of banding in gneiss formed by flattened quartz veins (running E-W). At "a" a new generation of crystallite-filled cracks crosscuts the foliation. Crossed polarizers. Scale bar:1cm.

in the cataclasites, i.e. that they were formed by crystal growth in (micro)faults.

2.5. Conclusions.

In microcracks in cataclasites the growth of silica minerals from a fluid phase took place, the crystallization products vary from chalcedony aggregates to large euhedral quartz crystals. Transitional relations of chalcedony with quartz crystals suggest that growth occurred from colloidal fluids. The investigated crystallization products represent growth in cracks formed in the latest stages of the deformation history.
A diagnostic microstructure for growth of quartz in free space is a narrow banding parallel to crystallographic planes, the boundaries of the bands are dislocation arrays associated with fluid inclusions.
Deformed veins indicate that in the deformation history of the rocks plastic deformation followed crystal growth. Plastically deformed veins are themselves brittly deformed, providing space for further crystal growth growth. In the history of these fault zones this cycle of brittle deformation, crystal growth and then crystal-plastic deformation appears to be repetitive.

CHAPTER III. THE TEXTURAL DEVELOPMENT OF MYLONITES FROM THE GRANITE-MYLONITE NAPPE.

3.1. Introduction.

The Granite-mylonite nappe (Asklund, 1960), which has been correlated with the Offerdal nappe (Gee, 1974; Reymer, 1979; Aukes et al., 1979) overlies the autochthonous basement directly in the northern and north-eastern edge of the Grong culmination. The thin veneer of parautochthonous Paleozoic meta-sediments separating the autochthonous from the Granite-mylonite nappe at the southern rim is encountered only locally (Aukes et al. 1979; Gee, 1980). The Granite-mylonite nappe comprises (foliated) granodiorites, augengneisses and mylonites. Whole rock chemical compositions of 17 samples of this rock unit are given in table A2 (appendix). Mean values are given below. Notwithstanding some variation in chemistry, these rocks can be distinguished as a group from the rocks of the autochthonous basement by relatively low contents of SiO_2 (61 vs 78%), high Al_2O_3 (16 vs. 11%), high FeO (4.5 vs. 0.5%), high MgO (2.3 vs. 0.2%) and high CaO (5 vs. 0.4%). The difference in chemistry is reflected in the mineralogy: rocks of the Granite-mylonite nappe contain a considerable amount of biotite and chlorite, Ca-bearing plagioclase and epidote-group minerals, all these are lacking or accessory in the autochthonous basement granites.

CIPW norms of all the measured samples plot in or next to the granodiorite field in a Streckeisen diagram, see Fig. 3.1.
Aukes et al. (1979) argued that the occurrence of the different rock-types is due to a heterogeneous strain distribution imposed by nappe formation in an originally more or less homogeneous igneous rock. This chapter is an account of the study of microstructures of rocks showing textural relations from plutonic to mylonitic. The Granite-mylonite nappe contains lense-shaped pods of relatively weakly or non-foliated rocks displaying an igneous texture. Locally within these pods shear zones are developed in which the rocks display textures gradational from igneous at the rims to mylonitic in the central parts. The study of the development of mylonitic textures in shear zones is a widely applied approach in structural geology since the classic paper of Ramsay and Graham (1970) which deals

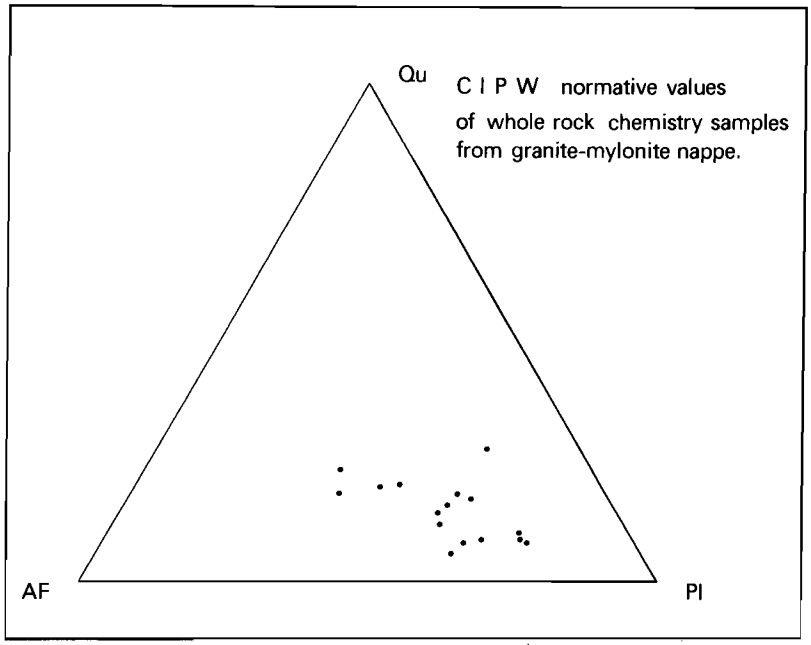

Figure 3.1. Plots of CIPW normative values of whole-rock chemistry of 16 samples from the Granite-mylonite nappe on a "Streckeisen" diagram.

with the strain distribution in such structures (Carreras et al., 1980). The presently described shear zone is located in an exposure 1 km south of Nordli (see Fig. 6.2).

3.2. Relation of meso- and microstructures in the shear zone.

Figure 3.2 is a drawing of the studied shear zone. Three structural domains have been distinguished, each showing specific mesoscopic and microscopic structures:

Domain A consisting of coarse grained, non-foliated rocks

- B in which the rocks contain a widely spaced foliation
- C displaying a fine grained, well foliated and lineated rock-type.

The chemical compositions of rocks from the different domains are similar (table A2).

The mineral composition of rocks found in domain A is plagioclase (ca. 35 vol.%), alkali feldspar (ca. 5-10 vol%), biotite (ca. 30 vol.%), epidote-group minerals (ca. 15 vol.%) and quartz (ca. 10 vol%); accessories are rutile, sphene, zircon and orthite. Feldspar minerals and biotite aggregates define irregularly outlined domains. Feldspar-rich volumes contain predominantly subhedral plagioclase crystals (Ø 2-10 mm) displaying development of prism planes and polysynthetic twinning (albite twins). Microprobe analyses reveal ca. 30% An. Various stages of alteration to white mica and epidote group minerals were observed. In some specimens irregularly outlines blebs of alkali-feldspar (Ø ca. 5mm) are found which display "flame perthitic" intergrowth structures (Smith, 1974) and locally crosshatch twinning in the K-feldspar phase. These perthites are rimmed by pure albite (width of the rims ca. 1mm).

Most feldspar-rich area's contain quartz blebs (Ø 3-5mm) which display undulose extinction.

Biotite-rich domains are composed of aggregates of brown-pleochroic biotite in a decussate arrangement (Vernon, 1974). Biotite often includes rutile needles, sphene, zircon and epidote.

Locally anhedral green pleochroic hornblende crystals are found in the biotite-rich volumes.

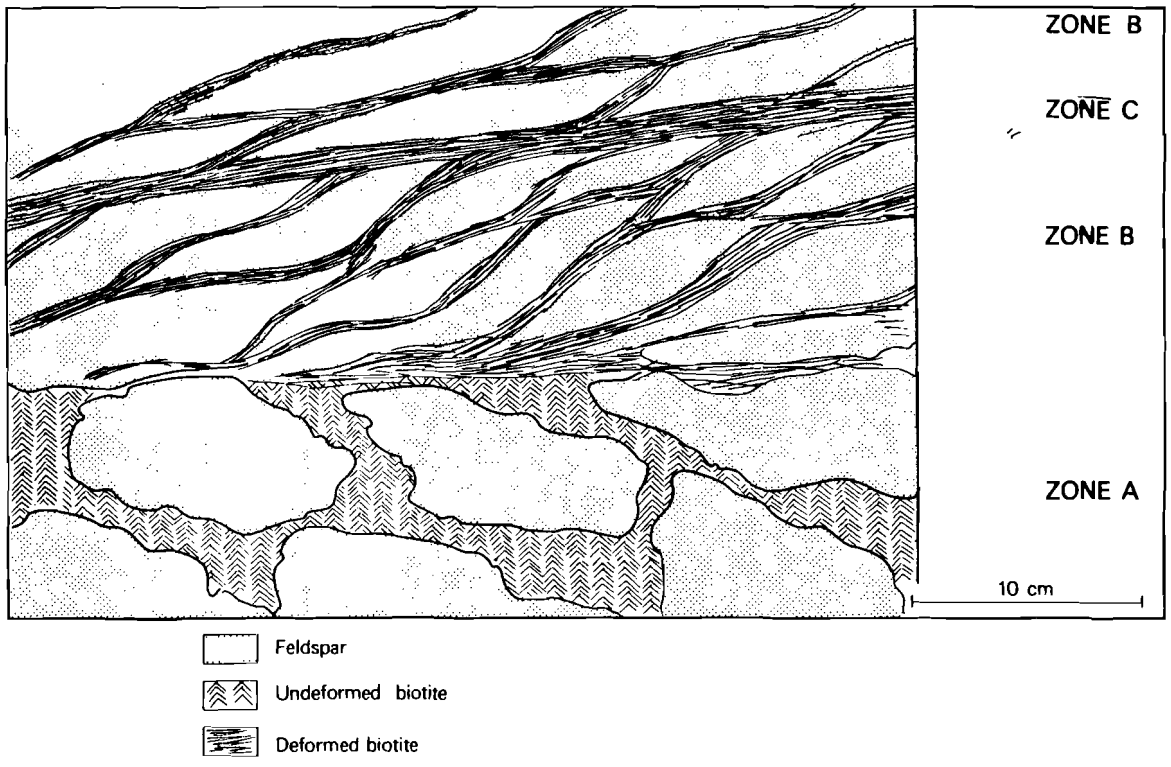

Figure 3.2. Sketch of shear zone in granodiotite. Zone A: relatively undeformed rock. Zone B: development of shear band cleavage by deformation of mica-rich domains; Zone C: band in which both feldspar and biotite are strongly deformed.

The texture of the feldspar-rich domains is typically igneous: subhedral plagioclase with interstitial anhedral quartz and alkali feldspar (Fig. 3.3) reflecting a crystallization sequence (Turner and Verhoogen, 1960). Subsolidus reactions modified the igneous texture, in alkali feldspars this is manifested by flame perthite due to exsolution and twinning of microcline by an ordering reaction (see also Chapt. 4). These processes are induced by cooling or later alteration (predominantly of plagioclase) by incipient retrogressive metamorphism.

The interpretation of the texture in the biotite-rich area's is not unambiguous since decussate aggregates may be interpreted as impingement structures due to growth or as grain boundary adjustment textures of highly anisotropic minerals (Vernon, 1976). Sagenite is thought to be a result of release of Ti by retrogressive metamorphism (cf. Miyashiro, 1973).

Rocks from domain B are affected by metamorphism and deformation and show an incipient foliation, predominantly in biotite-rich area's. Large biotite crystals are folded or kinked with crystallographic misorientations in kinks of approximately 20°, folds may be open, tight or isoclinal. Kinkband boundaries are oriented at large angles to (001), the dominant slip plane in micas (Bell, 1979; Bell and Wilson, 1981), in most cases they are decorated by aggregates of rutile and sphene (Fig. 3.4). This mineral association is also found at grain boundaries in deformed biotite aggregates. Locally epidote is found at such sites; it seems to have grown into the biotite. Grain boundaries and cleavage planes of biotite are decorated by opaque material. The relative amount of biotite vs. epidote+sphene+rutile+opaques in deformed regions varies from 9:1 to 1:1.

Locally there are aggregates of chlorite exhibiting a typical biotite-microstructure: decussate arrangement of the grains, a sagenite structure and occurrence of sphene and rutile at grain boundaries. This microstructure is interpreted as a pseudomorph of chlorite after biotite.

An incipient foliation is defined by irregularly spaced bands of 1-5 mm in width, composed of fine grained epidote, sphene, rutile (and occasionally chlorite and green biotite). These bands run approximately parallel to the trend of the shear zone. They may abut coarse grained, relatively undeformed biotite aggregates (Fig. 3.5). Since the mineral association in

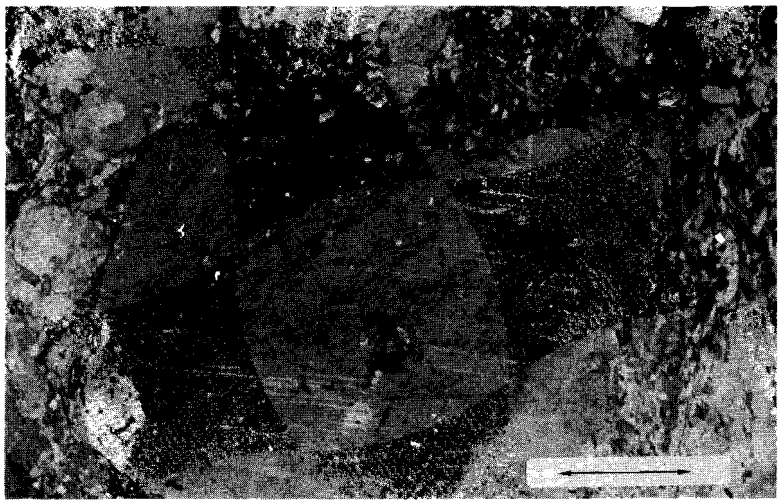

Figure 3.3. Micrograph of subhedral plagioclase crystal in relatively undeformed granodiorite. Crossed polarizers. Scale bar: 0.5mm.

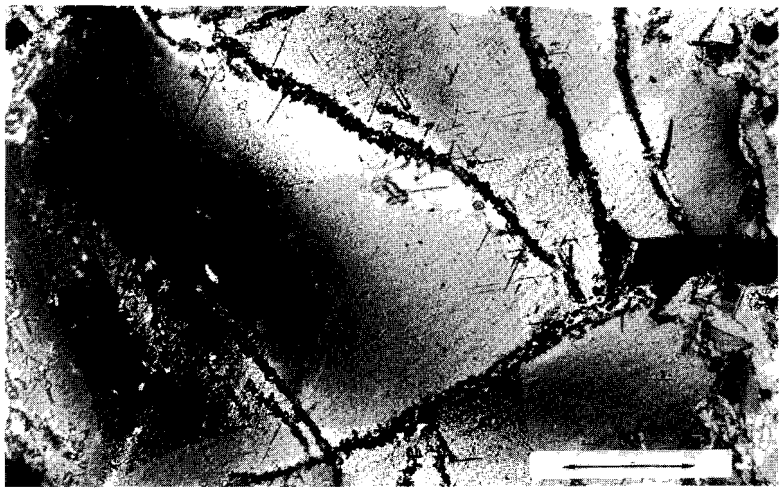

Figure 3.4. Kinked biotite with oriented rutile needles (sagenite). At kink band boudaries and cracks (as on this photograph) concentration of rutile, sphene and epidote. Plane of the photograph is parallel to the basal plane of biotite. Crossed polarizers. Scale bar: 0.2 mm.

these bands is similar to that found at kinkband and grain-boundaries of deformed biotite (aggregates) a genetic relation is suggested. The locally high relative amount of Ti-bearing minerals with respect to the amount of biotite suggests the operation of non-conservative processes: breakdown of biotite and subsequent selective transport of elements. The newly formed mineral association rutile+sphene+epidote would indicate loss of K and introduction of Ca in these regions (see also Chapt 5). Beach (1979, 1980) and Kerrich et al. (1980) described similar microstructures in biotites and attributed them to the operation of pressure solution and stress corrosion cracking. It is however difficult to discriminate between microstructures which originated by pressure solution and those formed by deformation-enhanced solution of an unstable phase.
The spaced bands of rutile+ sphene+epidote+opaques are thus interpreted as deformed biotite aggregates which were completely altered by solution and redeposition of elements.

Plagioclase crystals show further alteration to epidote-group minerals and white mica; these alteration products are also found in schlieren parallel to the foliation. This microstructure suggests transformation induced ductility (Beach, 1980).

Quartz shows grain boundary recrystallization and occasionally polygonization (White, 1977), producing elongate domains which contribute to the foliation.

The rocks of domain B become better foliated near the center of the shear zone; bands of sphene, rutile and epidote and those of white mica and epidote are found as more regularly spaced discontinuities. At this stage a second foliation oblique to the former is found (Fig. 3.6). This foliation can be described as a regularly spaced set of minor shear zones as older structural elements are progressively rotated and deformed. White et al. (1980) and Platt and Vissers (1981) described similar structures in mylonitic rocks and called them shear band cleavage or extensional crenulation cleavage. The formation of the structure is attributed to foliation boudinage due to strength anisotropy of a layered rock. The occurrence of one set of shear bands is thought to be indicative of a deformation approximating a simple shear (a conjugate set may indicate pure shear).

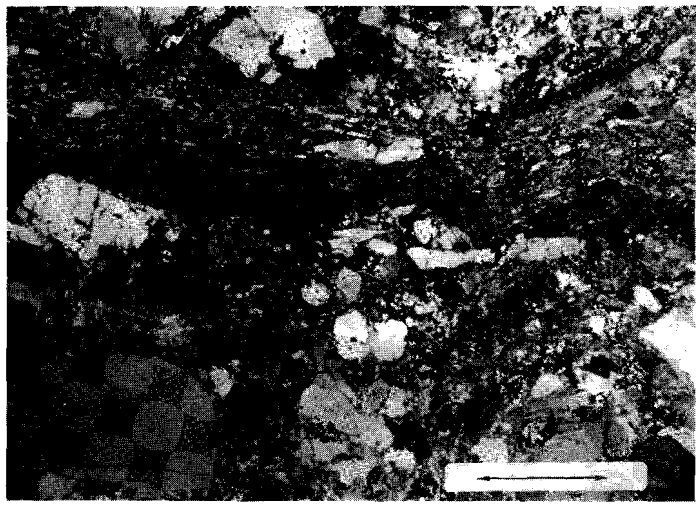

Figure 3.5. Incipient foliation development in granodioritic rock from shear zone. Dark band (d-b) consisting of fine grained rutile+sphene+epidote abutts biotite-rich domain (at b). Crossed polarizers. Scale bar: 1.5 mm.

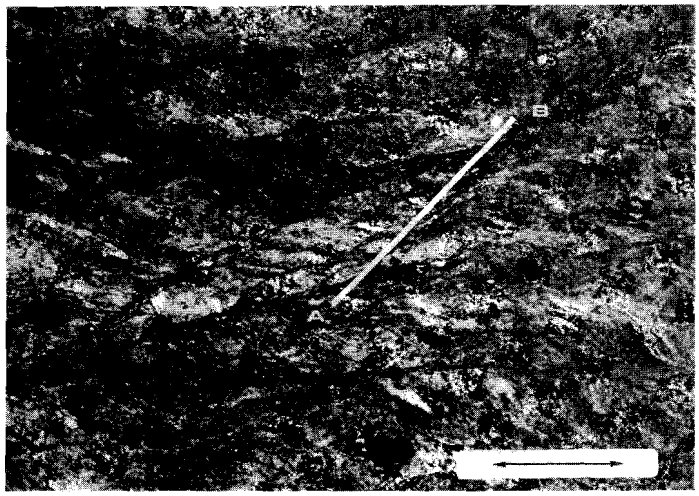

Figure 3.6. Micrograph showing second foliation in deformed granodiorite (parallel AB). Crossed polarizers. Scale bar: 3mm.

Domain C is situated in the center of the shear zone. The rocks are composed of fine grained epidote, phengite, green biotite, chlorite, albite and quartz; locally there are elongate saussuritized plagioclase relicts (aspect ratio 10:1) which are aligned with the foliation. The minerals are more or less evenly dispersed throughout the rock and the texture is mesoscopically homogeneous. The foliation is defined by oriented phengites. It is parallel to the trend of the shear zone.
Green biotite and chlorite occur intimately intergrown in stacks and microveins.

3.3. Metamorphic reactions and deformation mechanisms.

The textural variation of the rocks from the different structural domains of the shear zone is the result of a close interplay of deformation and metamorphism of an initially homogeneous granodiorite. Whole rock chemical analysis demonstrates that the mineralogical transformation was essentially isochemical (table A2). The microstructure suggests that the following mineral transformation has taken place:

brown biotite+ plagioclase = epidote group minerals+albite+phengite+green biotite+chlorite+sphene+rutile.

The newly formed mineral association found in the rocks points to middle greenschist facies conditions (Miyashiro, 1973; Frey, 1976; Graham et al. 1983).
The effect of the metamorphic reactions on the microstructure is that the initial domainal configuration of the granodiorite (plagioclase vs. biotite-rich domains) is lost by chemical and mechanical homogenization. Epidote growth in plagioclase-rich as well as in biotite-rich domains and phengite growth in plagioclase crystals suggests mobility and homogenization of K, Ca, Fe, and Mg. The newly formed phases may occur in vein-like structures (epidote, chlorite/green biotite) or dispersed throughout the rocks.

The deformation mechanisms which operated in the different minerals and mineral aggregates are diverse.
Quartz microstructures indicate intracrystalline deformation and associated recovery and recrystallization. Biotite shows intracrystalline deformation

structures (folds and kinks) and others which are associated with solution transfer processes. Plagioclase crystals are not deformed but show different stages of transformation to fine grained aggregates of phengite, albite and epidote, in which mica flakes are coating more or less globular albite and epidote. Since such aggregates occur also as elongate domains aligned with the foliation it is inferred that they underwent a considerable amount of deformation. Probably the deformation mechanism in such aggregates was pressure-solution-aided grain boundary sliding (cf. Kerrich et al., 1980). The chlorite-green biotite stacks which are found scattered throughout the rock (total volume may be as high as 10%) are interpreted to have grown in open spaces created by intergranular cracking associated with this process (Atkinson, 1982).

CHAPTER IV. OCCURRENCE, ORIGIN AND MICROSTRUCTURE OF ALKALI-FELDSPAR MEGACRYSTS IN THE GRANITE-MYLONITE NAPPE.

4.1. Introduction.

The granite-mylonite nappe encompasses several rock-types which are thought to represent different stages of deformation and metamorphism of a granodioritic source rock (see Chapt. 3). All these rock-types may contain pink K-feldspar megacrysts, the sizes of which are highly variable ranging from 1-20 cm in diameter. Some crysts display idiomorphism (Fig. 4.1); they may occur scattered throughout the rocks or are concentrated in bands which are parallel to the local mylonitic foliation (Fig. 4.2). Feldspar megacrysts-bearing gneisses are common rocktypes in lower structural levels of the Scandinavian Caledonides (cf. Strand and Kulling, 1972; Gee, 1980). The origin of this rock-type and in more detail the origin of the megacrysts have been topics of considerable debate in the literature (see Röshoff, 1978) and is rooted in the famous granite controversy (Holmes, 1965). According to Rui (1972), Strand (1951) and Rosenqvist (1944) the megacryst-bearing gneisses are metasomatically altered sediments. The feldspar megacrysts in this view are porphyroblasts. The idiomorphism of some megacrysts was claimed to indicate such an origin. Törnebohm (1898); Högbom (1920); Point (1975); Röshoff (1978) and Alm et al. (1980) maintain that the megacrysts-bearing rocks are tectonized basement granitoids, intensively deformed by nappe transport during the Caledonian orogeny. The feldspar megacrysts are interpreted to be original (pre-tectonic) constituents of the rocks; it is implied that they are porphyroclasts. Transitional relations of granodioritic rocks to augengneisses and augen-bearing mylonites support this interpretation (Röshoff, 1978; Aukes et al., 1979).

Although there is field evidence that the rocks have been formed by deformation of a granitic rock (see also Chapt. 3), the feldspar megacrysts have relationships with the countryrock which contradict a pre-tectonic growth. These structures are described in the following section.

4.2. Syn-tectonic feldspar generation.

In all the rock-types of the Granite-mylonite nappe K-feldspar veins are

Figure 4.1. K-feldspar megacrysts in mylonitic rock.

Figure 4.2. Concentration of K-feldspar megacrysts in bands parallel to the mylonitic foliation.

found which are discordant with respect to foliation and the width of which varies from 0.1-50 cm (Fig. 4.3). Most veins show deformation induced structures such as folds or/and demonstrate (partial) break-up into clasts which form new megacrysts (Fig. 4.4). The mechanism of this breaking-up process is closely related to the mechanical and metamorphic behaviour of alkali-feldspars in these rocks, as is discussed in chapter 3. Deformed discordant veins may be transected again by younger, smaller ones of the same composition. In some cases the microstructure suggests repetitive generation of microveins by a crack-seal mechanism (Ramsay, 1980), see Fig. 4.5. In some sites close to a major vein there is a concentration of (idiomorphic) megacrysts which may have a direct genetic relation to the vein.(Fig. 4.6).

Discussion.

The fact that the veins have grown discordantly to a mylonitic foliation and subsequently have been deformed suggests a syntectonic genesis. The occurrence of different generations of veins showing diverse time relations with deformation-induced structures indicates that veining has taken place over a considerable period and probably continued to a late stage in the tectonic history.

This phenomenon allows an alternative theory for the mechanism of feldspar-megacryst generation: syntectonic growth in veins which were subsequently broken-up during deformation.

Objective of chapter 4.

Some feldspar megacrysts in rocks from the Granite-mylonite nappe bear a genetic relation to discordant veins; the origin of these is clear. Most megacrysts occur scattered throughout the rocks and mesoscopic structures indicating their origin are lacking.

The present chapter is a report of an investigation into the possibility of discriminating between different modes of genesis of the K-feldspar megacrysts on the basis of microstructures.

The following reasoning suggests that such microstructural criteria could exist. If the K-feldspar megacrysts were original constituents of the rocks, the minerals should display microstructures induced by cooling, such as exsolution structures and twinning (Smith, 1974; Ribbe, 1974).

In the case that K-feldspar megacrysts would have generated syntectonically by veining and subsequent segmentation cooling effects should be absent

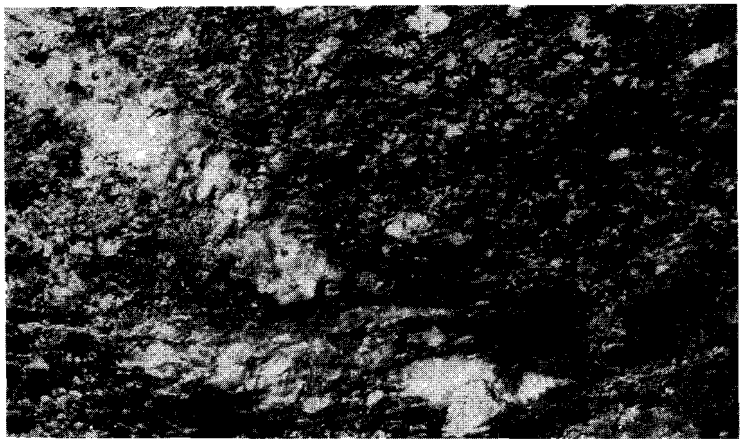

Figure 4.3. K-feldspar vein in deformed granodioritic rock. The vein is discordant with respect to the foliation (E-W on the photograph). Locality: Aane Width of the vein: 20cm.

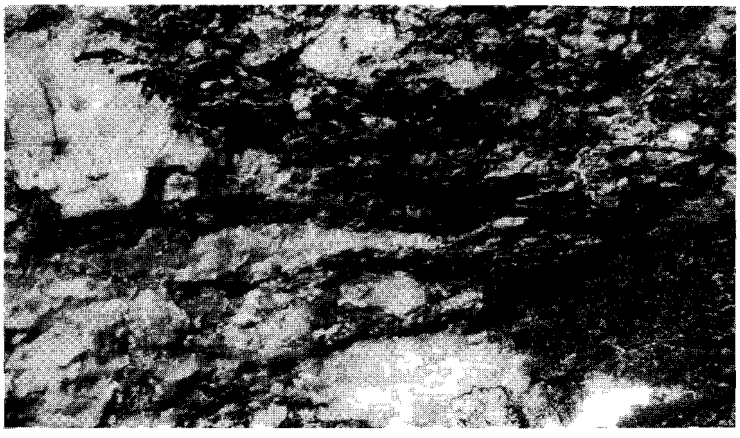

Figure 4.4. Detail of Fig. 4.3. showing fragmentation of the K-feldspar vein.

Figure 4.5. Micrograph of K-feldspar veinlets. Vein near "V" is built-up of several microveins, suggesting an origin by a crack-seal mechanism. Scale bar: 4 mm.

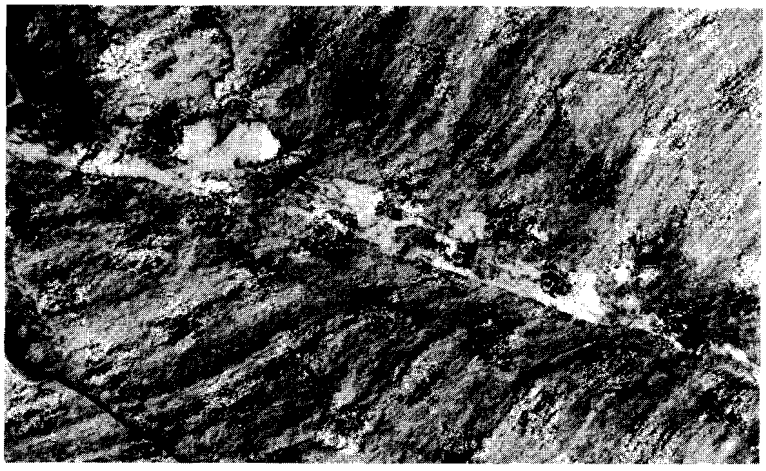

Figure 4.6. Discordant K-feldspar vein associated with shear zone in mylonite. Note the occurrence of individual megacrysts. Width of the vein: 4cm. Locality: 23 km. W of Nordli, south of the river Sandøla.

since deformation took place while the rocks were in greenschist facies conditions, i.e. in the stability field of "low-temperature" feldspars.

4.3. Microstructures induced by cooling of alkali feldspars.

At elevated temperatures K- and Na-feldspars form a solid solution series, the mineral exhibits monoclinic symmetry (space group C2/m).
Cooling may induce two processes in this mineral: decomposition to Na- and K-rich phases and a lowering of the symmetry elements of the decomposed phases by an ordering reaction. The subsolidus reactions are illustrated on the phase diagram in Fig. 4.7 (from Martin, 1974).

Microstructures induced by decomposition (exsolution).

The term perthite refers to an intimate intergrowth of Na and K-feldspar, the latter dominates the former in volume. In the literature different mechanisms of formation of this structure have been proposed: simultaneous growth of the two phases; exsolution from a K-Na solid solution feldspar and replacement of one phase by the other (see Smith, 1974).
Exsolution in alkali feldspars is thought to be a relatively fast process (compared with other silicates), since it only involves a redistribution of the alkali atoms while the Si-Al-O framework may remain unchanged (Yund, 1975).
Due to the same intrinsic property, replacement of one phase by the other is also a feasible process which can readily be performed in the laboratory (Orville, 1962).
Microstructures formed by exsolution and those generated by replacement in some cases are indistinguishable (Smith, 1974).
One special mechanism of exsolution of alkalifeldspars of intermediate composition that tentatively could yield diagnostic microstructures is spinodal decomposition followed by lamellar coarsening (cf. Yund, 1978). This process results in a rather uniform microstructure throughout one grain, it consists of regularly spaced lamellae of each phase, the orientation of the lamellae being crystallographically determined.
Due to strain induced by lattice-incoherency of the two phases, the albite lamellae are invariably twinned, the twin periodicity being dependent on the relative thic ness of the lamellae (Brown and Willaime, 1974).
Homogeneous or heterogeneous nucleation and growth is an alternative mechanism of exsolution. Microstructures produced by such a process are

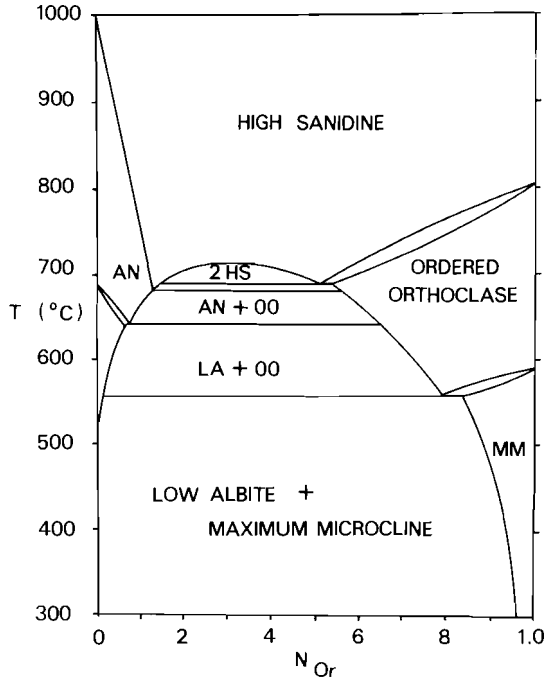

Figure 4.7. Phase diagram of alkali feldspars showing the relation of composition and temperature. MM=maximum microcline
LA= Low albite
00= Ordered orthoclase
AN= Anorthoclase

less regular than those generated by spinodal decomposition and might be easily confused with those resulting from replacement. It is thought that exsolution by nucleation and growth only occurs at very special conditions (cf. Brown and Parsons, 1983).
In conclusion it is stated that unless exsolution of alkali feldspars was spinodal decomposition, it may not be identified positively by microstructure

Microstructures induced by ordering.

The feldspar-crystal structure can be thought of as a double crankshaft of four-membered rings of AlO_4 and SiO_4 tetrahedra the structure was determined by Taylor (1933). Megaw (1974) constructed a simple model of the feldspar structure of which the smallest building stone is a tetrahedron representing an AlO_4 or SiO_4 group. Four tetrahedra are arranged in a ring as shown on Fig. 4.8-a. The feldspar structure can now be built-up by attaching similar rings in a way as shown on Fig. 4.8-b,c,d. In the ideal feldspar structure, i.e. the sanidine lattice all tetrahedral sites are equivalent and the distribution of Al-occupied sites throughout the structure is random. The unit cell is monoclinic, space group C2/m.
In an orthoclase structure the four tetrahedral sites in a ring are non-equivalent, the sites labelled T_1 on Fig. 4.8-c are preferentially occupied by an AlO_4 group (one in each four-membered ring). Both T_1 sites in a ring are equivalent and the symmetry of the unit cell is not lowered with respect to the sanidine structure.
In the microcline structure the two T_1 sites are non-equivalent; one T_1 site (labelled T_{1-o} on Fig. 4.8-d) is preferentially occupied by Al; the other site (labelled T_{1-m} on Fig. 4-8d) is occupied by Si. By this the symmetry of the microcline-unit cell is lower than that of sanidine; mirror and glide planes parallel (010) are absent, as are the two-fold axes parallel [010]. The symmetry is triclinic, space group $C\bar{1}$.
When a high-temperature feldspar (sanidine, orthoclase) is cooled, its structure tends to order to the low-temperature configuration (microcline) whether or not this transformation takes place depends on several factors (cooling rate, fluid content and composition, deformation; see Martin, 1974; Yund and Tullis, 1980; Yund, 1983).
The typical cross-hatching twin pattern displayed by most plutonic microcline crystals is interpreted to be the result of a symmetry inversion as described above. The albite (reflection twins with composition plane (010) and pericline twins (rotation axis [010]) mimick the lost symmetry elements

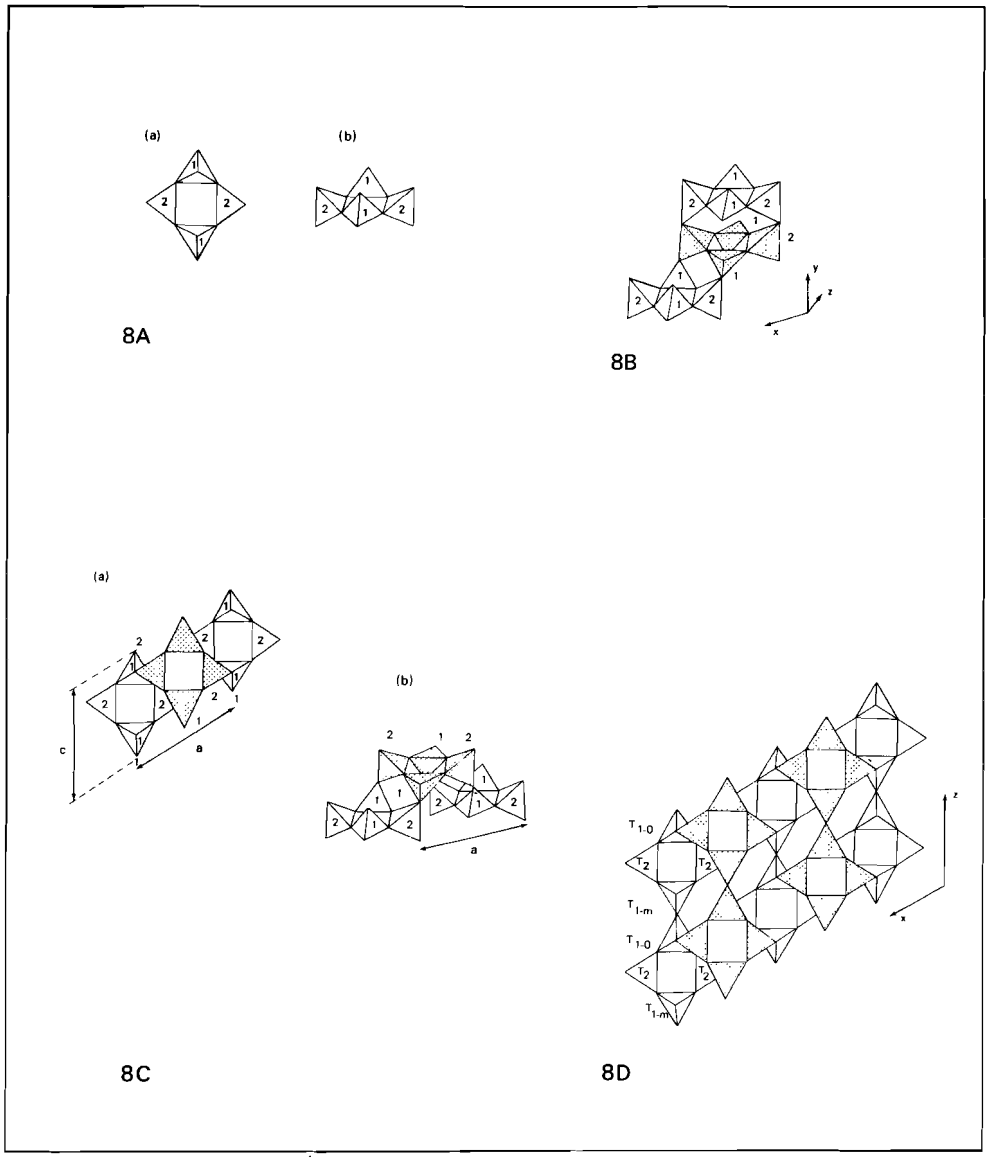

Figure 4.8. Megaw's model of feldspar structure. Each tetrahedron (8A) representing an Al/SiO_4 group. 8B-D shows the structure of the feldspar by attachment of different tetrahedra.. see text for discussion.

of the high temperature modification, respectively the (010) mirrors and the [010] rotation axes. Laves (1952) argued that the geometrical relation of the two sets of twins in microcline (shared twin axis) required an origin of the structure by symmetry transformation.
Mc Laren (1974) and Fitzgerald and McLaren (1982) found by electron microscopy that the two twins are each bound to specific areas in a mineral and hence on this scale could not confirm Laves' observations.
The structures of albite and pericline twins are such that two lamellae which are related to each other by either twin law differ in Si-Al ordering pattern; hence the lamellae can be regarded as ordering domains.
It is thought that the mechanism of twinning is restricted to the transformation induced one; mechanical twinning by simple shear of the lattice, as is the case in anorthite is not possible in ordered alkali feldspars since topochemically no symmetric relation can be achieved by conservative processes.
The results of Eggleton and Busseck (1980) are interesting in this respect. Using High Resolution Electron Microscopy these authors demonstrated the existence of a transitional form between domain-free, monoclinic orthoclase and triclinic, albite-twinned microcline. In the transitional domains the lattice shows sinusoidal bending. It was concluded that these domains are ordered structures with a pseudo monoclinic symmetry the lattice bending was interpreted as incipient albite twinning (see also Ribbe, 1974).
This interpretation thus confirms the consensus in feldspar literature that cross-hatch twinning in microcline is a result of a symmetry inversion due to ordering of Al and Si atoms in the structure.
A problematic microstructure is displayed by microcline crystals which are only partly or "patchy" twinned. Mäkinen (1913) and others described untwinned microcline with only local development of cross-hatch twinning in a twin-free, triclinic matrix. Goldsmith and Laves (1954) also studied Mäkinen's samples; they concluded that this microstructure is the result of a solid state domain coarsening, they however gave no arguments supporting this view.
In other cases occurrences of patchy twinned K-feldspar crystals could be attributed to a local development of ordering (Eggleton and Busseck, 1980), naturally in these cases patches of crystals which show the cross-hatching twin pattern occur as small islands in a monoclinic feldspar environment.
In section 4.4 microstructures are described which allow an alternative

explanation to the problem of patchy twinned triclinic K-feldspars.

Applicability of cross-hatching twin patterns to the study of the cooling history.

If at this stage it is accepted that cross-hatching twin patterns in microcline are the result of a symmetry inversion due to ordering, the usage of this microstructure to decipher a cooling history must be evaluated.
K-feldspars which grew below the monoclinic-triclinic inversion temperature (following Martin, 1974 this temperature is ca. 575°C, following Marfunin, 1966 it is an inversion trajectory) in most cases display cross-hatching twin patterns or monoclinic symmetry. This is due to the fact that although microcline is the stable low-temperature modification of K-feldspar, commonly at low temperatures a crystal tends to grow metastably in a high-temperature modification (Marfunin, 1966). The typical low temperature K-feldspar, which is found in alpine-type open joints etc. is adularia. The structure of adularia is complex in the sense that different parts of a crystal may show different structural states (Deer, Howie and Zussman, 1963; Smith, 1974). The mineral may occur as completely ordered, triclinic (space group $C\bar{1}$) or disordered monoclinic (space group C2/m). McConnel (1965) presented TEM micrographs of adularia showing two sets of mutually orthogonal distortion waves in a monoclinic lattice, and interpreted the structure as incipient albite and pericline twins (see also McLaren, 1974 and Eggleton and Busseck, 1980).
Typically the ordering domains are small in triclinic adularia, a phenomenon which has been attributed to the low diffusivity at low temperatures (Martin, 1974).
This section shows that there are serious restrictions concerning the applicability of ordering induced microstructures to establish a cooling history. However, the absence of such structures in triclinic K-feldspars as described by Martin (1974) and in the following section may be interpreted as the result of growth directly in the triclinic state. Growth of an ordered phase of a certain ordering series indicates that the temperature of formation did not exceed the upper stability temperature of that modification (Marfunin, 1966).
So the absence of an ordering induced structure in triclinic K-feldspars may be used as a criterion to establish that the mineral was generated in a low temperature environment.

4.4. Microstructures in the studied megacrysts

4.4.1. Perthite structures.

Most megacrysts studied display an intimate intergrowth of microcline and albite and thus can be classified as perthites. Two types have been distinguished on the basis of the type of occurrence of albite: string albite and vein albite (cf. Anderson, 1928).

Vein-albite perthite is the most encountered type in the megacrysts. Albite and microcline show syntaxial relationships. The albite phase is found in irregulary outlined vein-like structures and along the grain boundaries. The width of one vein-like structure is highly variable along its length. In some cases the albite veins are oriented parallel to the cleavage direction of the host (Fig. 4.9). Invariably the albite phase contains inclusion (haematite particles, fluid inclusions), the total volume of which may reach 5 vol.%. Some albite veins occur along the rims of healed cracks (microveins of newly crystallized K-feldspar, chlorite or quartz, see Fig. 5.6). Feldspar crystals displaying such vein-type perthite have a core-rim relation: the amount of albite veins increases towards the outer regions of the clasts, the rim consists of pure albite (Fig. 5.6). The relative width of the albite rim is variable: a narrow coating along the grain boundary and nearly completely albitized grains with a small core of K-feldspar are the two extremes of a wide variety of structures.

Discussion.

The preferential occurrence of albite along (healed) cracks and grain boundaries, the often irregular outline of the veins, the core-rim relation of albite and K-feldspar and the difference in relative amount of albite and K-feldspar in different megacrysts suggest that this vein-type perthite is a replacement structure.

Replacement of one K-feldspar by another under hydrothermal conditions can be readily performed in the laboratary (Orville, 1963; Helgeson, 1974). It is inferred that the preferential occurrence along cracks, cleavage planes and grain boundaries indicates that similar processes operated in the presently described feldspars, hydrothermal solutions had acces to the K-feldspar host along these structures.

In Chapt. 5 the origin of the relatively large amount of fluid inclusions is explained as due to lattice shrinkage by replacement of K-feldspar by

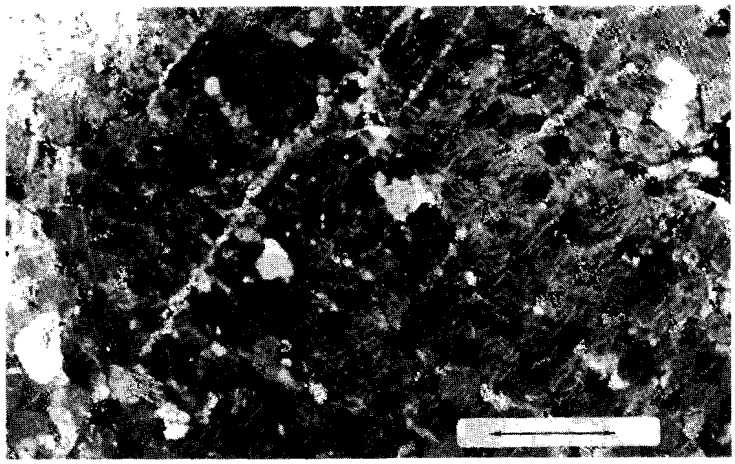

Figure 4.9. K-feldspar crystal (dark grey) with albite domains (light grey) along cleavages and the grain-boundary. Crossed polarizers. Scale bar: 1mm.

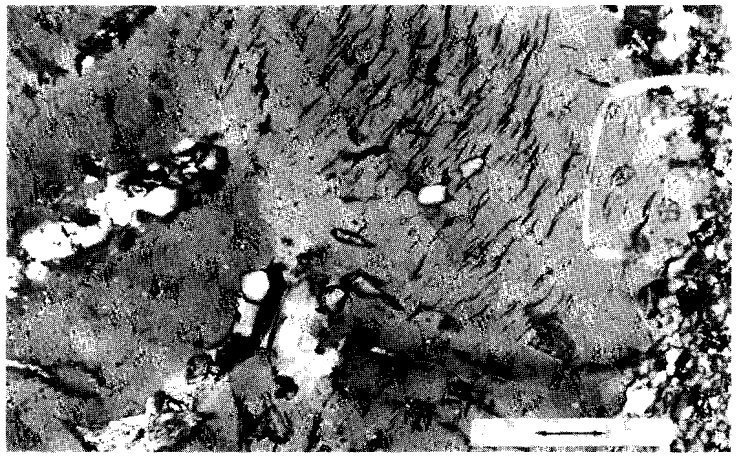

Figure 4.10. String-type perthite (albite: dark grey in light grey matrix of K-feldspar). Scale bar: 1mm. Crossed polarizers.

albite, the replacement taking place by an ion-exchange mechanism leaving the Si-O-Al framework intact.
It is difficult to establish whether exsolution processes contributed to the development of the microstructure. There are however megacrysts which are nearly pure $KAlSi_3O_8$, which show no perthite structure. This would indicate that the perthite structures in other megacrysts is a secondary process solely.

Conclusions.

-Alkali feldspar megacrysts originally were nearly pure K-feldspar.

-Replacement of K-feldspar by albite caused the development of a vein-type perthite.

-The mechanism of replacement was an ion-exchange mechanism under hydrothermal conditions.

String albite-type perthite.
Anderson (1928) described string albite as occurring in bodies typically 0.1-1mm long with a rounded, elliptical or lenticular cross section. This type of perthite is occasionally found in feldspar megacrysts, and also in late stage veins (Fig. 4.10). In contrast to vein albite, string albite shows a good crystallographic control on the dimensional orientation of the Na-rich phase: The longer axes of the elliptical bodies are approximately parallel to (100) of the host. Typically string albite occupies 5% of the volume of a feldspar crystal.

Discussion.
The origin of this microstructure is considered to be exsolution by nucleation and growth (Willaime et al., 1976; Champness and Lorimer, 1976). The value of the microstructure in establishing a cooling history is however limited due to the extremely low initial Na concentration. Moreover small concentration stability variations can also be induced by variations in the pressure (Luth, 1974).

4.4.2. Cross-hatching twin patterns in K-feldspar megacrysts in veins.

The K-feldspar megacrysts and veins display all the possible stages in the development of cross-hatch twinning: completely untwinned, patchy twinned and completely cross-hatched samples are found. The development of twinning was studied at partly twinned K-feldspars of which mesoscopical relations indicated a syn-tectonic origin. Segmented as well as non segmented veins were examined.
The study was performed using light-optical and transmission electron microscopy and X-ray and electron diffraction techniques.

X-ray data.

The structural state of the K-feldspar samples was determined by convential X-ray powder diffraction techniques (Goldsmith and Laves, 1954). The experiments were performed using a Guinier FR 552 ENRAF/NONIUS camera, operating with Cu-Kα_1 radiation.
Powder diffractograms of undeformed and untwinned as well as those of deformed, partly or totally twinned samples demonstrate splitting of (131) and ($1\bar{3}1$) (Fig. 4-11).
Using the formula of Goldsmith and Laves (1954) a triclinity value of 0.85-1 could be calculated, indicating that the K-feldspar can be classified as maximum microcline. Some samples show no clear peaks in the critical region. No samples were found to have a monoclinic symmetry.

Optical microscopy

Figure 4.12 is a micrograph of a folded K-feldspar vein in a mylonite. The fold is open, the axial plane is parallel to the foliation in the host rock. The hinge region of the fold (shown on Fig. 4.12) is segmented into clasts of ca. 0.5 cm in diameter. The clasts are inequant (aspect ratio ca. 1:3), the longer axes are parallel to the axial plane of the fold. The clasts display undulose extinction and they are embedded in a matrix of optical strain-free, equant grains of ca. 0-01 mm in diameter. The nature of the segmentation and the formation of the matrix grains will be discussed in Chapt. 5.
The optical properties of the clasts indicate triclinic symmetry (extinction angle γ=18°, see Steward, 1975).

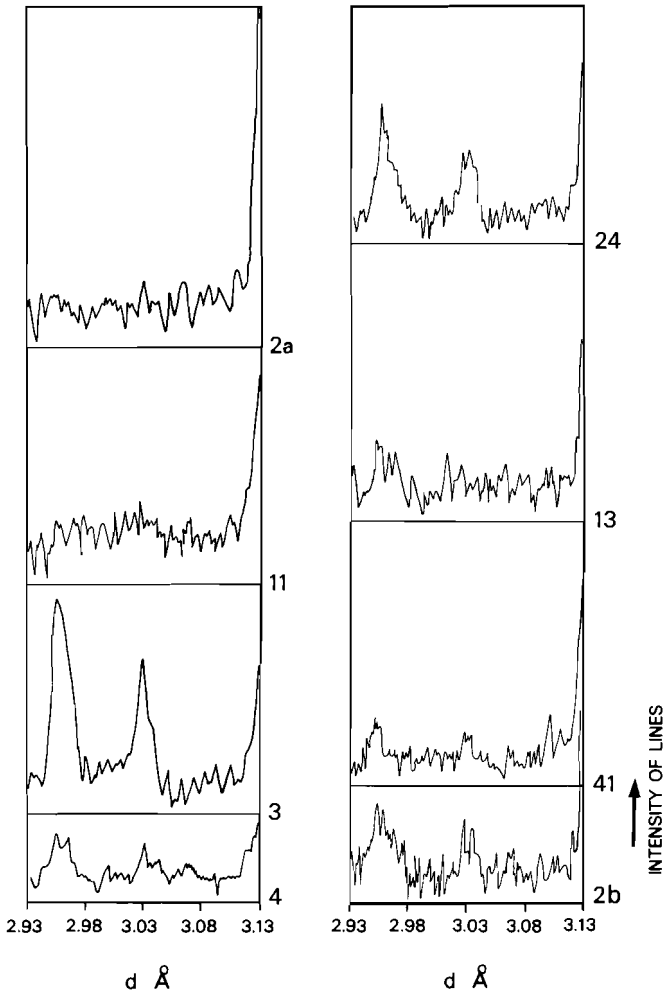

Figure 4.11 Intensities of lines of X-ray diffraction experiments (using Guinier camera) of powdered K-feldspar samples. Most specimens show splitting of 131 and $13\bar{1}$ lines (3.03 and 2.95 Å respectively).

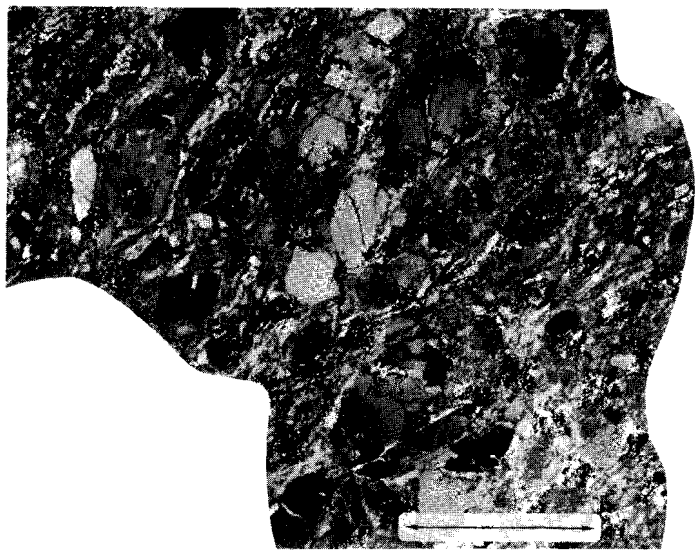

Figure 4.12. Folded K-feldspar vein showing segmentation into clasts. Scale bar: 3mm. Crossed polarizers.

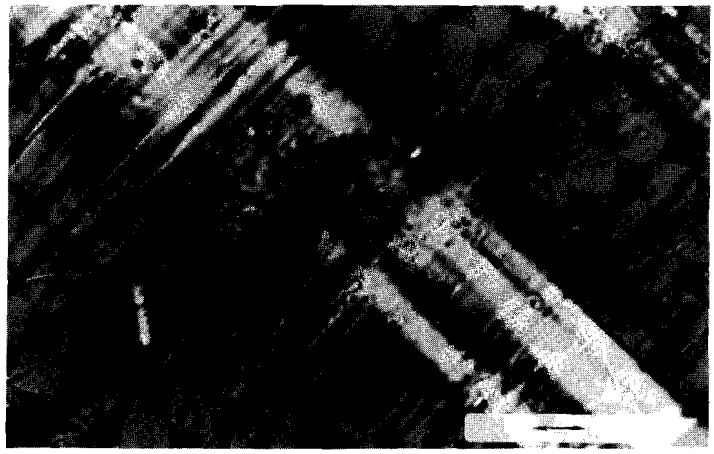

Figure 4.13. Kink in K-feldspar clast. Kink band is preferentially twinned. Note that the number of twins increases with the amount of crystallographic misorientation. Crossed polarizers. Scale bar: 0.8 mm. Detail of Fig. 4.12.

Some clasts are completely cross-hatched, most clasts are partly twinned and some bear no twins at all. In partly twinned specimens twins are found predominantly at sites of crystallographic misorientation (kink-like structures in which the number of twins is dependent on the amount of misorientation , see Fig. 4.13). Grain boundaries and cracks are other sites of preferential twin occurrence (Fig. 4.14).
In some cases relatively broad zones displaying cross-hatching twins separate large, untwinned domains which appear to have a twin relation to each other (Fig. 4.15). Each of these domains is in crystallographic continuity with one set of the twin lamellae.
Using optical microscopy, the twin lamellae were found to have an average width of 5 μm. As pointed out by McLaren (1974, 1978) however this value must be taken with some caution as the size of twins measured by optical and electron microscopy appears to be different.
The data above indicate that twins in the K-feldspars may occur predominantly at zones which are highly strained or at sites which are likely to behave as stress concentrators (grain boundaries, cracks) and that they are found in a triclinic matrix.

Transmission electron microscopy.

Samples of untwinned and partly twinned K-feldspar crysts were ion-thinned and studied by transmission electron microscopy (TEM).
Clasts of which mesoscopical relations suggest an origin by segmentation of a syntectonic vein, as well as isolated clasts and not segmented veins were examined.
The study was performed using a JEOL 200C TEM operating at 200 kV and a High Voltage Electron Microscope of the Metallurgical Institute of TNO, Apeldoorn, operating at 900 kV.
Specimens were mounted in a tilt-rotation stage which allows tilts of ± 60° around the stage axis and ±180° around the foil normal.
Most diffraction experiments were performed using a double tilt holder (allowing rotations of ± 60° around the stage axis and ± 35° around an axis normal to the foil normal and the stage axis).

Results.

Specimens which show on the light-optical scale relatively coarse twins (width of ca. 0.01mm), by TEM demonstrate much finer spaced lamellae (width of the lamellae ca. 0.1-1μm) the orientation of which is similar to

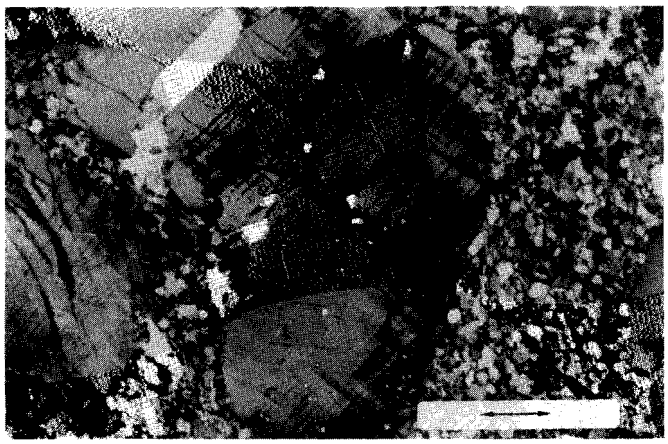

Figure 4.14. Preferential occurrence of twins at grain-boundary of K-feldspar clast. Detail of Fig. 4.12. Crossed polarizers. Scale bar: 0.5mm.

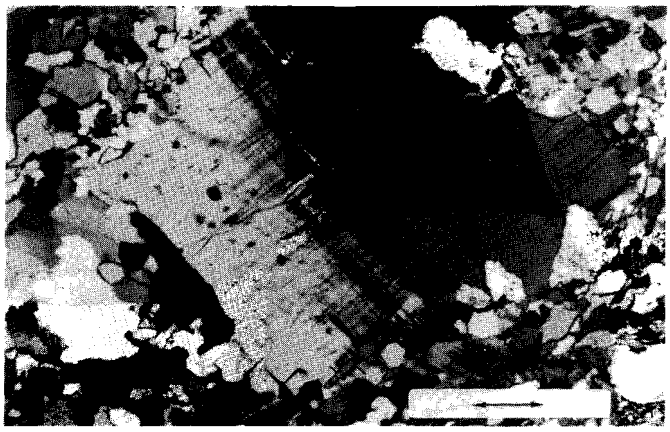

Figure 4.15. K-feldspar clast with a zone displaying cross-hatching twins which separates domains which are in crystallographic continuity with one of the twins. Scale bar: 0.5mm. Crossed polarizers. (Detail of Fig. 4.12).

the light-optical-visible twins (Fig. 4.16). Two sets of mutually perpendicular lamellae are found, one set is parallel to (010), the other is parallel to (h01), an irrational plane in between (100) and $(20\bar{1})$, close to $(20\bar{1})$. Areas which reveal a high concentration of lamellae parallel to (010) show extra spots in the diffraction pattern of the reciprocal plane (001)*(Fig. 4.17). The direction of splitting is parallel to [100].
Dark field images of a diffracted beam of a pair show only one set of lamellae reflecting. The lamellae boundaries are out of contrast using g= 040 for imaging, they are in contrast using any other g. These data indicate that the (010) lamellae are albite twin (cf. McLaren, 1974).
The boundaries of the other set of lamellae are out of contrast using g= $20\bar{1}$; 200 and 002, indicating a fault of $\frac{1}{n}$. 010 associated with such boundaries. Diffraction patterns of zones containing this type of lamellae show streaking or extra spots which are oriented such that a 180° rotation parallel to the b axis can be inferred.
These lamellae have been interpreted as pericline twins (cf. McLaren, 1974). The configuration of the lamellae is such that a true cross-hatching pattern can hardly ever be observed, instead, there are domains in which either of the sets occur (Fig. 4.16). Such a phenomenon was also described by Tibbals and Olsen (1977); McLaren (1974, 1978) and Fitzgerald and McLaren (1982).
Locally kink-like structures with irregular kink-band boundaries were found in areas containing twins. The number of twin lamellae in a kink-band appears to be larger than that in the matrix (Fig. 4.18).
Specimens which by light-optical microscopy appear untwinned or patchy twinned, show by TEM large untwinned regions of which diffraction patterns parallel to $(001)^*$ display triclinic symmetry (Fig. 4.19).
Very locally within these regions there are zones which show a cross-hatching pattern of wavy, ill defined bands on a very small scale. The orientation of these bands are those of albite and pericline twins (Fig. 4.20).
Most specimens which on light-optical scale do not show features indicating intracrystalline deformation are defect-free on the scale of TEM.
Specimens which show undulose extinction, by TEM demonstrate two sets of planar defects bound by dislocations (Fig. 4.21). In some cases the bounding dislocations are loops (Fig. 4.21), in other cases planar defects are found at one side of an isolated dislocation (Fig. 4.21"s").
One set of planar defects is parallel to (010): the "(010)"defects, the

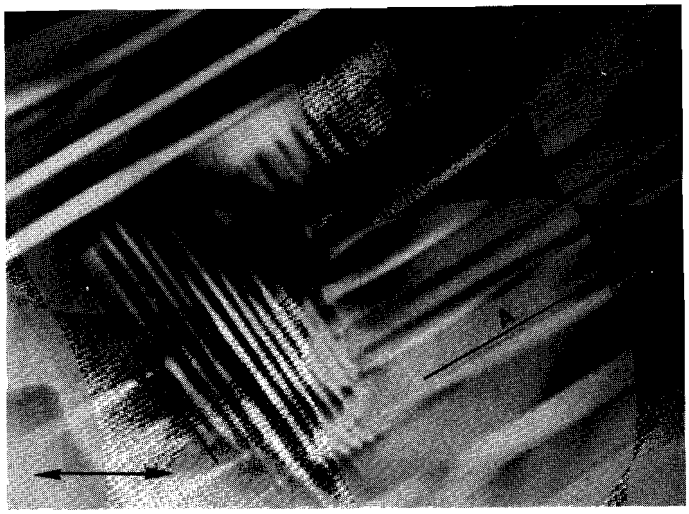

Figure 4.16 TEM micrograph of albite and Pericline twins (// A and P resp.). Note that each set of twins is bound to a specific domain. Scale bar: 0.2 μm

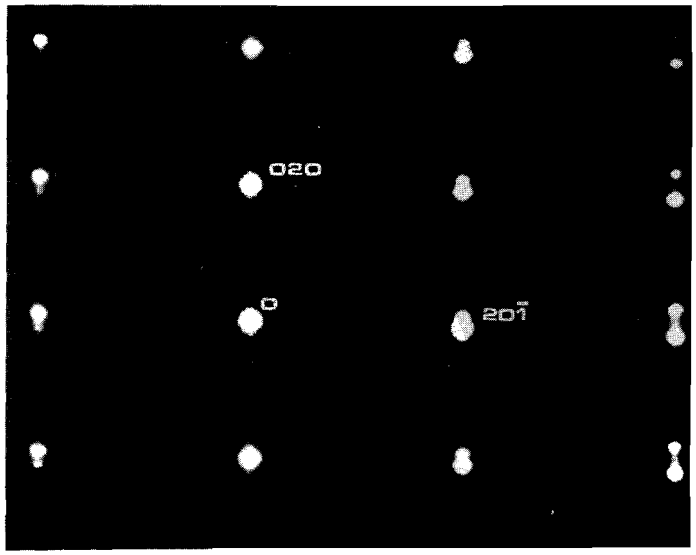

Figure 4.17 Diffraction pattern of microcline. Note splitting of spots due to albite twinning.

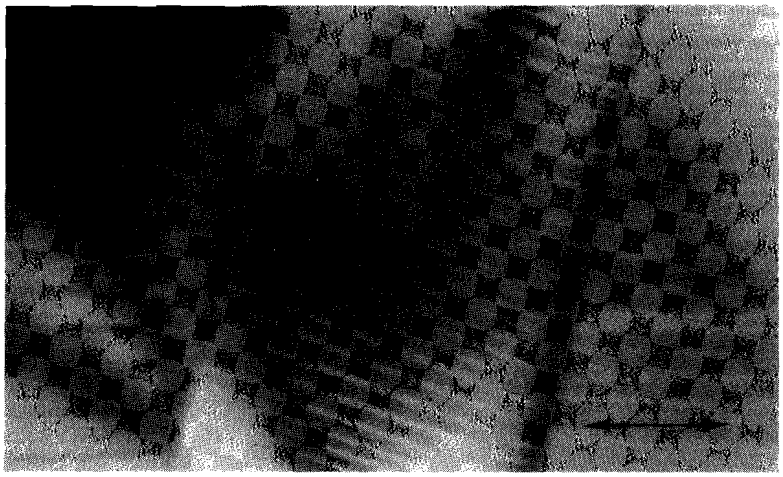

Figure 4.18 TEM micrograph of kink in twinned microcline. within the kink the number of twins is doubled with respect to that in the matrix. Scale bar: 0.025 μm

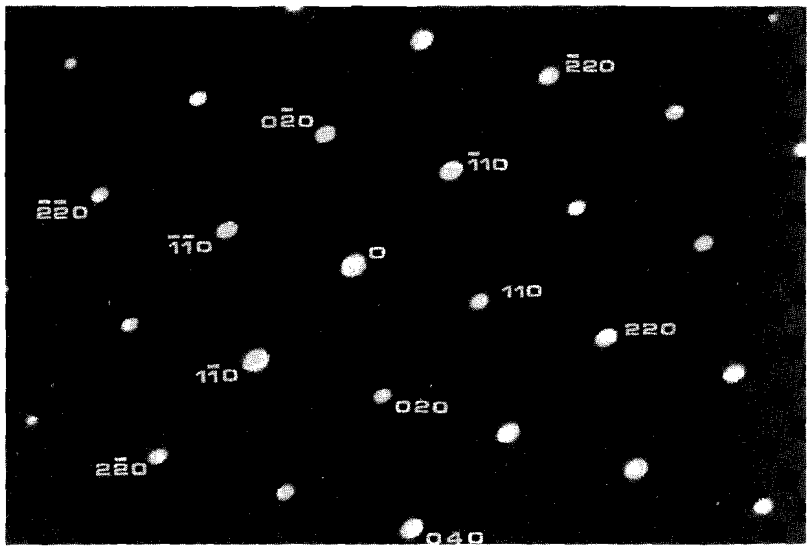

Figure 4.19 Diffraction pattern parallel the reciprocal plane $(001)^*$ displaying triclinic symmetry as (110) and $(\bar{1}10)$ are not equivalent.

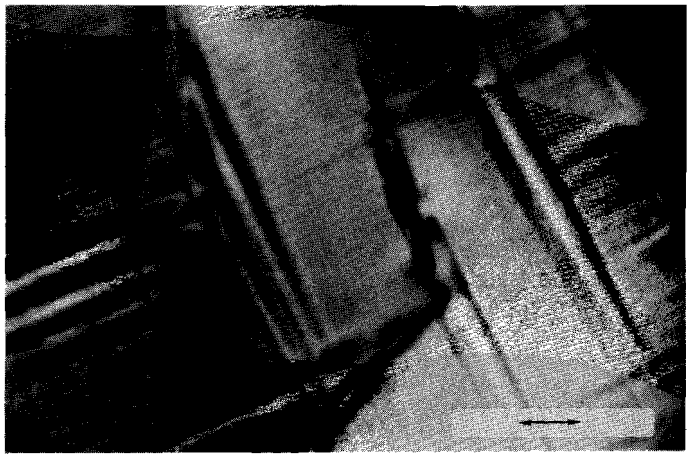

Figure 4.20. TEM. Modulated texture in K-feldspar defined by bands running parallel to albite and pericline composition planes. Scale bar: 0.05 μm.

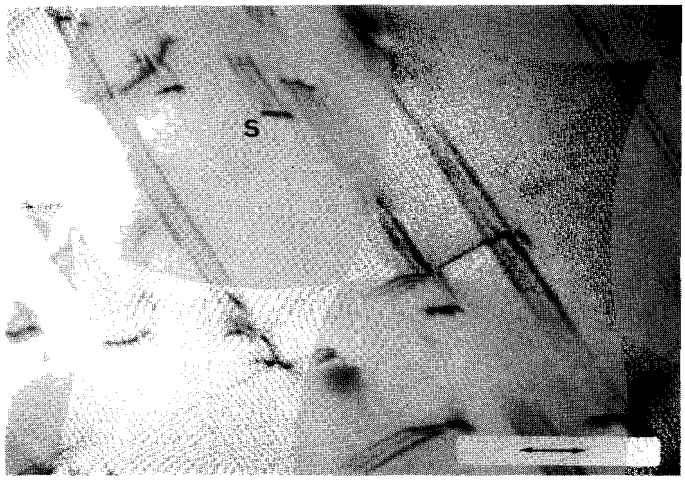

Figure 4.21. Dislocations associated with planar defects. The orientation of the planar defects is parallel to the albite and pericline-twin composition planes. Note that the planar defects are also associated with single dislocations (at "s"). Scale bar: 0.1 μm.

other defects are parallel to the pericline-twin composition plane: the "p"-defects.
The "010" defects and associated dislocations are out of contrast using g=040 for imaging (Fig. 4.22 A and D), they are in contrast for any other operating diffraction vector.

The "p" defects are in contrast for any g of the type (hkl), $k \neq 0$, and are out of contrast for any g of the type hol (Fig. 4.22 A-D).
The associated dislocations of the "p" defects are not out of contrast for g=hol, but demonstrate weak or symmetric contrast which is stable for small tilts

The defects may occur in various configurations:
-They may be concentrated in bands parallel to the trend of the planar defects (Fig. 5.2). Only one type of defect is found in such bands.
-The defects may occur isolated or as isolated patches (Fig. 4.21). Also high-dislocation-density areas containing both types of defects may be found
-The defects may be found in a regular cross-hatching pattern covering a relatively wide area
-The defects may be found at boundaries of relatively large volume defects such as grain boundaries or healed cracks

The nature of the defects.
The relation of the fault vector R of the planar defects and the Burgers vector b of the bounding dislocations is difficult to establish in the case of the "010" since they appeared to be out of contrast only when g=040 was used for image formation i.e. when these planar defects were (nearly) vertical. This suggests that the direction of the vector R lies in (010), the exact direction being un nown, but it is probably an irrational one.
"p" defects are out of contrast using g of the type (hol), indicating that the vector can be expressed as $\frac{1}{n}(010)$. The value of n is not known, it must be $\neq 2,4$ since the defects are in contrast for g= 040.
Using $g=20\bar{2}$ dislocation loops of "p" defects show "symmetric" contrast (stable at small variations from the Bragg angle) at parts where they have a direction close to [001] and faint contrast where the orientation is nearly parallel to [010]
This type of contrast is thought to indicate g.b=0 (cf. Kovacs and Gandais,

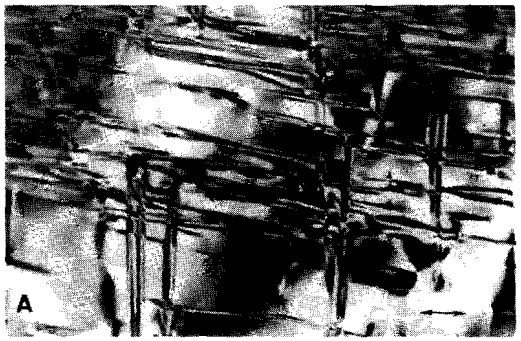

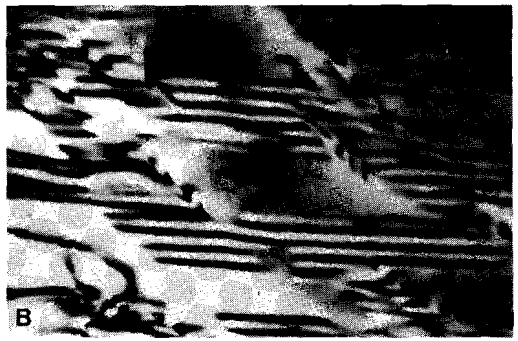

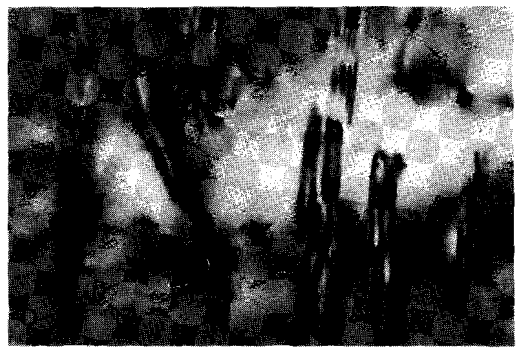

Figure 4.22 A-D are TEM micrographs of "p" and "(010)" defects in microcline at various diffraction conditions. All figures are from the same area. The "p" defects run N-S, the "010" defects run E-W on all the photographs. Scale bar 0.3 μm

Figure 4.22 A: both types of defects are in contrast; g=220

Figure 4.22 C: "p" defects are out of contrast; g=20$\bar{1}$

Figure 4.22B: "p" defects out of contrast; g=200

Figure 4.22D: "(010)" defects out of contrast; g=040

1979), indicating that $b=\frac{1}{n}$ 010 . As the directions of R and b are similar the planar defects can be classified as shear defects. The occurrence of these defects in deformed specimens only and their typical arrangements (e.g. in dislocation-rich bands which are interpreted as slip bands) suggest an origin by plastic deformation. "(p)" is however an unknown slip plane. Moreover, [010] is a "forbidden" slip direction (McLaren, 1975; Willaime et al., 1979) because of the strong coherency in that direction. This problem is discussed in the following lines.

There are different types of atomic arrangements which can yield a linear dislocation structure. One model implies the existence of a line of non-satisfied bonds, a structure which in the case of a primitive cubic cell can be thought of as an extra half plane inserted in a perfect lattice (Hull, 1975, see Fig. 4.23a).
Dislocations can be truly linear structures terminating at discontinuities or may be found as closed loop structures. Movement of a dislocation through the crystal causes relative movement of parts of the crystal, hence deformation. The same process takes place when a loop structure is expanding. In silicates the crystal lattice may not be restored after the passage of a dislocation. By such a process planar defects are created along the actual movement plane (McLaren, 1975; Willaime et al., 1979).
Another configuration yielding a dislocation structure is that found on a stepped surface of a twin boundary (Fig. 4.23b). This type of dislocation has a coherent structure, i.e. all the atomic bonds are satisfied, the (partial) dislocation being merely the termination of a monolayered twin lamella.
Another possible configuration could be one of mixed character of the two models described above: an incoherent dislocation loop of which the shear stress is relieved by a twin of one or more atomic layers in width (Fig. 4.23c).
Alternatively planar defects and associated dislocation loops can be platelets of a second phase of which the boundary with the host is semi-coherent (Friedel, 1963).
"p" and "010" defects have orientations and fault vectors which are consistent (in the case of the "010" defects not inconsistent) with pericline and albite (micro)twins respectively and hence they are interpreted as such. The defects are interpreted to be dislocation structures of the type

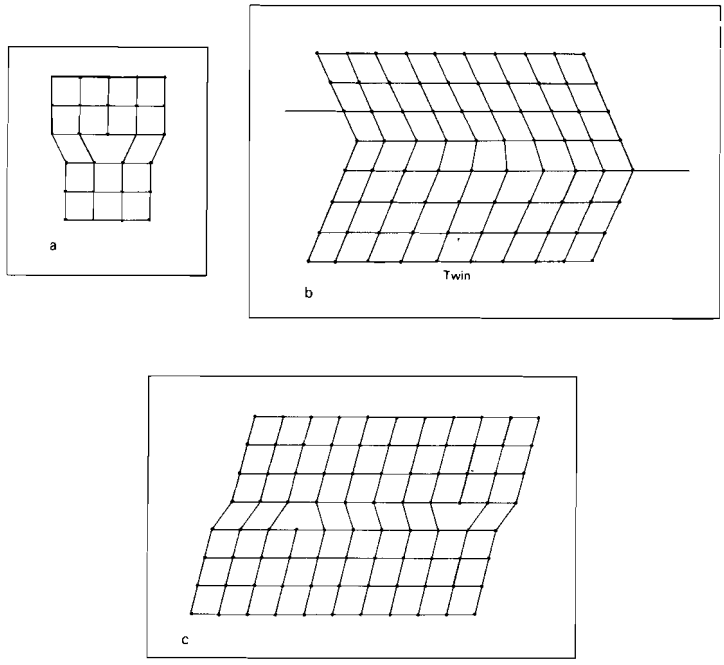

Figure 4.23. Three dislocation models:
4.23a: Dislocation model by insertion of extra half plane in a structure.
4.23b: Twinning dislocation
4.23c: Dislocation loop enclosing microtwin

as shown in Fig. 4.23c.
It is suggested that these microtwins were formed by a non-conservative process (local reordering of Al and Si atoms) during passage of a dislocation of which the core can act as a diffusion channel (Friedel, 1963).
Hence the process of formation is interpreted to be creep twinning in Laves' terminology (1974), this process is thought to take place also in ordered albite-rich plagioclase crystals.

Conclusions.

Microstructures on the scale of light-optical and transmission electron microscopy indicate that the cross hatching twins in the studied megacrysts are not the result of a symmetry inversion, but are induced by deformation.
The process of formation of the twins is thought to be similar to deformation induced twinning in plagioclase, designated as creep twinning, performed by a diffusional process following or associated with the passage of a dislocation.
The lack of symmetry-inversion-induced microstructures is thought to indicate that the microcline crysts were originally triclinic, implying a growth at relatively low temperatures.

CHAPTER V. THE MECHANICAL BEHAVIOUR OF ALKALI FELDSPARS AND ITS RELATION TO METAMORPHIC PROCESSES.

5.1. Introduction.

In the rocks from the Granite-mylonite nappe alkali-feldspars occur in two microstructural arrangements: as megacrysts which show little evidence of plastic deformation and in fine grained bands of which the microstructure suggests that the mineral underwent ductile deformation (section 5.2). In this chapter it is argued that the different microstructures are related to different metamorphic reactions which alternatively took place in the rocks.

5.2. Observations.

K-feldspar clasts of various sizes occur scattered throughout the rocks or are concentrated in bands which are aligned with the foliation (Fig. 4.2). In some cases the crystals are embedded in a fine-grained matrix of albite, K-feldspar and quartz grains of ca. 0.05 mm in diameter. Some porphyroclasts have elliptical outlines (aspect ratio 3/2) with the long axes parallel to the foliation (Fig. 5.1). The matrix grains form tails and mantles around the porphyroclasts; tails of different clasts may join to produce a compositional layering.

K-feldspar porphyroclasts show undulose extinction, lattice misorientations of ca. 5^{o} have been measured. At grain boundaries and cracks the mineral is twinned (see Chapt. 4).
By transmission electron microscopy (TEM) the dislocation substructure of K-feldspar was revealed. Figure 5.2 shows a band with a high dislocation density, consisting of micro-twin dislocation loops (see Chapt.4, see also Fig. 5.3).Bands with high densities of micro-twins are parallel to (010) or to the pericline-twin composition plane.
Isolated dislocations with Burgers vector [001] have been analyzed, probably representing the slip system (010)[001] (Scandale et al., 1982). There is little evidence of recovery structures in the mineral, observed dislocation walls, by correlation with optical microscopy, are thought to be growth structures. No recrystallization effects have been observed.

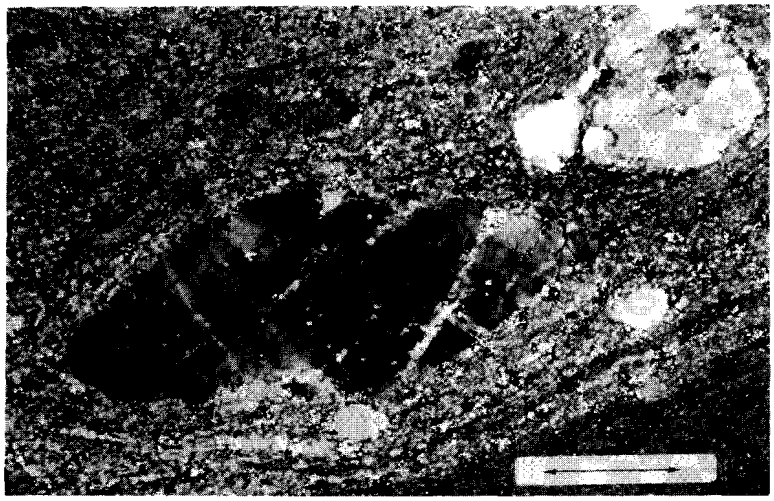

Figure 5.1. K-feldspar clasts in fine grained matrix in mylonite. Crossed polarizers. Scale bar: 2mm.

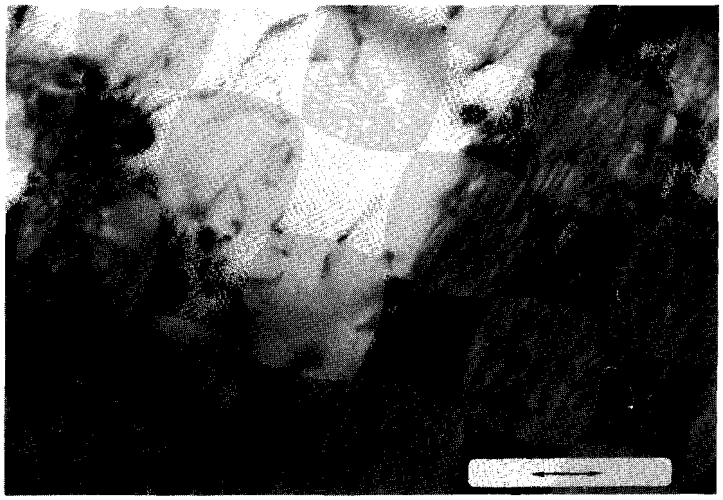

Figure 5.2. TEM micrograph of band with a high dislocation density. The band runs parallel (010). Scale bar: 0.1 μm.

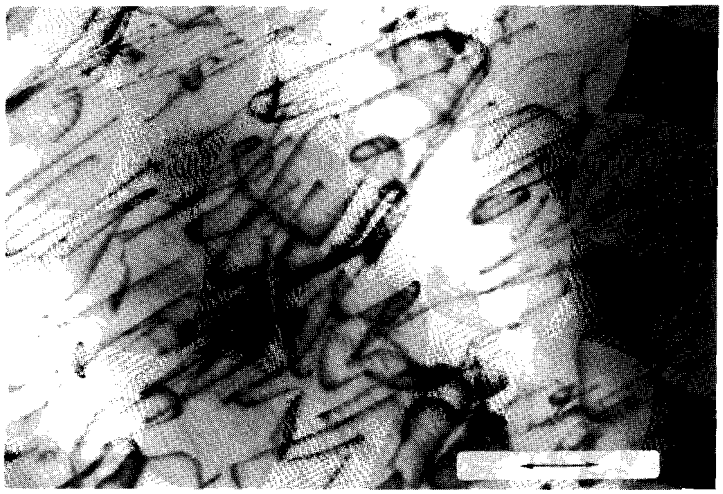

Figure 5.3. As Fig. 3.9. specimen tilted ca. 50°, showing that the dislocations are loops enclosing planar defects. Scale bar: 0.05μm.

The substructure is characteristic of plastic deformation at low temperature (relative to the melting temperature T_m) in which case diffusional processes are expected to be limited (cf. Nicolas and Poirier, 1976)

Nearly all K-feldspar porphyroclasts show evidence of brittle deformation. Three types of cracks have been distinguished on the basis of their "post-crack" history.

i) Healed cracks. The cementing mineral is newly crystallized K-feldspar, it constitutes microveins that are variable in width from 0.1-2mm.
The orientation of the microveins is such that a general extension parallel the local foliation can be deduced. In most cases the microveins occur in a conjugate pattern (Fig. 5.4). Between one set and its conjugate associate there is usually a generation difference (one set overprints the other in a consistent manner). Also, within one set different generations of veinlets can be found. The microstructure indicates repeated crack-seal events (cf. Ramsay, 1980).
The K-feldspar microveining need not be confined to older K-feldspar veins or crysts, often the microveins are continuous in the matrix (Fig. 4.3).
In most cases the cracks contain composite chlorite-K-feldspar veins.
The effect of the microveins is that older K-feldspar crysts actually grow during deformation in a direction parallel to the foliation.
The microveins are associated with haematite particles and fluid inclusions coating the vein wall and produce a cloudiness of the feldspar (in hand specimens the veinlets can be seen by the naked eye by different intensities of red-colouring caused by the haematite particles).

Figure 5.5 is a TEM image of a healed crack. The apparent difference in the defect structure between the host and the newly crystallized phase is taken as evidence for the genetic relation.

ii) Crack-like structures along which albite domains are found (Fig. 5.6).
The albite phase is in crystallographic continuity with the K-feldspar host. Albite in this microstructure contains fluid inclusions in an amount very much exceeding that in the host material (up to ca. 5 vol%). The width of of the albite phase along the cracks is highly variable (Fig. 5.6). In general the number of cracks increases from the core to the rim of a K-feldspar host; at the rim the albite domains join to produce a pure albite mantle.

Figure 5.4. Micrograph of K.feldspar vein which is built-up by micro-veins (healed cracks). Vein walls (parallel to AB and CD) are stained by haematite particles. Crossed polarizers. Scale bar: 1mm.

Figure 5.5. TEM micrograph of healed crack (h.c.)= micro-vein of neo-crystallized K-feldspar in host which is plastically deformed K-feldspar with high crystal-defect density. Scale bar: 0.1um.

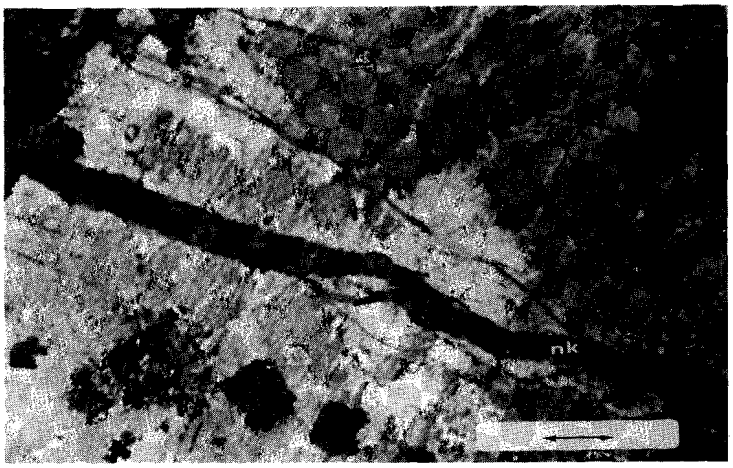

Figure 5.6. K-feldspar crystal (grey) with albitization along cracks and grain boundary (albite at white aera's). "nk": Microvein of neo-crystallized K-feldspar. Crossed polarizers. Scale bar: 1.5mm.

Figure 5.7. Type (iii) cracks (associated with albite grains) parallel the line XY on photograph in K-feldspar host. Type (i) cracks (healed cracks) run parallel the line KF on the photograph. Scale bar: 1.5mm. Crossed polarizers.

This structure is interpreted as being the result of the replacement of K-feldspar by albite, the replacement taking place by a cation-exchange through the pore fluid which finds acces through the cracks (cf. Orville, 1963). Heimann (1979) studied feldspar replacements experimentally and noted that due to the difference of molar volumes of albite and K-feldspar (100.3 versus 109.4 at 25°C and 1 atmosphere pressure, cf. Robie et al., 1978) albitization of K-feldspar by ion-exchange causes shrinkage of the Al-Si-O framework to produce holes in the albite phase.
The occurrence of a relatively large volume of fluid inclusions in the albite domains in this microstructure is thought to be the result of such a process. The microstructure is thought to be diagnostic.

iii) Crack-like structures along which rows of small, equant albite grains are found. The albite grains appear to corrode the K-feldspar host (Fig. 5.7). The albite in this microstructure differs in crystallographic orientation from the host.
TEM demonstrates a low crystal-defect density of the albite phase relative to the K-feldspar host (Fig. 5.8). The grainboundaries are smooth or lobate, suggesting corrosion. In some cases bubbles are found at the grainboundaries.
The microstructural relation of albite grains and K-feldspar host is similar to that which is found at the rims of porphyroclasts embedded in albite rich matrix.
This microstructure is interpreted as due to the replacement of K-feldspar by albite by a solution-neocrystallization process such as proposed by Petrovic (1974), the driving force for this process is considered to be an enhanced solubility by elastic strain at the albite-K-feldspar boundary.
According to Petrovic (1974) the type of feldspar replacement which will occur (cation-exchange in an existing Si-Al-O framework versus solution and neo-crystallization) is dependent on the compositional difference between the two phases (large compositional differences would favour the mechanism of solution-neocrystallization). However such a relation is not found in the rocks. Both in the microstructure occurring at type (ii) cracks as in that found at type (iii) cracks albite and K-feldspars are end-members in composition (pure K-feldspar and Na-feldspar).
In the present case a correlation between the type of replacement with the defect structure of the K-feldspar host is found. Porphyroclasts showing

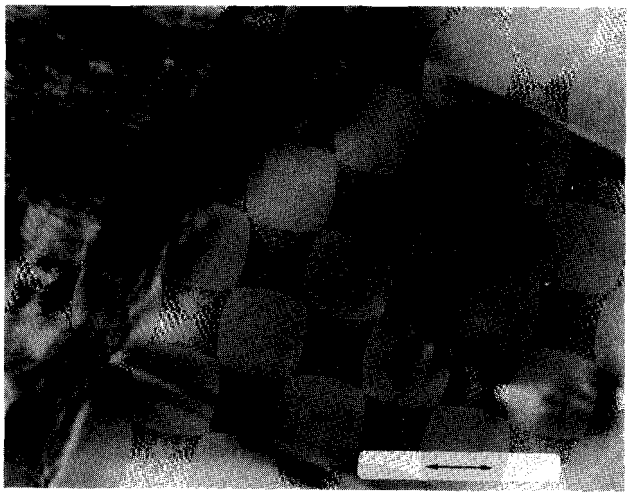

Figure 5.8. TEM micrograph of albite grain associated with type (iii) cracks. Note the difference in crystal defect density between albite (ab) and the K-feldspar host (K). Scale bar: 0.1 um. Locality "2".

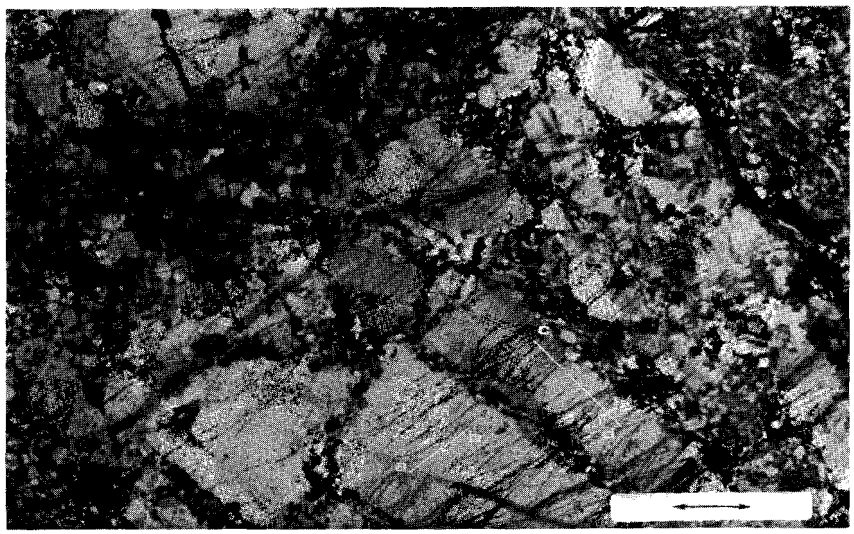

Figure 5.9. Overprinting of different types of cracks in a K-feldspar clast. At "1" type (i) crack overprints a type (iii) one. At "2" a type (iii) crack overprints a type (i) one. Scale bar: 1mm.

albitization microstructures in which the K-feldspar and albite are in crystallographic continuity are relatively undeformed, show no undulose extinction and in TEM demonstrate relatively low defect densities (dislocation densities $10^9/cm^2$) those which show microstructures suggesting a solution-neocrystallization process are deformed, show undulose extinction and have relatively high defect densities (dislocation densities up to $10^{12}/cm^2$ were measured).

Discussion.

The microstructures which are discussed above suggest that at greenschist facies conditions plastic deformation of K-feldspar does occur. The mechanism of deformation, such as the formation of slip bands, mechanical twinning, kinking and brittle failure are typical of a low-temperature environment in which diffusional processes are thought to be practically non-operative (cf. Nicolas and Poirier, 1976). Therefore the formation of a fine-grained K-feldspar matrix susceptible to plastic flow (as is typical of mylonites) is suppressed since such a matrix formation in most cases is a result of diffusion- controlled solid-state recrystallization (Hobbs et al., 1966; White, 1976; Poirier and Guillopé, 1979).

Other work on the natural deformation of feldspars confirms this conclusion (e.g. Hanmer, 1982).

Yet in some of the rockspecimens studied the relation of megacrysts to matrix seems to indicate that during the deformation K-feldspar megacrysts were replaced by fine-grained feldspar of different composition. The fine-grained material may constitute bands aligned with the mylonitic foliation suggesting a high ductility. Recently, similar observations have been made in granite-mylonites from other areas (Allison et al., 1979; Kerrich et al., 1980; Hanmer, 1982). These authors attribute the apparent ductility to a flow strength reduction by strain-induced recrystallization. Compositional variations of recrystallized material with respect to the host are thought to be indicative of diffusive mass transfer during deformation to allow grainboundary sliding ("superplasticity").

In metals and non-feldspar silicates the minimum temperature required for the operation of diffusion enhanced grainboundary sliding is found to be about $T = 0.5T_{melt}$ (Nicolas and Poirier, 1976).

Following Kerrich et al.(1980) in feldspars these processes are operating at much lower temperatures ($T=0.2T_{melt}$).

In the present case it is found that the role of the interaction between

pore fluid and the K-feldspar crystals is of vital importance for the formation of new strain-free grains. The microstructures suggest that strain-enhanced solution in the presence of a Na-rich fluid and neocrystallization of fine grained albite took place, thus reducing the strength of the rock. It is found that the composition of the pore fluid is of major importance for the mechanical behaviour of the rocks and as such may be denoted as an independent variable (cf. Ferry, 1983). In the present case this is illustrated by the difference of type (i) and type (iii) cracks. Only if the pore fluid is Na-rich, solution-neocrystallization takes place. If the pore fluid is K-rich cracks may heal and no grainsize reduction takes place.

Some microstructures indicate that the composition of the pore fluid changed several times during the deformation, they are discussed in the next section.

5.3. Microstructural differences of albite and K-feldspar.

Figure 5.9 illustrates that during the deformation of the rocks the composition of the pore fluid may have varied, causing different types of fluid-feldspar interactions. In this figure two directions are indicated, each aligned with a system of cracks.
Parallel to the line "a-b" healed cracks are found as revealed by the dust trails. The line "c-d" marks the direction of cracks along which albite grains appear to have corroded the K-feldspar host. The arrow "p" points to a microvein (type i) which overprints type (iii) cracks. In other cases type (iii) cracks overprint that of type (i).
It is concluded that the composition of the pore fluid changed alternately from Na-rich to K-rich. This phenomenon appears to be related to the microstructural relation of K-feldspar and albite with the porphyroclast which is different for each of these minerals:
K-feldspar is found in veins throughout the entire rocksuite (Chapt. 4), it is associated with microfaults and open cracks; it is thought that the mineral has grown in free space. Locally the veinlets are bimineralic, microcline being accompanied by chlorite.
In the rocks studied albite is never found in tension gashes or other sites where crystallization in free space could have taken place, instead the mineral is found solely as a replacement of K-feldspar.

Because all the specimens analyzed have chemical compositions close to that of granodiorite, assumed to be the parent-rock of the mylonites, and no large variations in the contents of K and Na were found, it is concluded that the change in the composition of the pore fluid did not result from an influx of material from external sources, but is due to internal factors. It is thought that the source material of K-feldspar (+chlorite) veins is derived from mica's undergoing incongruent pressure solution as follows:

$$\text{muscovite} + 6SiO_2 + 2K^+ = 3\text{K-feldspar} + 2H^+ \quad (1)$$

(cf. Wintch, 1975; Meyer and Hemley, 1976; Beach, 1982), or more general:

$$\begin{matrix} 5\text{biotite} + 3\text{white mica} \\ +9\text{quartz} + 4H_2O \end{matrix} = \begin{matrix} 8\ \text{K-feldspar} \\ +9\ \text{chlorite} \end{matrix} \quad (2)$$

(cf. Hoschek, 1973 and Graham et al., 1983).

The replacement of K-feldspar by albite is thought to be related to the overgrowth of plagioclase by epidote-group minerals and white mica (see Chapt. 3) following reaction (3) (Meyer and Hemley, 1976):

$$\begin{matrix} 4\text{anorthite} \\ +\text{K-feldspar} + 2H_2O \end{matrix} = \begin{matrix} 2\text{clinozoisite} \\ +\text{muscovite} + 2SiO_2 \end{matrix} \quad (3)$$

By reaction (3) Na^+ will be released to the pore fluid by break-down of the albite component of plagioclase and is available for albitization of K-feldspar.

In Chapt. 3 it is found that during plastic deformation of granodiorites under greenschist facies conditions retrograde mineral reactions take place which are qualitatively expressed as follows:

$$\begin{matrix} \text{plagioclase} + \\ \text{brown biotite} \end{matrix} = \begin{matrix} \text{white mica} + \text{green biotite} \\ +\text{epidote} + \text{albite (+rut, sphene)} \end{matrix} \quad (4)$$

Transformation (4) involves pressure solution of brown biotite and overgrowth of plagioclase by a new generation of mica.
So, dissolved mica appears to be incorporated in the rocks in two distinct

manners:

-as mica-overgrowth of plagioclase during plastic deformation (thereby releasing Na^+ of plag. which causes albitization of K-feldspar)

-as K-feldspar-chlorite veins following a brittle deformation event.

It appears that the different mineral reactions are related to distinct deformation mechanisms, as is illustrated by the following scheme.

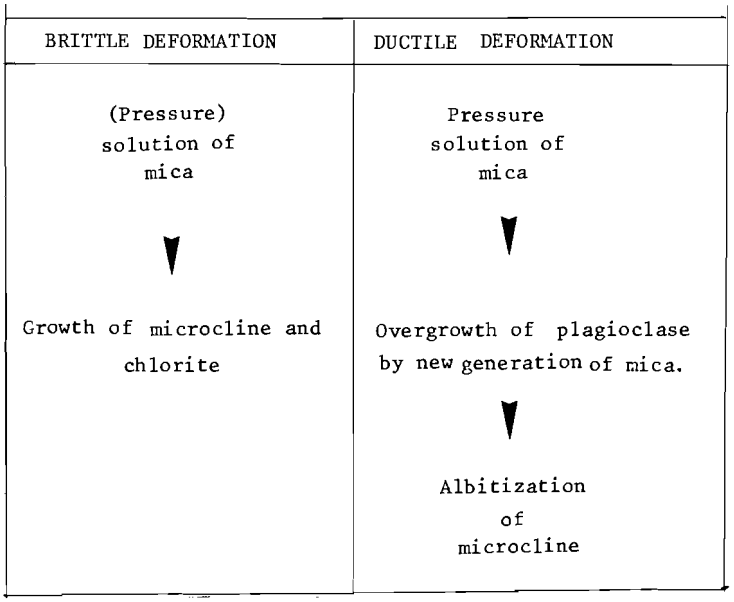

Figure 5.10 Schematic representation of the relation of metamorphic processes and deformation mechanism in the rocks from the Granite-mylonite nappe.

It is not known which factors govern the difference in mineral reactions associated with brittle and plastic deformation. Three possible parameters are given below:

i) pressure variations in the rocks
ii) variations in the temperature
iii) a change in the chemical activity of the pore fluid.

ad i) If the microcracks in a rock form a fluid-filled network extending over a considerable vertical distance, the pressure within these structures (pH_2O) is lower than the rock-pressure (Fyfe et al., 1976), thereby favouring K-feldspar growth over K-rich mica's (Meyer and Hemley, 1976). After the cementation of the microcracks the pressure will increase to a value equal to the rock pressure, favouring K-rich mica growth.

ad ii) Fluid migration in a rock through cracks may cause a fast heat transport, thereby governing a change in mineral reactions (Ferry, 1983). (in the present case, a sudden lowering of the temperature would favour K-feldspar+chlorite growth at the expense of mica).

ad iii)Brittle deformation involves migration of fluids present as H_2O films at grainboundaries to cavities in the rock in which case the fluid might be buffered, thereby changing its chemical activity and as a result favouring different mineral reactions (Graham et al., 1983).

A study of the composition of the fluid inclusions combined with that of the stable isotope distribution between the different phases would be necessary to evaluate the different possiblities. However a fluid inclusion study is hampered by the fact that due to the formation of a vast number of late tectonic microcracks leaking occurred causing most (former) fluid inclusions to be empty.

5.4. Conclusions.

Plastic deformation of K-feldspar in mylonites under greenschist facies conditions is limited. Operating processes are twinning, kinking and the formation of slip bands. No solid state recrystallization takes place due to the relatively low temperature.

Brittle deformation of the rocks involves the formation of open cracks in which new K-feldspar/chlorite veins are formed.
Intragranular cracking of K-feldspar porphyroclasts during plastic deformation of the matrix of the mylonites is associated with albitization. In relatively weakly deformed K-feldspar crysts albite inherets the Si-Al-O framework of the host; in strongly deformed specimens albite constitutes new, strain-free small grains, thereby causing grainsize refinement and probably a flow strength reduction of the rocks.

In the rocks brittle and ductile deformation mechanisms alternated, each process being associated with a specific mineral association:
K-feldspar+chlorite growth during a brittle event; biotite+white mica generation during plastic deformation.

CHAPTER VI. STRUCTURAL HISTORY OF THE MYLONITES AND CATACLASITES NW OF THE GRONG CULMINATION AND REGIONAL GEOLOGY

6.1. Introduction.

The deep erosion level in the Scandinavian Caledonides allows examination of basement-cover relations in a number of windows or domes. These domes predominantly occur along two "lines", which are known as the Scandinavian geanticlines (Ramberg, 1980), parallel to the Caledonian trend. One of these "lines" runs near the Norwegian coast, connecting the southern gneiss region with the Nordland granites (Fig. 1.4), the other is situated ca. 150 km to the east and connects the Olden culmination, the Borgafjell and Nasafjell windows. Most of these windows are relatively small (Ø ca. 25 km) and have nearly circular outcrop patterns. The stratigraphy in the cover rocks can be traced around the entire structures. Two basement highs lack such a symmetry and cross-cut the entire Caledonian belt: the Grong-Olden culmination in central Norway and Sweden and the Rombak antiform near Bodø. These two structures divide the orogen into the southern, central and northern Scandinavian Caledonides, the correlation of geological features between these parts often being uncertain.

According to Ramberg (1967, 1977, 1981), Cooper and Bradshaw (1980) and Nicholson and Rutland (1969) the western Scandinavian gneiss domes were formed as diapirs, as a result of an unstable density stratification after the emplacement of a relatively dense cover on a lighter granitic basement. The regular distribution pattern throughout the orogenic belt fits well with this diapiric model, and a comparison with the spatial distribution of salt domes can be made. Irregularities of this pattern are thought to be due to inhomogeneities in the basement (Cooper and Bradshaw, 1980) or in the cover (Ramberg, 1967).
Another interpretation is that the distribution of the domes in geanticlines point to an origin by large-scale folding of the basement, by lateral compression (Ramberg, 1981).

The relative age of the formation of the domes with respect to nappe transport is thought to be different for the western and eastern lines. Most domes occurring near the Norwegian coast, such as the Nordland granites, are involved in large recumbent folds (Nicholson and Rutland, 1967) which are interpreted as diapiric fold nappes (Ramberg, 1980). In this case the formation of the domes is thought to be a relatively early, syn-nappe emplacement structure.
The eastern series, such as the Nasafjell domes, the Borgafjell window and the Olden antiform are open structures, it is interpreted that their formation was late relative to the nappe emplacement (Gustavson, 1973; Gustavson and Grønhaug, 1960 ; Greiling, 1975; Thelander et al., 1980; Gee, 1980).

Dome formation and thrusting of the Caledonian nappes are two regional tectonic processes which possibly influenced the deformation history of the mylonitic rocks at the rim of the Grong culmination (cf. Stephansson et al., 1976; Grocott and Vissers, p.c.). In this chapter the mechanism and relative age of these large scale processes are discussed.

6.2. The structure of the Grong culmination.

Figure 6.1 is a geological map of central Norway and Sweden, showing the large scale structure of the Grong-Olden culmination and the overlying nappe units. The map is from Gee (1980) who interpreted the history of the culmination as "a transverse structure crossing the longitudinal grain of the orogen.....refolded by the Trøndelag and Snåsa synforms and the Tømmeras antiform". These folds belong to the Trondheim synclinorium which is the dominant structure of the southern Scandinavian Caledonides (see also Fig. 1.4). The extension of this structure to the north of the Grong culmination is not clear.

The geology of the southern rim of the Grong culmination was studied with emphasis on the basement-cover relations by Peacy (1967), Roberts (1967, 1968), Roberts et al., 1970 , Roberts and Wolff (1981) and Wolff (1979). East of Snåsa, metamorphic Caledonian nappes and basement are divided by a thin unit of weakly metamorphosed sediments which are thought to be the parautochthonous cover rocks of the basement. Along the entire basement-cover contact the foliation in the basement gneisses is parallel to that in

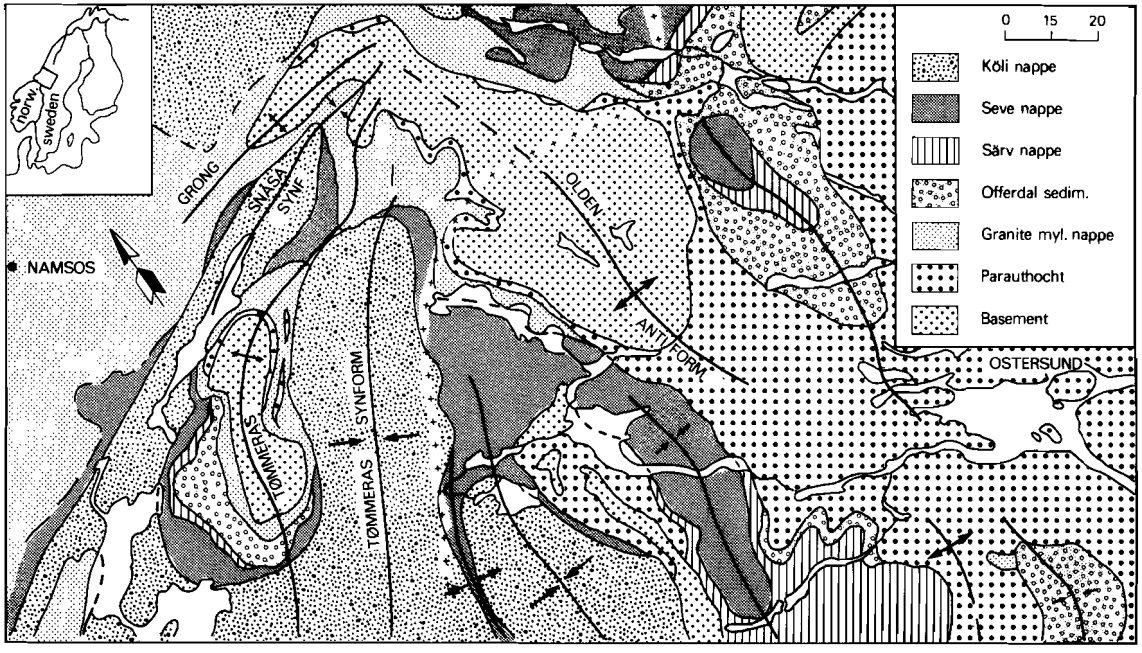

Figure 6.1. Map of the central Scandinavian Caledonides showing major rock units and structures (after Gee, 1980)

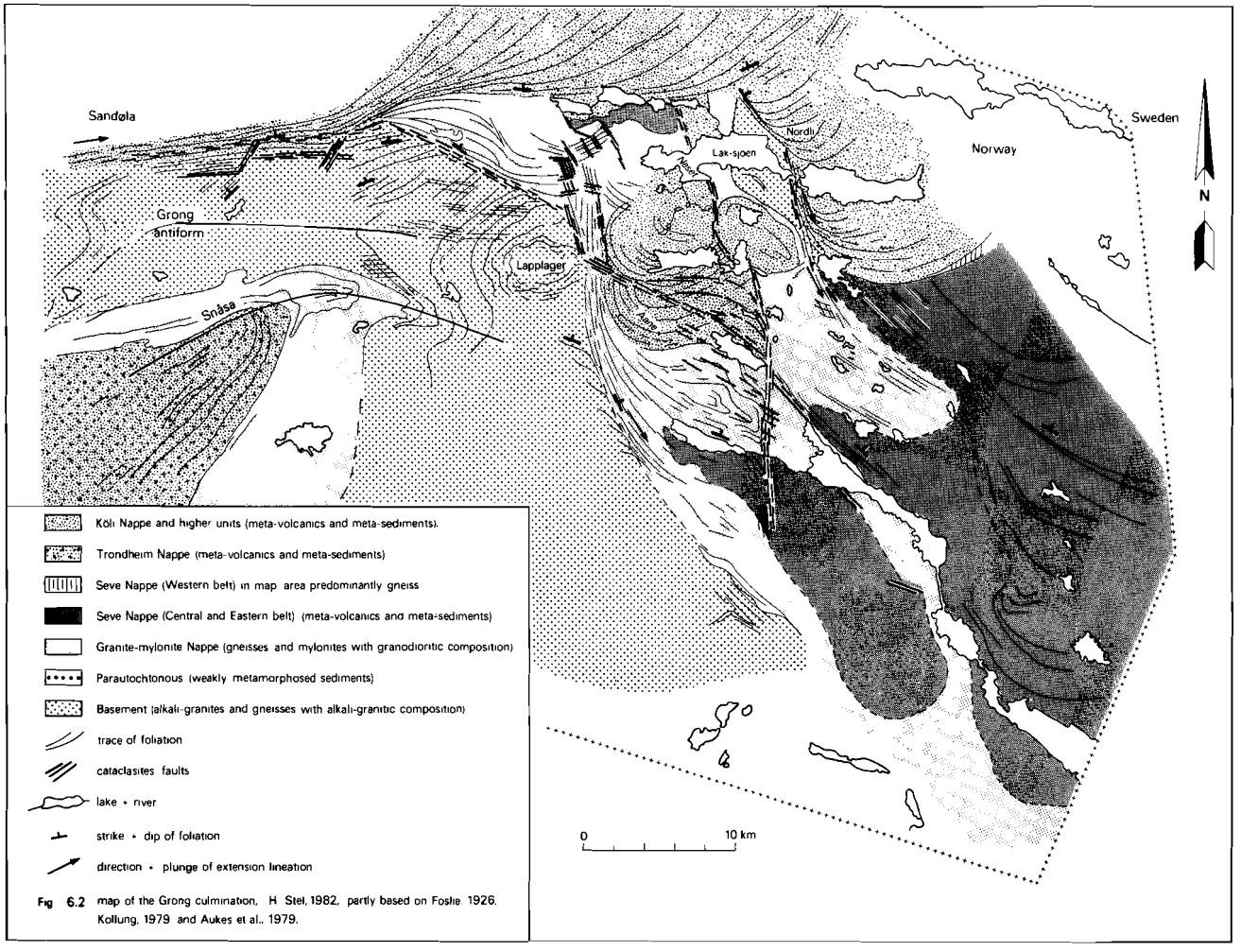

Fig 6.2 map of the Grong culmination, H. Stel, 1982, partly based on Foslie 1926, Kollung, 1979 and Aukes et al., 1979.

the nappes, a phenomenon which is supposed to be due to large strains which affected both rock units during nappe emplacement (Gee, 1980). Basement rocks and allochtonous units are concordantly folded by the northern extensions of the Trondheim synclinorium.

Figure 6.2 is a more detailed map showing the internal part of the Grong culmination and the northern basement-cover contact. The map is based on the work of Foslie (1929, 1929), Roberts (1967), Kollung (1979), Aukes et al. (1979) and additional mapping by the author.
The large scale folds affecting the southern basement-cover contact can be traced far into the culmination. The map shows the extension of the Snåsa synform, which is succeeded by the Grong antiform in the north. The trend of the folds of the Trondheim synclinorium changes abruptly from NE-SW (Caledonian) to W-E (transverse) in the central part of the culmination. The Grong antiform is relatively open and forms essentially the western part of the Grong culmination. At Lapplager this structure interferes with the N-S trending Olden antiform to produce the central dome structure of the culmination.

The northern and north-eastern basement-cover contacts transect the internal structure of the culmination. In general there is an abrupt change in the basement-foliation-orientation into zones of mylonite and, often, cataclasite at these contact sites. In some cases the reorientation is more gradual and the basement foliation swings into parallellism with the mylonites in dextral shear zones.

The northern cover rocks are formed by units belonging to the Köli and Seve nappes, in the map area consisting of metasediments and metavolcanics, and the Granite-mylonite nappe, consisting of gneisses and mylonites (see Chapt. 1). In all cover rocks the regional foliation shows a sudden swing in orientation near the contact with the basement. This reorientation of the foliation is accompanied by reorientation of fold axes and lineations towards parallellism with the dominant lineation in the mylonites.

6.3. Structural history of cataclasites and mylonites.

Cataclasites in the basement are predominantly found near the contact with the cover units. They transect older structures (Fig. 6.3), but due to

lack of stratigraphic markers the direction and amount of displacement cannot be determined. Cataclasites transect Köli and Seve units in the area south of Neset (in between the two basement highs), where they form a dense pattern of N-S and E-W trending zones which are nearly vertical. Some large cataclasite zones are associated with repetition of the stratigraphy, for instance across the Neset and Aane faults (Fig. 6.2). It appears that the structures are normal faults with an estimated displacement of 900-1100 m.
By analogy it is thought that the cataclasites found in the basement were also formed by normal faulting.

Mylonites are found between nappe units and at the basement-cover contact. Figure 6.3 shows an outcrop of the mylonite at the northern basement-cover contact in the Sandøla region (Fig. 6.2). The mylonites dip steeply north, the lineation, defined by parallel arrangement of mica flakes and quartz rods, is horizontal (E-W). Another type of lineation displayed by some mylonites is formed by steeply plunging slickenside striae. In the mylonites rootless isoclinal folds are found with foldaxes parallel to the main lineation (Fig. 6.4).
The mylonite belt at the basement-cover contact south of Nordli trends N-S also in this zone the lineation is nearly horizontal (N-S).
The structural relation of the cover rocks with respect to the mylonites (reorientation of the foliation and lineation accompanied by mylonitization) is similar to that of a dextral shear zone (Fig. 6.2). This leads to the conclusion that the mylonites were formed by shearing due to movement of the cover with respect to the basement.

The relative age of the cataclasites and mylonites varies at different places. Figure 6.5 illustrates these relations at the north-eastern corner of the culmination. It is a detailed map showing the trace of the foliation in the mylonites and the trend of the cataclasites. At Fisketjörna a N-S cataclasite zone cuts-off an E-W trending mylonite belt in the Granite-mylonite nappe. Further south this cataclasite grades into a mylonite, quartz veins which were formed during or after cataclasis are plastically deformed in a manner as described in Chapt. 2. Locally the rocks are pure quartz mylonites with a strong dimensional and crystallographic fabric (Fig 6.6, Fig.6.7). The mylonite belt cross-cuts the central dome structure of the Grong culmination at Lapplager.

Figure 6.3. Platy mylonites outcropping at the river Sandøla, 30 km. W of Nordli. Note the horizontal lineation.

Figure 6.4. Similar folds in mylonites.

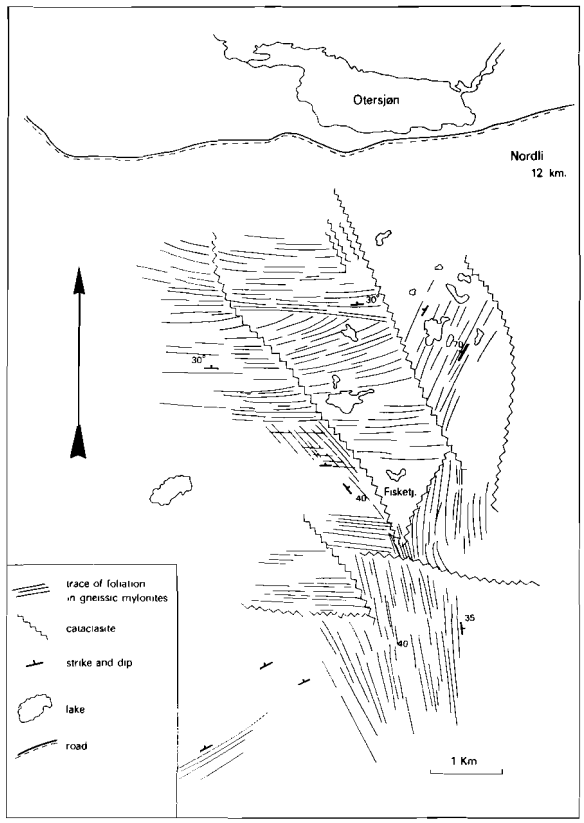

Figure 6.5 Detailed map of an area 12 km W of Nordli, showing the relationship of cataclasites an mylonites.

Figure 6.6. Microstructure of plastically deformed quartz vein. Scale bar:1mm. Crossed polarizers.

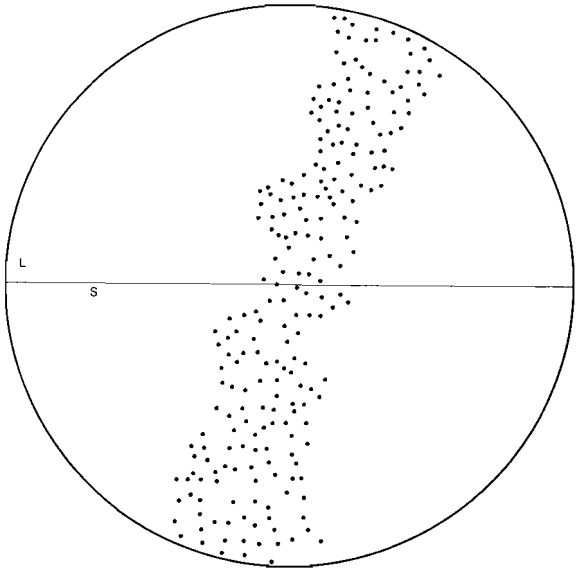

Figure 6.7

C-axes orientation pattern of quartz-rich mylonite, probably derived from a cataclasite in the basement. N=200; L=direction of the lineation; S marks the orientation of the foliation.

At several places this N-S trending mylonite zones is crossed by E-W trending cataclasites which themselves may grade into mylonites.

From the offset of stratigraphic markers it was concluded that cataclasites were formed by vertical movement of the basement relative to the cover. The structural relations of the cover rocks and mylonites show that the latter were produced by relative horizontal movement of the cover with respect to the basement, i.e by thrusting.
In the previous chapters it is shown that on a mesoscopic and microscopic scale there has been an alternation of brittle and plastic deformation in the rocks. Although much of the micro-faulting and associated veining could have been due to local brittle failure (for instance due to strain hardening), in this section it is argued that a similar switch in deformation has taken place also on a regional scale: block faulting of the basement (producing cataclasites) and concurrent thrusting of the cover rocks (causing plastic deformation of the cataclasites).
A possible explanation for such a switch in mechanisms on a regional scale is that block faulting of the basement resulted from movements in the deep underground. Such movements could for instance have been induced by episodic release of stresses due to uncompensated load (cf. Garfield, 1976), imposing a high strain rate type of deformation in the granitic upper crust. This process may have taken place while the relative warm cover rocks were plastically flowing over colder basement (cf. Andreasson and Bryhni, 1980).

6.4. The early structural history of the Grong culmination.

As described in section 6.2 the Grong-Olden culmination is formed by two interfering major folds: the Grong and Olden antiforms. According to Gee (1980) the E-W trend of the Grong antiform is an initial transverse structure, being refolded by N-S trending folds of the Trondheim synclinorium. However, Fig. 6.2 shows that one of these folds, the Snåsa synform, shows a reorientation of the axial plane from a Caledonian trend in the cover to a transverse one near the basement. Also the Tømmeras antiform and the Trøndelag synform show this change in trend.
Hence the interpretation of Gee is not satisfactory.
The author's interpretation is that the Grong and Tømmeras antiforms and the Snåsa and Trøndelag synforms belong to the same system of folds, namely the Trondheim synclinorium. This means that in this view the Grong

antiform initially was a fold with a Caledonian trend, reoriented towards a transverse structure (like the Tømmeras antiform and Snåsa and Trøndelag synforms) and subsequently refolded by the Olden antiform.
It is concluded that folding, and hence the formation of the Grong culmination, postdated nappe emplacement in the Scandinavian Caledonides because the cover and basement rocks are concordantly folded in relatively tight folds.

6.5. Late structural history of the Grong culmination.

Comparison of the basement-cover relations of the northern and southern rim of the Grong culmination indicates that there are a number of differences between these areas which indicate a discrepancy of the relative age of thrusting and the formation of the basement high and of the tectonic regime, namely:

- Whereas at the southern rim the basement is covered by a thin, but continuous veneer of parautochthonous sediments, in the north this unit is only locally found.
- The nature of the contact is different. In the north the contact is formed by shear zones and cataclasites, while in the southern region such structures have not been observed.
- In the southern region the foliation of the basement gneisses and that in the cover rocks is parallel, whereas at the northern rim there is always a discordant relation.
- At the southern edge, basement and cover rocks are concordantly folded by large scale folds which are persistent in the Grong culmination, whereas in the north the contact mylonites transect the internal structure of the culmination.

The occurrence of cataclasite zones has been correlated with blockfaulting in the basement. Because these structures are found only in the north, it is thought that this faulting is due to tilting of the basement along an axis which runs approximately E-W. In the previous section it was argued that cataclasis and mylonitization were alternating processes. Because it was found that mylonites are due to horizontal movement of the cover relative to the basement, it is concluded that late stage block-faulting was simultaneous with late stage thrusting. In this respect it is inter-

esting to discuss the pattern of the foliation in the cover rocks and mylonites around the north-eastern edge of the Grong culmination.

The swing in orientation of the foliation in the coverrocks towards parallellism with that in the mylonites at the northern and north-eastern rim of the Grong culmination has been attributed to folding of flat lying mylonites during updoming (cf. Kollung, 1979).
The alternative explanation is that the cover rocks moved around an existing basement culmination, thereby producing steeply dipping shear zones at the margins. In both cases a similar pattern of orientation of the foliation in the cover rocks would be found. However the pattern of the extension lineations in the mylonites around the culmination would be different.
When a rock undergoes a large progressive simple shear, the longest axis of the strain ellipsoid is nearly parallel to the shear direction (Ramsay, 1970). In mylonites this direction is parallel to the extension lineation, which in the case of quartz-rich rocks can be further defined with the quartz-c-axes orientation pattern (Tullis, 1977; Lister and Hobbs, 1980), in other rocks it is usually defined by alignment of inequant minerals (Hobbs et al., 1976). In mylonites formed during thrusting the shear direction, and thus the extension direction is parallel to the direction of the movement of the nappes (see discussion in section 1.3).
If the pattern of the foliation in the mylonites around the Grong culmination had been due to post-nappe folding, then the extension lineation in the mylonites should have been folded accordingly.
In all cases however this lineation is nearly horizontal, in the Sandøla region it plunges gently to the W., south of Nordli it is horizontal or gently plunging to the S. In Nordli the mineral lineation in the cover rocks curves around the north-eastern point of the culmination (Fig. 6.8). This pattern of lineation orientations is inconsistent with folding of initially flat lying lineation, but is compatible with the model of flow of the cover rocks around an existing basement high, the direction of thrusting having been influenced by the topography of the basement.

In the Scandinavian Caledonides all rock units tend to thin out westwards (Gee and Zachrisson, 1974). The rock units of the cover show wedge-like outcrop patterns at the northern basement-cover contact, which could be interpreted as the result from folding of the thinned-out strata. However, the western and central belt of the Seve nappe are cut-out against the base-

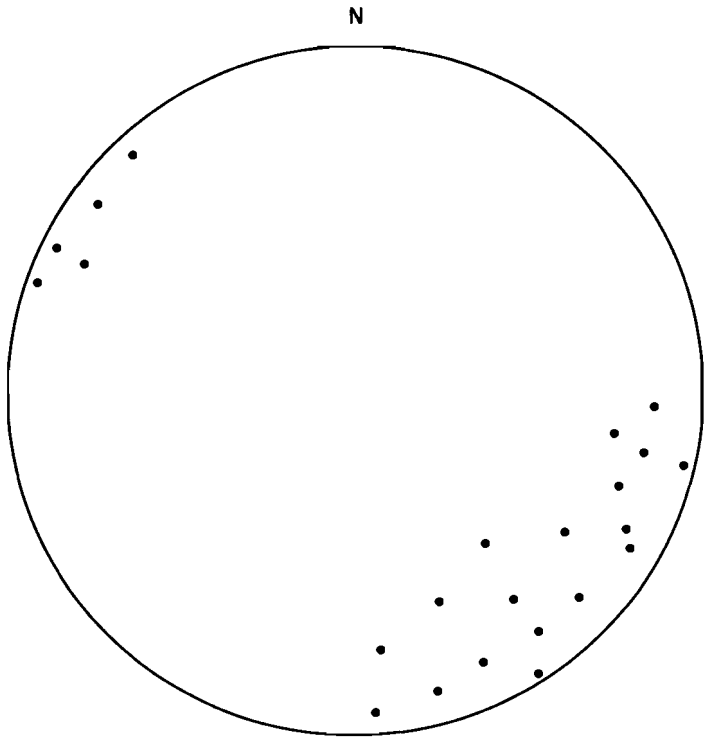

Figure 6.8 Orientation pattern of extension lineations in cover rocks around Nordli. (partly after Reymer, 1974).

ment-cover contact in Nordli, which is ca. 30 km E from the most western occurrence of these units in the central parts of the Caledonides (Williams and Zwart, 1977). Also the members of the Lasterfjäll and Tjopasi groups (middle and lower Köli units) wedge out anomalously. In Norldli the complete Lasterfjäll group (with a thickness of ca. 1000m) is cut out within a range of 50 m.
In the authors interpretation, the stratigraphic thinning was influenced by the Grong culmination, i.e. parts of the nappe pile were lost (sheared out of the succession) as a response to the obstruction,created by the culmination, to the movement of the nappes that overrode it at the time of emplacement.

There is both structural and stratigraphic evidence that (late stage) thrusting post-dated the formation of the Grong culmination at the northern basement-cover contact.
At the southern rim, basement and cover are both folded by tight folds partly form the Grong culmination. It is thought that in this region after the formation of these structures (and hence of the culmination) no further nappe transport took place.
Hence the acceptance of the model proposed in this section leads to the conclusion that north of the Grong culmination thrusting was younger, or alternatively lasted longer than south of this structure.

6.6. Thrusting in the southern and central Scandinavian Caledonides: a discussion.

The northern rim of the Grong culmination is a large scale shear zone, it is interpreted that this is the result of the fact that thrusting in the southern and central Scandinavian Caledonides was not synchronous.
It is interesting to speculate upon the question to what extent this difference in thrusting affected the large scale geology.

Comparing the geology of the central and southern Scandinavian Caledonides (north and south of the Grong culmination respectively) there are some marked differences, namely:

-The so-called Nordland granite suite, which consists partly of intrusives

in a regular pattern of 400 km in length along the Norwegian coast stops at the northern rim of the Grong culmination and cannot be traced south of it.

-In the southern Caledonides Seve units occur as far as 50 km West of Trondheim (Gee, 1980; Ramberg, 1980; Andreasson and Gorbatschev, 1980); in the central Caledonides the westerly extension of the Seve nappe is thought to be 150 km to the east, measured perpendicular to the grain of the orogen (cf, Zachrisson, 1973; Gee and Zachrisson, 1979).

-The Trondheim synclinorium, which is marked by strong negative magnetic anomalies that are correlated with the basement topography (Dyrelius, 1980) appears to die out at the Grong culmination. North of this structure no negative anomalies are found, the basement being a gentle basin in the area between the Grong culmination and the Borgafjell window (Kollung, 1979).

In short, the pattern of Caledonian intrusions, the cover stratigraphy and the structure of the basement differ markedly, and there is no horizon in both parts of the Caledonides which can be correlated.
There are two alternative ways to explain the discrepancy:
i) The tectono-metamorphic regime of the central and southern Caledonides was different.
ii) The cover of the two parts are shifted with respect to each other, e.g. by a difference in the amount of nappe transport.

According to Ramberg (1980) the Nordland granites represent the central part of the orogen. Supposing that this suite of intrusives originally was continuous throughout the entire orogenic belt, then because nappe movement was towards SE, its absence in the southern Caledonides could indicate that here the axial zone of the orogen is located W of the Norwegian coast. This would imply a dextral shift of the central Caledonides with respect to the southern.
The same relative movement could be deduced from the fact that the westerly extension of the Seve in the central Caledonides is located 150 km east of the most western Seve occurrence in the southern Caledonides.
Speculating further on this idea, the reorientation of the folds belonging to the Trondheim synclinorium from a Caledonian trend in the south to a

transverse trend in the Grong culmination could also be the result of a dextral shear.

This interpretation implies that the nappes in the central Scandinavian Caledonides were thrusted considerably further eastwards than those in the south.

REFERENCES.

Allison, J., Barnett, R.L. and Kerrich, R.; 1979: Superplastic flow and changes in crystal chemistry of feldspars. Tectonophysics 53:T41-T46

Alm, O., Röshoff, K. and Stephansson, O.; 1980: Microstructures and mechanical characteristics of the Tännas augen gneiss, Swedish Caledonides. Geol. Fören. Förhand. 102:319-334

Anderson, O.; 1928: The genesis of some types of feldspar from granite pegmatites. Norsk Geol. Tidskr. 10:116-207

Andreasson, P.G. and Gorbatschev, R.; 1980: Metamorphism in extensive nappe terrains: a study of the central Scandinavian Caledonides. Geol. Fören Förhand. 102:335-358

Asklund, B.; 1938: Hauptzuge der Tektonik und Stratigraphie der mitteren Kaledoniden in Schweden. SGU C417:1-99

Asklund, B.; 1955 Norges geologi och fjällfjedje problemen, 1955: Geol. Fören. Förhand. 77

Asklund, B.; 1960: The geology of the Caledonian mountain chain and adjacent areas in Sweden. SGU 16:1-47

Atkinson, B.K.; 1982: Subcritical crack propagation in rocks: theory, experimental results and applications. Journal of Structural Geology 4:41-56

Augevine, C.L., Turcotte, D.L. and Furnish, M.D.; 1982: Pressure solution lithification as a mechanism for the stick-slip behaviour of faults. Tectonics 1:151-160

Aukes, P.G., Reymer, A.P.S., de Ruiter, G.W.M., Stel, H. and Zwart, H,J.; 1979: The geology of the Lierne district, north-east of the Grong culmination, central Norway. Norges Geol. Unders. Publ. 354: 115-129.

Bambauer, H.U.; 1961: Spurenelementgehalte und Farbzentern in Quarzen aus Zerklüften der Schweizer Alpen. Schweiz. Miner. Petrogr. Mitt. 41:335-369

Beach, A.; 1979: Pressure solution as a metamorphic process in deformed terrigenous sedimentary rocks. Lithos 12:51-58.

Beach, A.; 1980: Retrogressive metamorphic processes in shear zones with special reference to the Lewesian complex. Journal of Structural Geology 2:257-263

Beach, A.; 1982: Deformation mechanisms in some cover sheets from the external French Alps. Journal of Structural Geology 4:137-149.

Behr, H.J., Ahrendt, H., Schmidt, A., and Weber, K.; 1981: Saline horizons acting as thrust planes along the southern margin of the Damara orogen (Namibia, SW Africa) in: Thrust and Nappe Tectonics (McClay and Price eds.). Geol. Soc. London, special issue no.9:167-173

Behrmann, J.H. and Platt, J.P.; 1982: Sense of nappe emplacement from quarz-c-axis fabrics; an example from the Betic Cordilleras (Spain) Earth and Planet. Sci. Let. 59: 208-215

Bell, T.H.; 1979: The deformation and recrystallization of biotite in the Woodroffe thrust mylonite zone. Tectonophysics 58:139-158

Bell, T.H.; 1981: Foliation development-The contribution, geometry and significance of progressive, bulk inhomogeneous shortening. Tectonophysics 75:273-296

Bell, T.H. and Etheridge, M.A.; 1973: Microstructure of mylonites and their descriptive terminology. Lithos 6:337-348

Bell, T.H. and Etheridge, M.A.; 1976: The deformation and recrystallization of quartz in a mylonite zone, central Australia. Tectonophysics 32:234-267.

Bell, I.A. and Wilson, C.J.L.; 1981: Deformation of biotite and muscovite: TEM microstructure and deformation model. Tectonophysics 78: 201-229

Boland, J.N.; 1974: Dislocation substructures in naturally and experimentally deformed olivine. In: Swann, P.R.,(ed.); High Voltage Electron Microscopy. Academic Press, London: 312-316

Boullier, A.M. and Gueguen, Y.; 1974: SP-mylonites. Origin of some mylonites by superplastic flow. Contrib. Mineral. Petrol. 50:312-316

Brown, W.L. and Parsons, I.; 1983: Nucleation on perthite-perthite boundaries and exsolution mechanisms in alkali feldspars. Phys. Chem. Minerals 19:55-61

Brown, W.L. and Willaime, C.; 1974: An explanation of exsolution orientations and residual strain in cryptoperthites. In: MacKenzie, W.S. and Zussman, J. (eds.); The Feldspars. Manchester Univ. Press, Manchester:440-460

Brunner, G.O., Wondratschek, H. and Laves, F.; 1959: Uber die Ultrarotabsorption des Quartzes. Naturwissenschaften, 24:661

Byerlee, J.D., 1967: Frictional characteristics of granites under high confining pressure. J. Geophys. Res. 72:3639-3648

Byerlee, J.D. and Brace W.F.; 1972: Fault stability and pore pressure. Bull. Seismol. Soc. Am. 62:657-660

Carreras, J., Estrada, A. and White, S.; 1977: The effect of folding on the c-axis fabric of quartz mylonite. Tectonophysics 39:3-24

Carreras, J., Cobbold, P.R., Ramsay, J.G. and White S.H. 1980 : Shear zones in rocks. Special Issue of the Journal of Structural Geology Vol. 2, 287 pp.

Carreras, J., Julivert, M. and Santanach, P.; 1980: Hercynian mylonite belts in the eastern Pyrenees: an example of shear zones associated with late foldings. Journal of Structural Geology 2:5-9

Carter, N.L., Christie, J.M. and Griggs, D.T.; 1964: Experimental deformation and recrystallization of quartz. J. Geol. 72:687-733

Champness, P.E. and Lorimer, G.W.; 1976: Exsolution in silicates. In: Wenk, H.R. (ed.) Electron Microscopy in Mineralogy. Springer Verlag, Berlin: 174-204

Christie, J.M.; 1960: Mylonitic rocks of the Moine thrust zone in the Assynt region, north west Scotland. Trans. Edinburgh Geol. Soc. 18: 79-93

Christie, J.M.; 1963: The Moine thrust in the Assynt region, north west Scotland. Univ. Calif. Publs. Geol. Sci. 40:345-419

Claesson, S.; 1980: A Rb-Sr isotope study of granitoids and related mylonites in the Tännas augen gneiss nappe, southern Swedish Caledonides. Geol. Fören. Förhand. 102:403-420

Cooper, M.A.; 1981: The internal geometry of nappes: criteria for models of emplacement in: McClay, K.R. and Price N.J. (eds) Thrust and Nappe Tectonics. Geol. Soc. London Special publication no. 9: 225-234.

Cooper, M.A. and Bradshaw, R.; 1980 The significance of basement gneiss domes in the tectonic evolution of the Salta region, Norway. Geol. Soc. London J. 137:231-240

Deer, W.A., Howie, R.A. and Zussman, J.; 1963: Rock forming Minerals, vol. 4. Framework Silicates. Longmans, Green and Co., Ltd. London 435pp.

Dieterich, J.H.; 1972: Time-dependent friction in rocks. J. Geoph. Res: 3690-3697

Dieterich, J. H.; 1978: Time dependent friction and the mechanism of stick slip. Pure Appl. Geophys. 116:790-806
Dyrrelius, D.; 1980: Aeromagnetic interpretation in a geotraverse area across the central Scandinavian Caledonides. Geol Fören. Förhand. 102: 421-438
Eggleton, R.A. and Buseck, P.R.; 1980: The orthoclase-microcline inversion: a high resolution transmission electron microscope study and strain analyses. Contrib. Mineral. Petrol. 74:123-133
Elliot, D.; 1976: The motion of thrust sheets. J. Geoph. Res. 81:949-963
Ferry, J.M.; 1983: Regional metamorphism of the Vassalboro formation, South Central Maine, USA: a case study of the role of fluid in metamorphic petrogenesis. J. Geol. Soc. London 140: 551-576
Fitz Gerald J.D. and McLaren, A.C.; 1982: The microstructures of microcline from some granitic rocks and pegmatites. Contrib. Mineral. Petrol. 80:219-229
Foslie, S. 1958. Map sheet Sandøla. Geologisk karten. Norges Geol. Unders. Oslo.
Foslie, S.; 1959: Map sheet Nordli. Geologisk karten. Norges Geol. Unders. Oslo.
Foslie, S.; 1960: Map sheet Sørli. Geologisk karten. Norges Geol. Unders. Oslo.
Frey, M., Hunziker, J.C; O'Neill, J.R. and Schander, H.W.; 1976: Equilibrium disequilibrium relations in the Monte Rosa granite, western Alps: petrological, Rb-Sr and stable isotope data. Contrib. Mineral. Petrol. 55:147-179
Friedel, J.; 1964: Dislocations. Pergamon Press, Oxford: 491 pp.
Friedman, M., Logan, J.M. and Rigert, J.A.; 1974: Glass-indurated quartz gouge in sliding-friction experiments on sandstone. Bull. Geol. Soc. Am. 85:937-942
Frondel, C.; 1978: Characteristics of quartz fibers. Am. Mineral. 63:17-27
Fyfe, W.S., Price, N.J. and Thompson, A.B.; 1978: Fluids in the Earth's Crust. Elsevier, Amsterdam: 383pp
Garland, G.D.; 1979: Introduction to Geophysics. Saunders, Philadelphia, 493 pp.
Gee, D.G.; 1974:Comments on the metamorphic allochton of northern Trøndelag, central Scandinavian Caledonides. Norsk Geol. Tidskr. 54:435-440
Gee, D.G.; 1975a: A tectonic model for the central part of the Scandinavian Caledonides. Am. J. Sci. 275-A:468-515
Gee, D.G.; 1975b: A geotraverse through the Scandinavian Caledonides-Ostersund to Trondheim. SGU, C717: 66pp.
Gee, D.G.; 1978: Nappe displacement in the Scandinavian Caledonides. Tectonophysics 47:393-419
Gee, D. G., 1980: Basement-cover relations in the central Scandinavian Caledonides. Geol. Fören. Förhand. 102:455-474
Gee, D.G. and Zachrisson, E.; 1974: Comments on stratigraphy, faunal provinces and structure of the metamorphic allochton, central Scandinavian Caledonides. Geol. Fören. Förhand. 96:61-66
Gee, D.G. and Zachrisson, E.; 1979: The Caledonides in Sweden. SGU, C742, 1-35.
Goldsmith, J.R. and Laves, F.; 1954: Potassium feldspars structurally intermediate between microcline and sanidine. Geochim. Cosmochim. Acta 6: 100-118
Graham, C.M., Greig, K.M., Sheppard, S.M. and Turi, B.; 1983: Genesis and mobility of the H_2O-CO_2 fluid phase during regional greenschist and epidote amphibolite facies metamorphism:petrological and stable isotope study in the Scottish Dalradian. J. Geol. Soc. London. 140: 577-599

Graham, R.H.; 1981: Gravity sliding in the Maritime Alps. in McClay, K.R. and Price, N.J. (eds.) Thrust and Nappe Tectonics. Geol. Soc. London Special publication no. 9: 335-352
Gratier, J.P.; 1982: Approche experimentelle et naturelle de la déformation des roches par dissolution et cristallisation avec transport de matiere. Bulletin Minéralogie 105:291-300
Greiling, R.; 1975: Der Südrand des Børgefjell Fensters. Zeit. Deutschen Geol. Ges. 126: 155-165
Griffith, A.A.; 1924: A theory of rupture. Proc. 1st Int. Cong. on Applied Mechanics, Delft, 55
Griggs, D.T.; 1938: Deformation of single calcite crystals under high confining pressure. Am. Mineral 23: 28-33
Griggs, D.T. and Handin, J. (eds) Rock Deformation. Geol. Soc. Am. Mem. 79
Gustavson. M and Grønhaug, A.; 1960: En geologisk undersøkelse på den nord vestlige del av kartblatt Børgefjell. Norges Geol. Unders. 211: 26-74
Gustavson, M.; 1973: Borgefjell- Beskrivelse til det berggrunnsgeologiske gradteigskart. Norges Geol. Unders. 298:1-43
Hanmer, S.K.; 1982: Microstructure and geochemistry of plagioclase and microcline in naturally deformed granite. Journal of Structural Geology 4:197-215
Heimann, R.B.; 1979: Hydrothermale Verdrängingsreaktionen an Alkalifeldspäte der Zusammensetzungen $Or_{93}Ab_7$ und $Ab_{96}Or_4$ Neues Jahrb. Min. Abh. 137:1-19
Helgeson, H.C.; 1974: Chemical interaction of feldspars and aqueous solutions.. In: McKenzie, W.S. and Zussman, J. (eds.); The feldspars. Manchester Univ. Press, Manchester: 184-218
Higgins, M.W.; 1971: Cataclastic rocks. U.S Geol. Surv, Prof. Pap. 687: 1-97.
Hobbs, B.E., Means, W.D. and Williams, P.F.; 1976: An Outline of Structural Geology. Wiley, New York. 571 pp.
Högbom, A.E.; 1920: Geologisk beskrivning över Jämtlands Län. SGU C140, 98 pp.
Holmes, A.; 1965: Principles of Physical Geology. Nelson and Sons, London 1288 pp.
Hoschek, G.; 1973: Zur stabilität metamorpher biotit paragenesen. Tschermaks Mineral. Petrol. Mitt. 20: 48-58
Hoskins, E.R., Jaeger, J.C. and Rosengren, K.J.; 1968: A medium-scale direct friction experiment. Int. J. Rock mech. Min. Sci. 5:143-154
Hull, R.; 1975: Introduction to Dislocations. Pergamon Press. 271 pp.
Jaeger, J.C.; 1943: The effect of absorption of water on the mechanical properties of sandstones. J. Inst. Eng. Aust. 15:164-166
Johansson, L.; 1980: Petrochemistry and regional tectonic significance of metabasites in basement windows of the central Scandinavian Caledonides. Geol. Fören. Förand. 102:499-514
Johansson, L.; 1981: The relationship between the Vestranden gneiss area and the Grong-Olden basement complex. Terra Cognita 1: 54

Kerrich, R.; 1977: An historical review and synthesis of research on pressure solution. Zentralbl. Geol. Paleont. H5/6:512-550
Kerrich, R., Allison, I., Barnett, R. L., Moss, S. and Starkey, J.; 1980: Microstructural and chemical transformations accompanying deformation of granite in a shear zone at Miéville, Switzerland; with implications for stress corrosion cracking and superplastic flow. Contrib. Mineral. Petrol. 73:221-242

Klingspor, I. and Troëng, B.; 1980:Rb-Sr and K-Ar age determinations of the Proterozoic Olden granite, central Caledonides, Jämtland, Sweden. Geol. Fören. Förhand.102:515-523

Kohlstedt, D.L. and Goetze, C.; 1974: Low stress, high temperature creep in olivine single crystals. J.Geoph.Res. 79:2045-2051

Kollung, S.; 1979: Stratigraphy and major structures of the Grong district, Nord Tröndelag. Norges Geol. Unders. 354:1-52

Kovacs, M.P. and Gandais, M.; 1979: Transmission electron microscopy study of experimentally deformed K-feldspar single crystals. The (121) 101 and 010 100 slip sysytems. Phys. Chem. Minerals 6:61-76

Lapworth, C.; 1885: The highland controversy in British geology; it causes, course and consequences Nature 32:558-559

Lamouroux, C., Soula, J.C., Déramond, J. and Debat, P.; 1980: Shear zones in the granodiorite massifs of the central Pyrenees and the behaviour of these massifs during the Alpine orogenesis. Journal of Structural Geology 2:49-53

Laves, F.; 1952: Mechanische Zwillungsbildung in Feldspaten in Abhangigheit von Ordnung-Unordnung der Si/Al Verteling innerhalb des $(Si,Al)_4O_8$-Gerüstes. Naturwiss. 39:546-547

Laves,F.; 1974: Domain and deformation textures in plagioclases and their investigation by photo-emission electron microscopy (PEEM) and by transmission electron microscopy. in: McKenzie, W.S. and Zussman, J. (eds); The Feldspars. Manchester Univ. Press, Manchester:522-536

Lister, G.S. and Hobbs, B.E.; 1980: The simulation of fabric development during plastic deformation and its application to quartzite: the influence of deformation history. Journal of Structural Geology 2: 355-371

Luth, W.C.; 1974: Analysis of experimental data on alkalifeldspars: unit cell parameters and solvi. in: McKenzie, W.S. and Zussman, J. (eds) The Feldspars, Manchester Univ. Press, Manchester:247-296

Mäkinen, E.; 1913: Die Granitpegmatite von Tamella in Finnland und uhre Minerale. Bull.Geol. Soc. Finl. 35:101pp

Marfunin, A.S.; The Feldspars-Phase Relations, Optical properties, and Geological Distribution. Israel Prog. Sci. Translations:Jerusalem 317 pp.

Marshall, D.B, Vernon, R.H. and Hobbs, B.E.; 1976: Experimental deformation and recrystallization of peristerite. Contr. Mineral. Petrol. 57: 48-54

Martin, R.F.; 1974: Controls of ordering and subsolidus phase relations in the alkali feldspars. in McKenzie, W.S. and Zussman, J. (eds) The Feldspars. Manchester Univ. Press, Manchester:313-336

McConnell, J.D.C.; 1965: Electron optical study of effects associated with partial inversion in a silicate phase. Phil. Mag. 11:1289-1301

McLaren, A.C.; 1974: Transmission electron microscopy of the feldspars. in McKenzie, W.S. and Zussman, J. (eds) The Feldspars. Manchester Univ. Press, Manchester:378-423

McLaren, A.C.; 1975: Microstructures of the plagioclase feldspars. Proc. of EMAG 75, Univ. Bristol (Venables, J.A, ed) Academic Press:461-466

McLaren, A.C.; 1978: Defects and microstructures in feldspar. Chem. Phys. Sol. and Surf., The Chemical Society, London:1-30

Megaw, H.D.; 1974: The architecture of feldspars. in: McKenzie, W.S. and Zussman, J. (eds) The Feldspars. Manchester Univ.Press, Manchester: 2-24

Meyer, C. and Hemley, J.J.; 1967: Wall rock alteration. in: Barnes,L. (ed) Geochemistr of hydrothermal ore deposits. Holt, Rinehart and Winston Inc. New York:166-235

Miehe, G., Graetsch and Flörke, O.W.; 1984: Crystal structure and growth fabric of length-fast chalcedony. Phys. Chem. Minerals 10:197-199
Mitra, G.; 1978: Ductile deformation zones and mylonites, the mechanical processes involved in the deformation of crystalline basement rocks: Am.J.Sci Vol.278 no.8: 1057-1084
Mitra, G,; 1979: Ductile deformation zones in Blue Ridge basement rocks and estimation of finite strains: Geol. Soc. Am.Bull.90:935-951
Miyashiro, A.;1973: Metamorphism and Metamorphic Belts. Allen and Unwin, London. 492pp.
Murrel, S.A.F.; 1981: The rock mechanics of thrusts and nappe formation. in McClay, K.R. and Price, N,J.(eds) Thrust ans Nappe Tectonics. Geol.Soc. London, special publication no. 9:99-110
Nabarro, F.R.N., 1967: Steady state diffusional creep. Phil. Mag. 16:231-237
Nassau, K. and Prescott, B.E.; 1978: Growth induced radiation developed pleochroic anisotopy in smoky quartz. Am. Mineral. 63:230-238
Nicholson, R. and Rutland, R.W.R.; 1969: A section across the Norwegian Caledonides: Bodø to Sulitjelma. Norges Geol. Unders. 260: 88pp.
Nicolas, A. and Poirier, J.P.; 1976: Crystalline Plasticity and Solid State Flow in Metamorphic Rocks. Wiley and sons; London. 444pp.
Nickel, E.; 1978: The present status of cathode luminescence as a tool in sedimentology. Miner. Sci. Eng. 10(2)
Oehler, J.W.; 1976: Hydrothermal crystallization of a silica gel. Geol. Soc. Am. Bull. 87:1143-1152
Oftedahl, C.; 1956: Om Grongkulminasjonen og Grongsfeltet skyvedekken. Norges Geol. Under. 195: 57-64
Orville, P.M.; 1962: Alkali metasomatism and feldspars. Norsk Geol. Tidskr. 42:283-316
Orville, P.M.; 1963: Alkali ion exchange between vapor and feldspar phases Am. Journ. Sci. 261-237
Passchier, C.W.; 1982: Mylonitic Deformation in the Saint Barthélemy Massif, French Pyrenees, with Emphasis on the Genetic Relationship between Ultramylonite and Pseudotachylite. GUA papers of geology series 1, no. 16, 171 pp.
Paterson, M.S.; 1978: Experimental Rock Deformation-The Brittle Field. Springer Verlag Berlin. 254 pp.
Peacey , J.S., 1964: Reconnaissance of the Tømmeràs anticline.Norges Geol. Unders. 227
Petrovic, R.; Diffusion of alkali ions in alkalifeldspars in: McKenzie, W.S. and Zussman, J. (eds) The Feldspars. Manchester Univ. Press, Manchester: 174-182
Platt, J.P. and Vissers, R.L.M.; 1980: Extensional structures in anisotropic rocks. Journal of Structural Geology 2:397-410
Point, R.; 1975: Mylonites et orogenèse tangentielle, nature, géochimie, origine et age des gneiss oeillés dans les nappes Caledoniennes externes. Bull. Soc. Geol. France 7:664-679
Poirier, J.P. and Guiloppé, M.; 1979: Deformation induced recrystallization of minerals. Bull. Minéral. 102:67-74
Ramberg, H.; 1952: Origin of Igneous and Metasomatic Rocks. Univ. Chicago Press, 273pp.
Ramberg, H.; 1967: Gravity, Deformation and the Earth's Crust as studied by Centrifuged models. Academic Press, New York, 241pp.
Ramberg, H.; 1972: Theoretical model of density stratification and diapirism in the earth. J. Geoph. Res. 77:877-889
Ramberg, H.; 1977: A tectonic model for the central Scandinavian Caledonides. Am. Journ. Sci. 277:647-656

Ramberg, H.; 1980: Diapirism and gravity collapse in the Scandinavian Caledonides. Journ. Geol. Soc. London. 137:261-270
Ramberg, H.; 1981: The role of gravity in orogenic belts. in McClay, K.R. and Price, N.J. (eds) Thrust and Nappe Tectonics. Geol. Soc. London, special publication no. 9:125-140
Ramsay, J.G.; 1980: The crack-seal mechanism of rock deformation. Nature 284:135-139
Ramsay, J.G. and Graham, R.H.; 1970: Strain variations in shear belts. Canadian J. of Earth Sci., 7:786-813
Råheim, A., Gale, G.H. and Roberts, D.; 1979: Rb-Sr ages of basement gneisses and supracrustal rocks of the Grong area, Nord Tröndelag. Norges Geol. Unders. 354:116-131
Read, A., 1953: Dislocations in Crystals. Wiley, New York, 211pp.
Reymer, A.P.S.; 1975: The geology of the Nordli area. Internal report Univ. Leiden, 75pp.
Reymer, A.P.S.; 1979: Age determinations on reworked crystalline basement. Norges Geol. Unders. 354:143-149
Ribbe, P.H.; 1974: The chemistry, structure and nomenclature of feldspars. in: Ribbe, P.H. (ed) Min. Soc. Am. Short Course Notes vol.2: Feldspar Mineralogy. Washinton D.C. :R1-R28
Roberts, D.; 1967: Structural observations from the Koppera-Riksgrensen area and discussion of the tectonics of Stjørdalen and the NE Trondheim region. Norges Geol. Unders. 245:64-122
Roberts, D.; 1968: Geological investigations in the Snåsa-Lurudal area, N-Tröndelag. Norges Geol. Unders. 247:18-38
Roberts, D., Springer, J. and Wolff, F.C.; 1970: Evolution of the Caledonides in the northern Trondheim region, central Norway: a review. Geol. Mag. 107:133-145
Roberts, D. and Wolff, F.C.; 1981: Tectonostratigraphic development of the Tronheim region Caledonides central Norway. Journal of Structural Geology 3: 487-494
Robie, R.A., Hemingway, B.S. and Fisher, J.R.; 1978: Thermodynamic Properties of Minerals and related substances at 298.15°K. and 1 Bar (10^5P) Pressure and at Higher Temperatures. Geol.Surv. Bull. 1452, 456pp.
Rosenqvist, I.; 1944: Metamorphism and metasomatism in the Opdal area (Sör Tröndelag, Norway) Norges Geol. Unders. 299
Röshoff, K; 1978: Deformation structures in the Tännas augen gneiss. Proceedings of the interdisciplinary conference on mechanisms of deformation and fracture. Luleå. 150-162
Röshoff, K.; 1978: Structure of the Tännas augengneiss nappe and its relation to under- and overlying units in the central Scandinavian Caledonides. SGU C739:1-35
Rui, I.; 1972: Geology of the Röros district, south eastern Trondheim region, with special study of the Kjöliskarvene-Holtsjoën area. Norsk Geol. Tidskr. 52: 1-21
Rutter, E.H.; 1976: The kinetics of rock deformation by pressure solution. Philos. Trans. R. Soc. London. Ser. A, 283:203-213
Rutter, E.H.; and White, S.H.; 1979: Effects of water, temperature and time on the microstructural and mechanical properties of experimentally produced fault gouge. Bull. Minéral. 102:93-101
Scandale, E., Gandais, M., and Willaime, C.; 1982: Transmission electron microscopic study of experimentally deformed K-feldspar single crystals. The (010) 001 . (001)$\frac{1}{2}$[$\bar{1}$10] and (110)$\frac{1}{2}$[$\bar{1}$12] slip systems. Phys. Chem.Minerals 9:182-187
Schmidt, S.M., Boland, J.N. and Paterson, M.S.: 1977: Superplastic flow in fine grained limestone. Tectonophysics 43:257-292

Scholz, C., Molnar, P. and Johnson, T.; 1972: Detailed studies of frictional sliding of granite and implications for the earthquake mechanism. J. Geoph. Res. 77: 6392-6406
Sibson, R.H.; 1977: Fault rocks and fault mechanisms. J. Geol. Soc. London 133:191-213
Sibson, R.H. , McMoore, J. and Rankin, R.H.; 1975: Seismic pumping- a hydrothermal fluid transport mechanism. J. Geol. Soc. London. 131; 653-659
Sibson, R.H., White, S.H. and Atkinson, B.K.; 1981: Structure an distribution of fault rocks in the Alpine zone, New Zealand. in: McClay, K.R. and Price, N.J. (eds.) Thrust and Nappe Tectonics. Geol. Soc. London, special publication no.9:197-210
Smith, J.V.; 1974: The Feldspars. 2 volumes. Springer Verlag, Berlin.
Spiers, C.J.;1979: Fabric development in calcite polycrystals deformed at 400°C. Bull. Minéral. 102:282-289
Spry, A.; 1969: Metamorphic Textures. Pergamon Press, Oxford. 350 pp.
Stel, H.; 1981: Crystal growth in cataclasites: diagnostic meicrostructures and implications. Tectonophysics 78: 585-600
Stenina, N.G., Bazarona, L.Sh. Scherbakova, M.Ya and Mashkontsev, R.I.; 1984: Structural state and diffusion of impurities in natural quartz of different genesis. Phys. Chem. Minerals 10:180-186
Stephansson., O.; 1976: A tectonic model of the Offerdal-Olden area, Jämtland, Sweden. Geol. Fören. Förhand. 98: 112-119
Stephens, M.B.; 1977: Stratigraphy and relationships between folding, metamorphism and thrusting in the Tärna-Björkvattnet region, northern Swedish Caledonides. SGU C726:1-146
Steward, D.B.; 1975: Optical properties of alkali feldspars. in: Ribbe, P.H. (ed.) Feldspar Mineralogy. Miner. Soc. Am. Short Course Notes, Vol. 2:S1-S12
Stocker, R.L. and Ashby, M.; 1973: On the rheology of the upper mantle. Rev. Geophys. Space Phys. 11: 391-426
Strand, T.; 1951: The Sel and Våga map areas. Norges Geol. Unders. 178:5-114
Strand, T. and Kulling, O.; 1972: The Scandinavian Caledonides. Wiley Intersciences, New York, 302pp.
Strömberg, A.; 1961: On the tectonics of the Caledonides in the south-western part of the county of Jämtland, Sweden. Bull. Geol. Inst. Univ. Uppsala 3 :1-92
Taylor, W.H.; 1933: The structure of sanidine and other feldspars. Z. Krist. 85: 425-442
Thelander, T., Bakker, E. and Nicholson, R.; 1980: Basement-cover relation ships in the Nasafjellet Window, central Swedish Caledonides. Geol. Fören. Förhand. 102: 569-580
Tibbals, J.E. and Olsen, A.; 1977: An electron microscope study of some twinning and exsolution textures in microcline amazonites. Phys. Chem. Minerals 1:313-324
Törnebohm, A.E.; 1898: Grunddragen af det centrale Skandinaviens bergbyggnad. Kungl. Sv. Vet. Akad. Hand. 28
Trouw, R. A. J., 1973: Structural geology of the Marsfjällen area, Caledonides of Vâsterbotten, Sweden. SGU C689:1-115
Tullis, J.A.; 1970: Quartz: preferred orientation in rocks produced by Dauphiné twinning. Science 168:1342-1344
Tullis, J.; 1977: Preferred orientation of quartz produced by slip during plane strain. Tectonophysics 39: 87-102
Tullis, J.; Christie, J.M. and Griggs, D.T.; 1973: Microstructures and preferred orientations of experimentally deformed quartzites. Geol. Soc. Am. Bull. 84:297-314

Turner, F.J. and Verhoogen, J.; 1960: Igneous and Metamorphic Petrology. McGraw-Hill, New York
Vernon, R.H.; 1974: Metamorphic Processes. George Allen and Unwin Ltd. London, 247 pp.
Voll, G.; 1960: New work in petrofabrics. Liverpool Manchester Geol. J. 2:503-567
Wakefield, J.; 1977: Mylonitization in the Lethakane shear zone, eatern Botswana. Geol. Soc. Lond. J. 133:263-275
Webster, R.; 1970: Gems. Butterworth, London. 838 pp.
White, S.; 1976: The effect of strain on the microstructures, fabrics and deformation mechanisms in quartzites. Phil. Trans. R. Soc. London Ser. A: 283: 69-86
White, S.; 1977: Geological significance of recovery and recrystallization processes in quartz. Teconophysics 39:143-170
White, S.; 1979: Strain and sub-grain size variations across a mylonite zone. Contrib. Mineral. Petrol. 70 :193-202
White, S.H., Burrows, S.E., Carrerras, J., Shaw, N.D. and Humphreys, F,J.; 1980: On mylonites in ductile shear zones. Journal of Structural Geology 2:175-187
Willaime, C. and Gandais, M.; 1977: Electron microscopy study of plastic defects in experimentally deformed alkalifeldspars. Bull. Soc. Franc. Min. Crist. 100:263-271
Willaime, C.; Christie, J. and Kovacs, M.P.; 1979: Experimental deformation of K-feldspar single crystals. Bull. Minéral. 102:168-177
Williams, P.F. and Zwart, H.J.; 1977: A model for the development of the Seve-Köli Caledonian nappe complex. in: Sanema, S.K. and Bhattacharji, S. (eds.) Energetics of geological processes. Springer Verlag Berlin: 169-187
Wilson, C. J. L.; 1973: The prograde microfabric in a deformed quartzite sequence, Mt Isa, Australia. Tectonophysics 19:39-81
Wilson, C. J. L.; 1980: Shear zones in a pegmatite, a study of albite-mica-quartz deformation. Journal of Structural geology 2:203-209
Wintsch, R.P.; 1975: Solid-fluid quilibria in the system $KAlSi_3O_8$-$NaAlSi_3O_8$-$Al_2Si_2O_5$-SiO_2-H_2O-HCl. J. Petrol. 16:57-59
Wolff, F.C.; 1979: Beskrivelse til de berggrunns geolgiske kart Trondheim og Ostersund 1:250000 NGU Skr. 31, 76 pp.
Yoshimura, J., Miyazaki, T., Wada, T., Kohra, K., Hosaka, M., Ogawa, T. and Taki, S.; 1979: Measurements of local variations in spacing and orientation of lattice planes of synthetic quartz. J. Cryst. Growth 46:691-700
Yuen, D.A., Fleitont, L., Schubert, G.; 1978: Shear deformation along major transform faults and subducting slabs: Geoph. J. 54: 93-119
Yund, R.A.; 1975: Subsolidus phase relations in the alkalifeldspars with emphasis on coherent phases. in: Ribbe, P.H. (ed.) Feldspar Mineralogy. Min. Soc. Am. Short Course Notes Vol. 2: Chapt. 5, 25pp.
Yund, R.A.; 1983: Diffusion in feldspar. in: Ribbe, P.H. (ed.). Feldspars. Min. Soc. Am. Rev. Mineralogy, revised Vol. 2:203-222
Yund, R.A. and Davidson, P.; 1978: Kinetics of lamellar coarsening in cryptoperthites. Am. Min. 63:470-477
Yund, R.A. and Tullis, J.; 1980: The effect of water, pressure and strain on Al/Si- order-disorder kinetics in feldspars. Contrib. Mineral. Petrol. 72:297-302
Zachrisson, E.; 1973: The western extension of Seve rocks within the Seve-Köli nappe complex in the Scandinavian Caledonides. Geol. Fören. Förhand. 95: 243-251

Zwart, H.J.; 1958: La faille de Mérens dans les Pyrenees Ariégeoises. Bull. Soc. Géol. France 8: 793-796

Zwart, H.J.; 1974: Structure and metamorphism in the Seve-Köli Nappe Complex (Scandinavian Caledonides), and its implication concerning the formation of metamorphic nappes. Cent. Soc. Géol. Belgique. Géol. des Domains Cristalline, Liège: 129-144

APPENDIX I

Whole rock chemical analyses of 13 samples from the autochthonous basement (in weight %).

Nr.	89.b	79.32	79.17	8c	79.20	89.a	79.8	79.20	81.10	81.15	79.31	77.22	79.5b[x]
SiO_2	78.20	76.59	79.90	74.10	77.15	78.84	78.52	78.68	77.30	78.01	76.77	78.51	84.10
TiO_2	.06	.23	.07	.27	.26	.06	.07	.10	.24	.15	.24	.13	.02
Al_2O_3	11.85	11.60	10.66	13.39	11.22	11.86	11.69	11.78	12.03	11.88	11.63	11.41	7.82
Fe_2O_3	.76	.87	.76	.55	.46	.69	.85	.41	.33	.51	.67	.63	.44
FeO	.30	.55	.10	.68	1.29	.44	.42	.69	.41	.38	.58	.47	.13
MnO	.02	.03	.03	.06	.02	-	.05	-	-	.04	.02	.03	.02
MgO	.07	.31	.07	.32	.55	.07	.04	.09	.06	.08	.31	.28	.19
CaO	.07	.63	.05	.79	.53	.05	-	.28	.41	.33	.61	.31	.10
Na_2O	3.49	2.87	3.27	3.11	2.20	3.49	3.52	3.22	3.09	3,28	3.18	3.12	2.17
K_2O	4.72	5.04	4.41	5.87	5.08	4.96	4.94	5.23	5.11	5.03	5.14	5.63	3.49
P_2O_5	.01	.06	.02	.08	.06	.02	.02	.02	.04	.06	.02	.03	.04
H_2O	.28	.44	.28	.42	.67	.27	.26	.29	.31	.43	.42	.31	.58
CO_2	-	-	-	-	-	-	-	-	-	-	-	-	-
Tot.	99.83	99.22	99.62	99.14	99.49	100.85	100.53	100.79	99.33	100.19	99.59	100.86	99.10

Specimen 79.5b is quartz-enriched by veining (Ch.2).

APPENDIX II

Whole rock chemical analyses of samples of the Granite-mylonite nappe (in weigth %).

Nr.	00.78	79.26	81.1c	81.1b	81.1b'	81.9a	79.24'	80.39	81.21	78.04	81.56	81.56'	81.60	80.86	79.28	78.89
SiO_2	59.70	67.77	57.19	58.00	57.36	57.19	67.53	63.43	61.28	62.11	62.41	65.18	62.49	62.38	63.52	60.27
TiO_2	.72	.71	.66	.67	.72	.66	.67	.70	.73	.58	.70	.68	.69	.73	.71	.68
Al_2O_3	17.73	15.05	17.32	17.20	17.19	17.40	14.90	16.32	16.44	16.58	17.36	16.63	17.13	17.32	17.09	16.28
Fe_2O_3	.50	.17	2.68	2.80	2.89	2.20	1.31	1.05	.78	.63	1.04	.43	.51	1.06	.45	.81
FeO	4.57	2.91	3.21	3.25	3.25	3.40	1.78	3.56	4.02	4.43	3.51	3.27	3.28	3.62	3.22	3.88
MnO	.09	.08	.08	.05	.07	.07	.02	.06	.03	.06	.07	.08	.09	.06	.10	.04
MgO	2.33	.94	2.75	2.89	2.90	2.91	.91	2.63	3.41	2.27	2.86	2.43	1.36	2.24	1.24	3.52
CaO	5.00	2.96	6.00	6.44	6.44	6.00	1.92	4.32	4.36	4.79	4.35	3.57	3.75	3.68	2.88	4.58
Na_2O	3.77	3.54	3.01	4.27	4.16	3.94	3.70	3.41	4.02	3.98	3.37	3.62	4.18	3.75	4.21	3.88
K_2O	3.65	5.44	4.72	2.60	2.62	2.90	5.92	3.52	3.98	4.13	3.58	2.61	4.56	4.11	4.70	4.14
P_2O_5	.37	.25	.38	.40	.39	.37	.24	.28	.27	.36	.26	.24	.22	.32	.24	.38
H_2O	1.36	.76	1.29	1.35	1.32	1.83	.50	.68	1.38	.56	.72	1.12	.81	.68	.92	1.42
CO_2	-	-	-	.08	.20	.10	-	-	.10	-	-	-	-	-	-	-
Tot.	99.79	100.58	99.29	100.10	99.51	98.97	99.40	99.96	99.98	100.48	100.23	99.97	99.07	99.94	99.48	99.88

Sample nr's 81a-c are from one shear zone (Ch.3)

Curriculum Vitae

De schrijver van dit proefschrift behaalde in mei 1971 zijn diploma H.B.S.-B aan de Chr. H.B.S. te Assen.
In oktober 1974 werd het kandidaatsexamen in de geologie afgelegd aan de Rijksuniversiteit te Groningen.
In mei 1978 werd het doctoraalexamen afgenomen (hoofdrichting geologie, met eerste en tweede bijvak structurele geologie)
Na zijn studie was de schrijver werkzaam als wetenschappelijk assistent by de Nederlandse Organisatie voor Zuiver Wetenschappelijk Onderzoek op de afdeling strukturele en toegepaste geologie o.l.v. Prof. dr. H. J. Zwart.

ERRATUM: p 13, map of the Scandinavian Caledonides

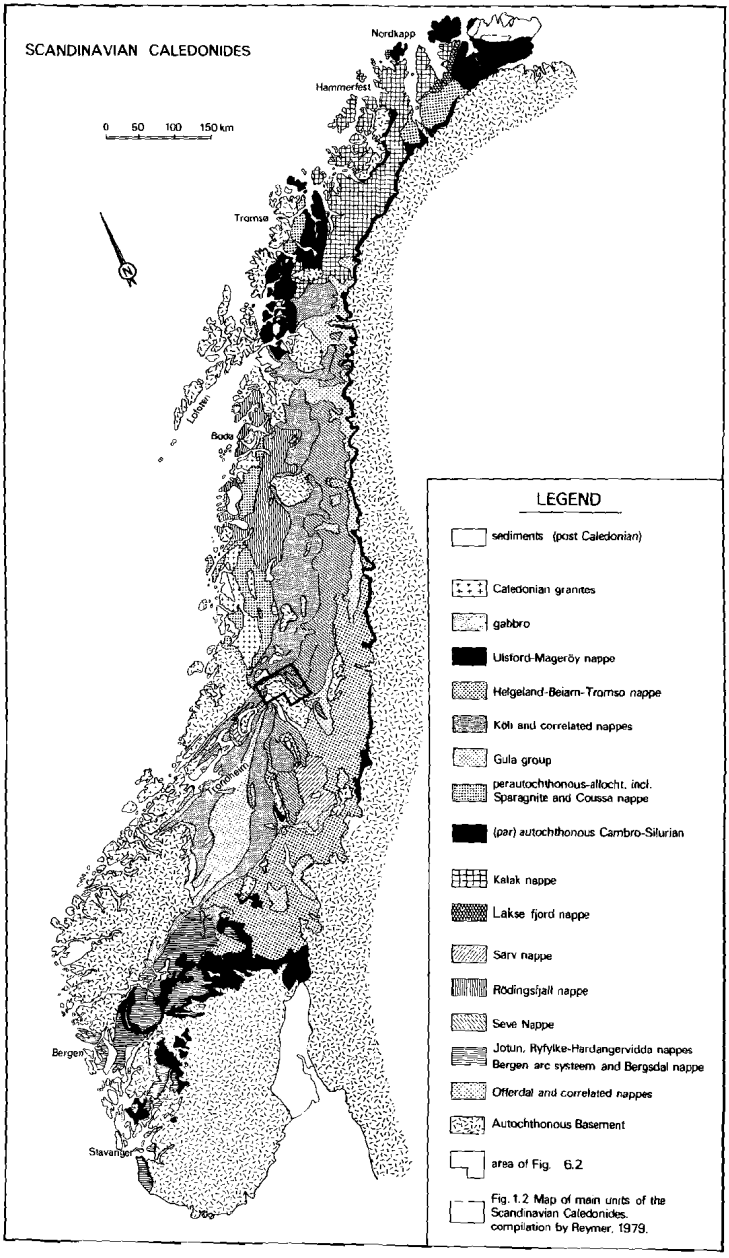

Fig. 1.2 Map of main units of the Scandinavian Caledonides, compilation by Reymer, 1979.